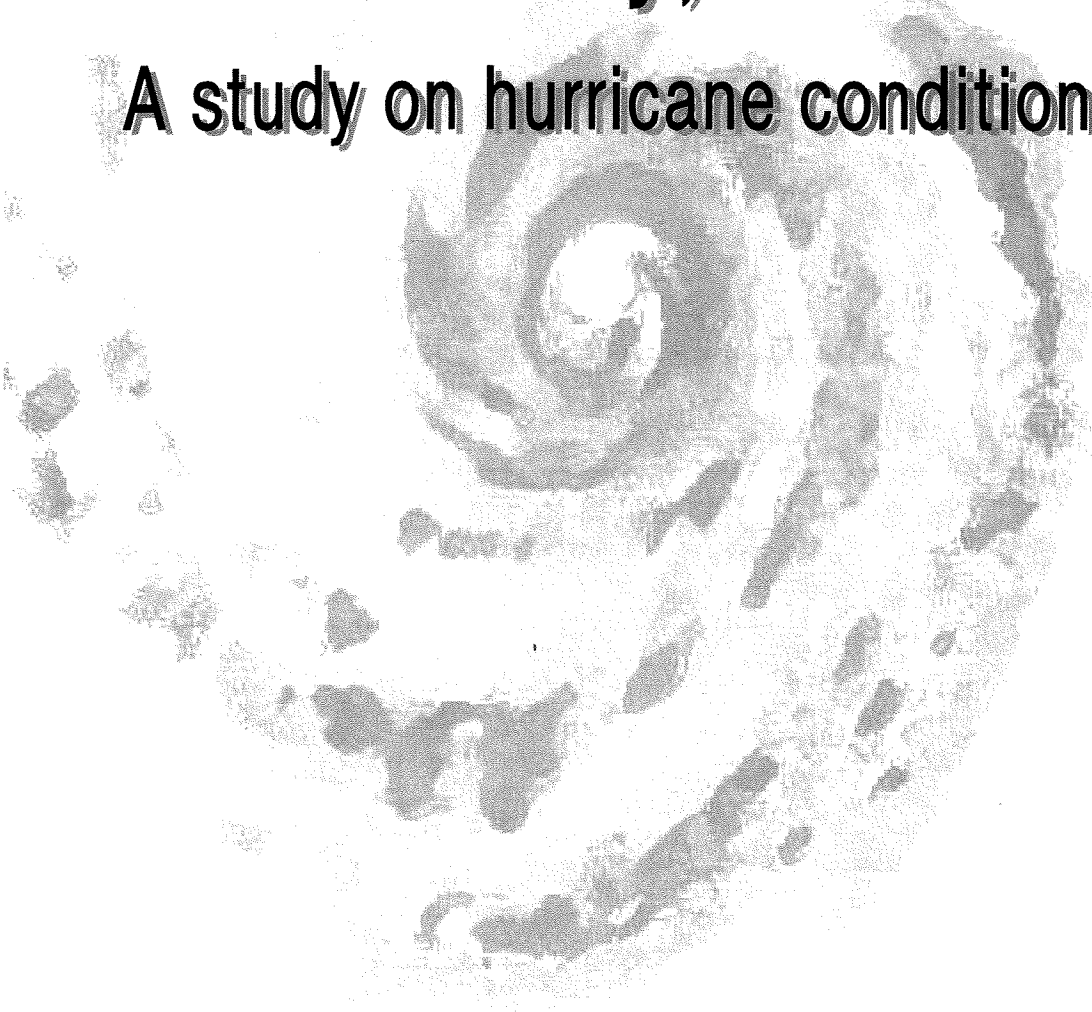# Fort Bay, Saba

A study on hurricane conditions

Master of Science Thesis Report
WL. Van Vilsteren (C9889076)
October 2000 till October 2001

TU Delft Delft University of Technology	Faculty of Civil Engineering and Geosciences
	Subfaculty of Civil Engineering
	Hydraulic and Offshore Engineering Division

Witteveen + Bos	Hydraulic Infrastructure Division
	Department: Rotterdam, The Netherlands

Witteveen + Bos

water

infrastructure

environment

construction
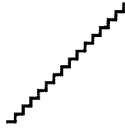
Fort Bay, Saba
A study on hurricane condities

registered	projectcode	status
	ZZWI5009	final version 001
project manager	**project director**	**date**
W.L. van Vilsteren	Ir. H.E. Nieboer	October 10, 2001

authorisation	name	initials
approved	Ir. S.C. van der Biezen	

The Quality management system of Witteveen+Bos has been approved to NEN-EN-ISO 9001 : 1994

PROJECT INFORMATION

Principal	Witteveen+Bos Consulting Engineers
Student	W.L. van Vilsteren (C9889076)
- University	Delft University of Technology
- Faculty	Civil Engineering and Geosciences
- Subfaculty	Civil Engineering
- Division	Hydraulic and Offshore Engineering
Traineeship	Witteveen+Bos, Hydraulic Infrastructure Division
	Rotterdam, The Netherlands
Period	October 2000 till October 2001
Committee	- Prof. drs. ir. J.K. Vrijling (TU Delft)
	- Ir. T.J. Zitman (TU Delt)
	- Ir. S.C. van der Biezen (Witteveen+Bos)
	- Dr. ir. L.H. Holthuijsen (TU Delft)

PREFACE

Hurricanes are often the called "The greatest storms on Earth". They have earned this title through their devastating impacts on people and economics of many nations including those in and around the *Caribbean Sea*. The island of *Saba* (*Netherlands Antilles*) is an example of such a nation where people and economics are relatively often affected by these impacts. The most recent economical impact was the devastation of the island's economical harbour, *Fort Bay*, during hurricane *Lenny* , November 1999 (See box below).

Local authorities on *Saba* are not satisfied with the present status of the harbour and therefore they commissioned *CEC* (*Civil Engineering Caribbean*, a subsidiary company of *Witteveen+ Bos* (*W+ B*)) to come up with a restoration plan. Initiated by the severe damages of hurricane *Lenny*, there exists a general believe that hurricane frequencies and intensities may have been increased during the existence of *Fort Bay* harbour (1972 till today (2000)). Therefore, before coming up with a restoration plan, *CEC* prefers to have an analysis of the conditions taking place during the presence of hurricanes in the area near *Fort Bay* harbour.

A part of the analysis forms the subject of my graduation project at *Delft University of Technology* (*TUD*), the Netherlands. The present report describes the partial analysis and it forms the contents of my Master of Science thesis.

In the first place I would like to thank Mr. T. Zitman for his patience and his critical comments. Secondly my thanks goes to Mr. S.C van der Biezen and Mr. H.E. Nieboer for their remarks and for making this graduation project possible. Acknowledged are also Prof. J.K. Vrijling, Dr. L.H. Holthuijsen and Dr. N. Booij for their remarks and professional support. Special thanks goes to *Digital Hydraulics Holland B.V* for the permission of using the computer model *DOLPHIN-B1*. Finally I would like to thank the people at the office of *Witteveen + Bos* in Rotterdam for their support and the stimulating working ambience during my 12 months of staying.

Wouter van Vilsteren.

October 2001

Hurricane Lenny
Hurricane Lenny was an extremely unusual event. Not only was it the strongest late-season hurricane on record, but it took a particularly rare course, starting in the central Caribbean to the south of Jamaica and then travelling east towards the northern Leeward Islands. Since most sea defences are built to protect against storms moving from east to west, Lenny's unusual route left the region, encompassing at least 16 islands particularly vulnerable to damage.

On 17th November, Lenny crossed St. Croix, ripping off roofs, washing 50 boats ashore, destroying a pier, and knocking out power to over 70% of the population. The hurricane then stalled while over St. Bartholomew, St. Maarten and Saba, and damage was reported most severe in the low-lying coastal areas on the south side of these islands. In Anguilla, storm surges created 12-foot waves, stripping away beaches, which attract tourists and provide the British Islands' largest source of revenue. Late on Friday, Lenny started to move away to the southeast and weaken. Overall, 17 people died as a result of Hurricane Lenny, and the damage is expected to cost around US$330 million (Source: Tropical Prediction Center).

SUMMARY

Fort Bay harbour is a small harbour, located at the South of the island of *Saba*. This island is part of the *Netherlands Antilles* and it is situated in the *Caribbean Sea* where hurricanes may occur several times a year. Since its construction in 1972, *Fort Bay* harbour has experienced several hurricanes. Unfortunately some of these hurricanes were responsible for damage to the harbour structures (mostly to the breakwaters). One of the most devastating hurricanes that hit *Fort Bay* and the area around it was hurricane *Lenny* (1999). It caused severe damage particularly to the armour layers and the monolithic heads of the two breakwaters of the harbour. Although some small-scale recoveries have been applied since then, the harbour structures are still in a poor condition today (2000). To improve this situation, local authorities of *Saba* have commissioned *CEC* to produce a plan focused on a full restoration of the original harbour facilities in combination with an economically feasible protection against hurricane conditions.

A basic element in this restoration plan is to identify what has caused the apparent damage to the *Fort Bay* harbour structures. The first part of the present study is meant to contribute to such an identification. From an overview of the history of *Fort Bay* harbour, an inventory is made of possible reasons why the harbour structures have not been able to withstand the conditions they have been exposed to. This analysis has a qualitative character. One of the items that have come forward in this analysis is a worsening of atmospheric and hydraulic conditions in the area around *Saba*. Looking at the damage caused by hurricanes that have occurred in the past few decades, there is a possibility that such adverse conditions show an increase in both frequency and intensity. Verification of this potential increase is the subject of the second (and also the last) part of the present study.

Hereafter the contents and main conclusions of both parts of the study are summarised.

PART 1
Looking back at the history of *Fort Bay* harbour, three moments of time marked the biggest changes of the harbour design. The moments of time are:
- 1972: Original harbour design
- 1990: Reconstruction design
- 1995: Present design

The original harbour design (1972) consisted of a single breakwater. The breakwater was made of caissons and the revetments of the head and the trunk sections were made of several gradings of rock. This harbour design functioned reasonably well till 1988. In that year, local authorities identified a need to extend the harbour facilities. To fulfil this need, an additional breakwater was constructed in 1990. Just as the original breakwater (indicated as main breakwater), the additional one (indicated as fishery breakwater) consisted of caissons. This time the revetment at the trunk section of the main breakwater consisted of *Accropode* elements instead of rock. These elements were used at the trunk section of the new fishery breakwater as well. At the breakwater heads, the rocky revetment was penetrated with hydrocrete with the aim to create a monolithic structure.

The two breakwaters of the reconstructed harbour remained in a good shape until 1995, when hurricanes *Luis* and *Marilyn* caused severe damage to both breakwaters (head and trunk sections). To regain safety against hurricanes, the head of the fishery breakwater was reconstructed and its trunk section was penetrated with hydrocrete to form one monolithic unit with the head. In addition, the original breakwater has been reconstructed with *Accropode* elements. Unfortunately, these repair works lasted a few years only. In 1999 hurricane *Lenny* devastated both breakwaters (head and trunk sections).

In general, damage to a structure may be caused either by under-estimating or even neglecting loads that may occur during the anticipated lifetime of the structure, or by an over-estimation of its strength. In the present study, we have assessed both possibilities within the context of the damages that have occurred till so far; meaning the damages to the first re-design (1990) and the reconstruction works (1995) that have been carried out since. This qualitative assessment has lead to a series of research questions. Each of these questions refers to a specific phenomenon or mechanism that may

contribute considerably to explaining the damage that has occurred. If we discriminate between (hydrodynamic) load and strength, these questions may be grouped as mentioned hereafter.

Questions regarding the loads on the structures
The breakwaters are exposed primarily to hydrodynamic loads of which the worst are generated by hurricanes. In particular, it concerns wave attack in combinations with water level changes driven by waves, wind and spatial variations in atmospheric pressure. In the determination of design wave conditions, distinction has been made between generation of waves in comparatively deep-water in front of *Fort Bay* harbour and propagation of waves from deep-water to the breakwaters. With respect to the first of these two steps, the following question could be put forward:
1. Did deep-water wave conditions (in the area of *Fort Bay* harbour), generated during hurricanes, worsen significantly (higher waves and changed directions of wave propagation) during the existence of *Fort Bay* harbour (1972-2000)?

and with respect to the second step the following two other questions could be formulated:

2. What changes do the deep-water waves experience while propagating at the relatively steep sloping shore (1:10) towards *Fort Bay* harbour?
3. What are the effects on the near shore wave conditions by taking water level variations into account?

Questions regarding the strength of the structures
The damages to the breakwaters that have occurred till so far were concentrated mostly to the *Accropode* revetments and the revetments made of rock penetrated with hydrocrete. Besides the aforementioned phenomena, which were related to the loads, other phenomena related to the strength of the harbour structures could have been responsible for the damages. In the case that some of these phenomena were not foreseen in previous harbour designs, unwillingly the strength of the breakwaters could have been overestimated. The following two questions are dealing with this possibility.

4. Is it possible to formulate mechanisms or phenomena that could have been responsible for the damage to the revetments consisting of *Accropode* elements, given the applied design wave conditions.
5. Is it possible to formulate mechanisms or phenomena that could have been responsible for the failure of the revetments consisting of rock penetrated with, given the applied design wave conditions.

PART 2
The second part of the present study deals with the possibility of hurricane conditions having worsened over the past decades to a level not foreseen in the latest breakwater design of 1995 (See research question 1). In this respect, an extensive hindcasting exercise of deep-water wave conditions during hurricanes in the area around *Saba* has been carried out and the results have been subjected to a statistical analysis. In this analysis, conditions before 1986 and after 1986 have been intercompared. The year 1986 has been used as a turning point, because the design of the latest harbour (1995) was based on a hindcast study (performed by the American organisation *Oceanroutes Inc.*) concerning hurricanes that have occurred in the period between 1900 and 1986. Since the damages to the breakwaters of the harbour were concentrated in the period after 1986, a worsening of wave conditions could have taken place after this year.

Unfortunately, the analysis could not be performed to its full potential, as hardly any field data (like satellite or buoy data) were available for the present study. This made it impossible to verify the results of the hindcast computations properly. However, it appeared that differences between the hindcast computations and the scarcely available field data were to some extend of a systematic nature. This was substantiated by a comparison of the hindcast computations with a hindcast study, performed by the American organisation *Oceanroutes Inc.* in support of the latest harbour design. A certain systematic difference between these hindcasts could be observed as well. Against this

background, it has been reasoned that the hindcast computations can be used to identify changes in hurricane conditions encountered before and after 1986. However, it was not possible to quantify the consequences of these changes in terms of breakwater design conditions with certainty. The hindcast computations and the statistical analysis are described hereafter.

Hindcast computations
The hindcast computations have been carried out with the use of the physical- mathematical wave model *DOLPHIN-B1*. Based on hurricane track information this model gives wave conditions as a function of time for a pre-selected location. For the present study this location was situated at relatively deep-water and within a relatively short distance to *Fort Bay* harbour. The hurricanes selected for the hindcast
- have occurred between 1972 and 2000;
- and have neared *Fort Bay* harbour to a distance less than 1000 [km].

Statistical analysis
The results of the hindcast exercise have been subjected to a statistical analysis. For the statistical analysis, each of the hindcasted hurricanes was characterised by two wave parameters, viz. the maximum significant wave height ($H_{s,max}$) and the corresponding direction of wave propagation (θ) as computed by *DOLPHIN-B1*. Selecting these two wave parameters is straightforward in the sense that they occur in commonly used basic design rules for breakwaters and similar harbour structures. The statistical analysis compared the hindcasted deep-water wave conditions before 1986 and after 1986. Concluded was that deep-water wave conditions, occurred after 1986, were significantly worse than those encountered before that time.

CONCLUSIONS AND RECOMMENDATIONS
The main conclusions and recommendations are:
- According to the statistical analysis of the results of the hurricane hindcasting exercise, a significant worsening of the deep-water wave conditions has taken place during the existence of the harbour (1972 till 2000). As a result an adjustment of the deep-water design wave condition, as applied by *CEC* to the latest harbour design, is necessary.
- In shallow waters and on gentle sloping shores, the maximum wave height is directly related to the available water depth (depth limited). However, in the case of *Fort Bay* harbour, relatively large (hurricane generated) waves propagate on a steep sloping shore (1:10) and have not enough time to adjust their wave height to the available water depth, because the water depth decreases too fast. To get insight into the behaviour of waves on the steep sloping shore near the *Fort Bay* harbour it is strongly recommended to perform a study on this phenomenon.

TABLE OF CONTENTS

Fort Bay harbour, Saba. A study on hurricane conditions

vii

NOMENCLATURE AND ABBREVIATIONS

Accropode	See Annex III
ARGOSS	Advisory and Research on Geo Observation Systems and Services
Armour layer	Protective layer on rubble mound breakwater composed of armour units
Armour unit	Large quarrystone or special concrete shape used as primary (wave) protection
Bathymetry	Topography of sea/estuary/lake bed
BMO	British Meteorological Office, also: Met. Office. They provide environmental and weather-related services (Bracknell, Berkshire, United Kingdom)
Boulders	In the present study defined as large concrete blocks used to support the revetment of a breakwater.
Breakwater	A construction to protect a harbour against significant wave action and silting-up
Caisson	Concrete box-type structure
CEC	Civil Engineering Caribbean consulting engineers is a subsidiary company of *Witteveen+ Bos*
Colloidal concrete	Concrete with extra cohesion
CYCLONE	Build-in tool of DOLPHIN-B1 for creating theoretical hurricane shaped wind fields
Desalination plant	Equipment for transforming salt sea water into fresh water
DOLPHIN-B1	Wave model to forecast or hindcast the two dimensional wave spectrum at a set of locations and times in arbitrary wind fields over the ocean [Lit 6]
ENDEC	Wave model (ENergy DECay) that takes account of the effect of depth-induced breaking in near shore regions
Fath	Fathom
Fetch (length)	Relative to a particular point (on the sea), the area of sea over which the wind can blow to generate waves at the point. The fetch length depends on the shape and dimensions of the fetch area, and upon the relative wind direction
Hindcast	Reconstruction of wave conditions based on historical information
Hurricane	A hurricane is a type of tropical cyclone acting on the Northern Hemisphere. Tropical cyclone is a generic term for a low pressure system that generally forms in the tropics. The cyclone is accompanied by thunderstorms and, in the Northern Hemisphere, a counter clockwise circulation of winds near the earth's surface.
Hydrocrete	See Colloidal concrete
Km	Kilometer
Knt/knts	Knots
LWS	Low Water Spring tide level
Max. sustained wind speed	The 1-minute maximum surface wind speed at an elevation of 10 [m] above mean sea level
Mb	Milibar
MW	Meter Water column
NACO BV	Netherlands Airport COnsultants BV. An Independent airport consultancy and engineering firm (The Hague, The Netherlands)
NHC	National Hurricane Center. Subdivision of the NOAA
Nmi	Nautical mile
NOAA	National Oceanic and Atmospheric Administration, located in the U.S. Department of Commerce (Washington, The United States)
Oceanroutes Inc.	Provider of marine information services, like weather routing services, forensic meteorology and studies and consulting (Sunnyvale, The United States)
Omni-directional	In this report it means: waves coming from every direction
Refraction	Change in direction of wave propagation, when a wave propagates in water with a different depth
Return period	In statistical analysis an event with a return period of N years is likely, on average, to be exceeded only once every N years
RMS	Root Mean Square difference. See Annex VI
Ro-Ro	Means Roll on Roll off. A quay used for Roll on and Roll off transhipment
Rubble mound	A general description of broken pieces of rock
s or sec	Seconds
Saffir-Simpson scale	See Annex IV

Shoaling	Changing of the wave height when a wave propagates in water with a different depth
Significant wave height	Also $H_{1/3}$. The average of the highest third part of all waves in a wave field
Stochastic	Having random variations in statistics
Swell	Also "old" waves. Waves that penetrate an area, but are not generated in that area
Time serie	A time serie is a registration of satellite observations covering a period of 14 days. They are available from the *ARGOSS* databases
Toe	Lowest part of the seaward and port-side breakwater slope, generally forming the transition to the sea bed
TUD/TU Delft	Delft University of Technology (Delft, The Netherlands)
ULS	Ultimate Limit State
Uplift	The upward pressure in the pores of a material or on the base of a structure
Wash out	Removing of sandy material due to wave action
Wash probes	Pointing a water jet towards an arbitrary kind of soil for a period of time and measure the level of scour.
Wave spectrum	Distribution of the wave energy over the frequencies
W+B	Witteveen+Bos Consulting engineers
Weibull	Name of a family of extreme value distributions
WL|Delft Hydraulics	Waterloopkundig Laboratorium: is an independent consulting and research institute (Delft, The Netherlands)

Conversions

For winds (knots = nautical miles per hour; mile = statute mile)

1 mile per hour	= 0.868 knot
1 mile per hour	= 1.609 kilometers per hour
1 mile per hour	= 0.4470 meter per second
1 knot	= 1.853 kilometers per hour
1 knot	= 0.5148 meter per second
1 meter per second	= 3.6 kilometers per hour

For pressures

1 inch of mercury	= 25.4 milimeters of mercury
1 inch of mercury	= 33.86 millibars
1 inch of mercury	= 33.86 hectopascals
1 milibar	= 100 newton per square meters

For distances/depths

1 fath	= 1.8288 meter
1 foot	= 0.3048 meter
1 nautical mile	= 1.1515 statute miles
1 nautical mile	= 1.853 kilometers

LIST OF SYMBOLS

Δ	Relative density i.e. for rock $\Delta = (\rho_r/\rho_w)-1$ [-]
α	Weibull shape parameter [-]
α	Slope angle of the shore [°]
θ	Direction of wave propagation relative to North [°]
β	Threshold value
σ	Weibull scale parameter
λ	Average number of hurricanes per year (N/T) [1/year]
γ_0	Breaker depth ratio (H/d) [-]
ξ_0	Irribarren number, defined at deep-water [-]
ρ_a	Mass density of air [kg/m^3]
ρ_r	Mass density of rock [kg/m^3]
ρ_w	Mass density of water [kg/m^3]
$\mu_{\underline{x}}$	Mean value of the stochastical value $\underline{x}$
$\sigma_{\underline{x}}$	Standard deviation of the stochastical value $\underline{x}$
a and b	Constants for the determination of the data sample probability
d	Water depth [m]
D	Representing the samples in a data set [-]
D_{n50}	Median diameter of armour unit [m]
f_{cor}	*Coriolis* parameter [1/sec]
f_m	Mean frequency of wave spectrum [Hz]
f_p	Peak frequency of wave spectrum [Hz]
g	Gravitational acceleration [m/s^2]
H	Wave height [m]
H_{max}	Maximum individual wave height [m]
H_s	Significant wave height [m]
$H_{s,max}$	The maximum H_s of all the hindcasted H_s, during the occurrence of a hurricane at an arbitrary location [m]
K_d	Stability coefficient in *Hudson* formula [-]
L	Wave length [m]
L_0	Deep-water wave length [m]
m	Rank of data sample. m= 1 refers to the highest sample
N	Number of samples in a data set [-]
P	Pressure at an arbitrary location [mbar]
P_a	Atmospheric pressure at mean sea level [mbar]
P_{diff}	Pressure difference between infinity and the centre of a hurricane [mbar]
P_{eye}	Pressure in the center of a hurricane [mbar]
P_{inf}	Environmental pressure at the outer limits of a hurricane, where the cyclonic circulation ends (also pressure at infinity) [mbar]
R	Distance from the centre of a hurricane to an arbitrary point where one wants to know the wind velocity [km]
R	Radius to maximum wind speeds [km]
R	Strength or Resistance descriptor in probabilistic calculations
R	Radius of a hurricane eye [km]
R_p	Return period [year]
S	Loading descriptor in probabilistic calculations
s(D)	Standard deviation of the samples in a data set
T	Wave period [s]
t	Time
t	Student's-t-Test parameter [-]
T	Hindcast period [year]
T_s	Significant wave period [s]
U_g	Gradient wind speed [m/s]
$U_{g,max}$	Maximum gradient wind speed [m/s]
$U_{g,max,sust}$	Maximum sustained wind speed [m/s] or [knts]
X	x-co-ordinate of the centre of a hurricane [°]
$\underline{x}$	Stochastical value of x
Y	y-co-ordinate of the centre of a hurricane [°]

Z	Reliability function in probabilistic calculations
Z	Definition of a hypothesis
z_a	Rise of mean water level, or storm surge [m]

LIST OF FIGURES

LIST OF TABLES

1. INTRODUCTION

1.1. Scope

Fort Bay harbour is a small harbour, located at the South of the island of *Saba*. The island of *Saba* is part of the *Netherlands Antilles* and it is situated in the *Caribbean Sea*. The harbour is divided in a fishery port and a multipurpose port, both protected by two single breakwaters. In this part of the *Caribbean Sea* hurricanes occur several times a year. Therefore during its existence, *Fort Bay* harbour had to deal with the occurrences of several hurricanes. Unfortunately, some of these hurricanes were responsible for severe damage to the harbour structures. Repair works and adjustments were carried out to prevent new hurricane damages. However, in 1995 the latest adjustments were not able to withstand the most recent hurricane conditions during hurricane *Lenny*, which passed the area between 13th and 21st November 1999. Especially the two breakwaters, suffered severe damage (in particular to the armour layers). As a result the harbour structures are in a poor condition and the harbour activities are hindered in an unacceptable way. An overview of the present (year 2000) status of the harbour is given in Figure 1.

Source: W+ B and CEC [Lit 9]

Figure 1: Overview Fort Bay harbour (2000)

Local authorities of *Saba* are not satisfied with the present state of the damaged harbour. Therefore they commissioned *CEC* (*Civil Engineering Caribbean*, a subsidiary company of *Witteveen+ Bos* (*W+ B*)) to come up with a restoration plan for the *Fort Bay* harbour. The restoration plan must take care of a full recovery of the harbour in combination with an economically feasible protection against hurricane conditions.

A fundamental element in this restoration plan is to identify the causes of damage to the *Fort Bay* harbour structures. In general there are two factors that could have been responsible for these damages. First, under-estimation of the loads (wave conditions) that may occur during the anticipated lifetime of the structures. Secondly, over-estimation of the strength of the structures. Before coming up with the final restoration plan, *CEC* wants to have an analysis of these two possibilities.

1.2. Objective

The meant analysis in Section 1.1 forms the subject of the present study. The first part of the study will contribute to this analysis, by giving possible reasons why the harbour structures have not been able to withstand the hurricane conditions they have been exposed to. After a thorough study of the design reports and other sorts of information related to the *Fort Bay* harbour, these reasons will be derived. In advance on Chapter 3, one of the reasons that have come forward is a worsening of wave conditions during hurricanes in the area around *Saba*. Whether or not this worsening has taken place and till what extend it was responsible for the occurred damages, will be verified in the second part of the present study.

Resuming, the objective of the present study is formulated as:

> *Identify the cause(s) of damage to the Fort Bay harbour structures and find out till what extend a worsening of wave conditions during hurricanes contributed to these damages.*

1.3. Structure of the Thesis study

The present study is divided into two parts. Part 1 is devoted to the identification of the possible reasons that could have been responsible for the damages to the harbour structures. Part 2 describes the study of one of these reasons, namely a potential worsening of hurricane wave conditions. Hereafter, both parts will be described in more detail.

Part 1

The present study starts with an overview of the history of *Fort Bay* harbour in Chapter 2. Apart from information regarding the problems *Fort Bay* harbour is confronted, the overview contains a qualitative assessment of the applied design wave conditions and the stability of the harbour structures. The assessments led to a series of research questions. Each of these questions refers to a specific reason that may contribute in the explanation of the occurred damages. In Chapter 3 these research questions are described.

Part 2

The second part of the present study describes the analysis necessary to determine whether or not a potential worsening of hurricane wave conditions has contributed to the damage of the *Fort Bay* harbour structures. In fact this boils down to finding an answer on the first research question (see Chapter 3). This question will be answered by conducting a new hurricane hindcast study. The hurricane hindcast is carried out with a wave model capable of hindcasting deep-water wave conditions based on hurricane track information. A description of the wave model, its restrictions and the model set-up are given in Chapter 4. Hereafter in Chapter 5 an effort is made to verify the model output with other registrations of hurricane wave conditions. At the end of this Chapter the actual hurricane hindcast will be carried out. Results from the hindcast are statistically analysed in Chapter 6. The statistical analysis estimates whether or not during the existence of the harbour the deep-water hurricane wave conditions have been increased significantly. Finally in Chapter 7 it is illustrated what a possible increase of these deep-water wave conditions means for the design conditions of the two breakwaters at *Fort Bay* harbour.

Part 1

Derivation of research questions

Fort Bay harbour, Saba. A study on hurricane conditions

3

2. BACKGROUND

This Chapter describes the history of *Fort Bay* harbour and the background of the problems the *Fort Bay* harbour is confronted with. The content is based mainly on information from reports of *CEC* and *W+ B* and partly on information from other available literature. First the geographical situation and some characteristics of *Saba* and the *Fort Bay* harbour will be presented. Secondly, the different harbour designs that have been applied during the existence of the harbour are described. In this part the applied design wave conditions as well as the stability of the harbour structures will be analysed.

Three different harbour designs have been applied since the construction of *Fort Bay* harbour. The harbour designs are listed hereafter:
- 1972: Construction of the original harbour design made by *NACO* (*Netherlands Airport Consultants BV*)
- 1990: Construction of the reconstruction design made by *CEC*
- 1995: Construction of the present-day design made by *CEC*

2.1. Geographical situation of Saba and the Fort Bay harbour

Saba is located about 1970 [km] (1225 [nmi]) Southeast of *Miami* (*Florida*) and 310 [km] (195 [nmi]) east of *San Juan* (*Puerto Rico*) near the northern end of the *Upper Antilles*. The island forms the westernmost corner of a triangle of islands including *Sint Maarten* (46 [km]/28 [nmi] Northeast) and *Sint Eustatius* (32 [km]/20 [nmi] southeast). There is only one main road, which runs from the airport at the north-eastern side of the island through the villages of *Hell's Gate*, *Windwardside*, *St John's* and *The Bottom*, and continues down to *Fort Bay*, the island's main port. A second road connects *The Bottom* with *Well's Bay* on the island's north-western side. In Figure 2 the location of *Saba* in the *Caribbean Sea*, as well as an overview of the island of *Saba* are given.

Source: Lonely Planet Word Guide [Lit 21]
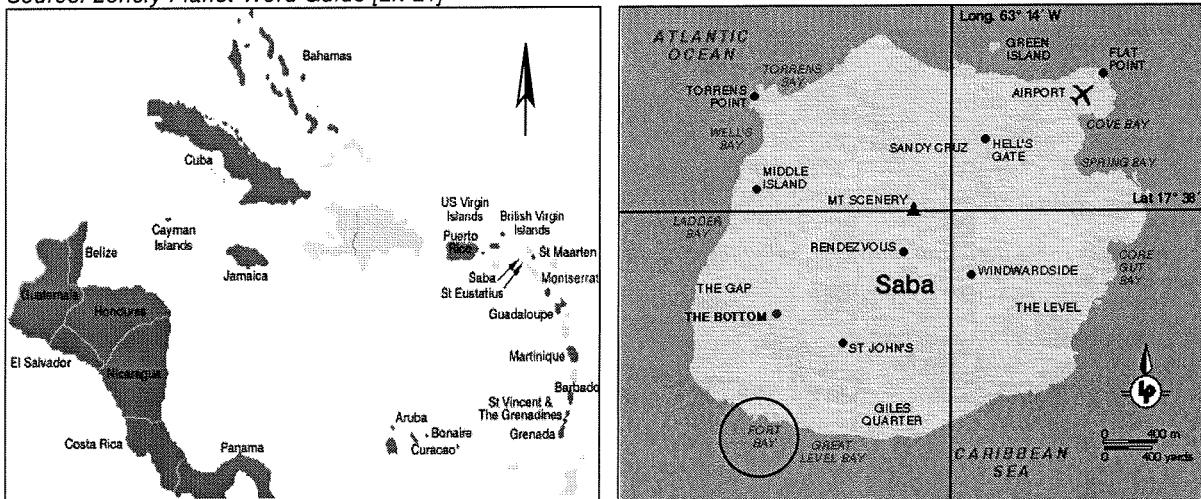
Figure 2: Map of the Caribbean and the island Saba

As the tip of an immense underwater mountain, the island juts out of the sea with no pause for lowlands or beaches. *Saba's* central volcanic peak, *Mt Scenery*, has an elevation of 890 [m] relative to mean sea level. There are no rivers or streams on the island. The *leeward* (western) side is dry with cacti and scrub, the *windward* (eastern) side has thicker vegetation and the mountainous interior is given over to lush jungle growth such as tall tree ferns, palms and mahogany trees. The average monthly temperature is 27 [°C] (80 [°F]), with few degrees difference between summer (June to August) and winter (December to February). Because of the difference in elevation, temperatures are a bit cooler in *Windward* side than in the *Bottom*. A kilometer long road leads to *Fort Bay*, the island's commercial port, on the south-western coast. *Fort Bay* has dive shops, the marine park office, the

island's power station, a water desalination plant and *Saba's* only gas station. In Table 1 some general characteristics of *Saba* are listed.

Table 1: Characteristics of Saba in year 1999

Characteristics	
Area	13 [km^2]
Population	1200 persons
Capital city	*The Bottom*
Government	Municipality of the *Netherlands Antilles*
GDP (Gross Domestic Product)	US$ 2.4 billion for *Netherlands Antilles* as a whole
GDP per head	US$ 10,000
Growth rate	0%
Inflation	3%
Major industries	Tourism
Major trading partners	*USA, Venezuela, Colombia, The Netherlands, Japan*
Currency	*Netherlands Antilles* florin (Naf)

Source: Lonely Planet Word Guide [Lit 21]

Fort Bay harbour, Saba. A study on hurricane conditions

5

2.2. Fort Bay harbour: Original design made by *NACO* (1972)

The original design of the *Fort Bay* harbour is made by *NACO* in the period between 1966 and 1968. The construction of the harbour based on the original design was finished in 1972. Information about the used design wave conditions is not available for the present study. However, back in 1966 *WL| Delft Hydraulics* conducted scale model tests for a cross section of a breakwater, which is similar to the applied breakwater at *Fort Bay* harbour. For the present study it is again unknown which significant wave height or other wave characteristics have been used as design condition for the scale model breakwater. Because of the lack of information a further evaluation of the design can not be carried out. The rest of the information of the original design of 1972 is only given in order to provide a complete picture of the history of the *Fort Bay* harbour. The layout of the harbour after completion in 1972 is given in Figure 3, the various structures are listed in Table 2. Cross-sections are available in Annex I. The harbour structures in Table 2 have been assigned by numbers that can be looked up in Figure 3.

Source: CEC project file 1988 [Lit 3]
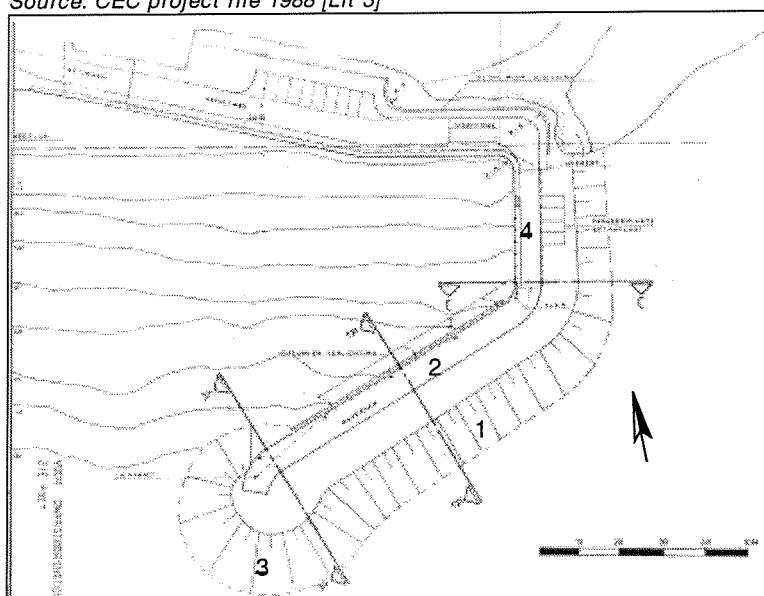
Figure 3: Layout harbour (1972)

Table 2: Main harbour structures in (1972)

Structure	Part	Construction material
Main breakwater (1)	Core	Rock 0-500 [kg]
	Secondary armour layer	Rock 500-4000 [kg]
	Primary armour layer	Rock 4000-7000 [kg] slope 1:1.5
	Toe	Not available
Main breakwater head (3)	Foundation	Bags filled with concrete
	Core	Rubble mound, sizes are not available
	Primary armour layer	Concrete cubes, sizes are not available
Main quay (2, 4)	Foundation	Bags filled with concrete
	Upper structure	Concrete caissons

2.3. Fort Bay harbour: Reconstruction design made by CEC (1990)

In the period from 1972 till 1987 recurrent damages were reported to the armour layers of the main breakwater (1) and main breakwater head (3), see Figure 3. The damages consisted of recurrent losses of armour layer material (rock) during hurricane conditions. To prevent the losses of armour material and because of the need to extend the harbour facilities, a reconstruction design was necessary. The reconstruction design was part of the framework of an integral development plan for *Saba*. The *Department for Development Co-operation* (*DEPOS*) commissioned *CEC* to prepare the reconstruction. According to the *Fort Bay* harbour design papers of 1990 [Lit 1] and [Lit 2], the reconstruction design had to comply with the following terms:

- Reduction of the losses of armour material in the future to an economically acceptable level;
- Extension of the harbour with a fishery port;
- Creating a more tranquil wave environment in the harbour basin (results in an improvement of transhipment activities).

2.3.1. Inspection of harbour status (1987)

Before coming up with a reconstruction plan, a harbour inspection was carried out in 1987 under auspices of *CEC*. In Table 3 the results are listed.

Table 3: Inspection results (1987)

	Inspection results
1	At some places under the caissons of the main quay (2), the concrete filled bags have disappeared;
2	Close to the main breakwater head (3) a big hole exists under the first caisson;
3	A few big holes have been encountered under the main quay (2);
4	Accretion has taken place along the entire quay (2);
5	From wash probes, the bottom consists of rock;
6	According to the design of 1972 the armour layer of the main breakwater (1) should consist of 4-7 [ton] stones. Inspection concluded that rock weights did not match with this norm. The weights were less. At some places holes are detected in the armour layer of the main breakwater (1). Due to wave attack armour units were moved to the toe of the breakwater;
7	Armour units from the main breakwater (1) and the main breakwater head (3) have been relocated in the harbour basin.

Source: Annex to harbour design paper of 1990 [Lit 2]

2.3.2. Survey of wave conditions at Fort Bay harbour (1988-1989):

As mentioned already in Section 2.2, information on the design wave conditions of the *Fort Bay* harbour was not available from the design of 1972. Therefore, before designing a reconstruction plan, a wave climate study near *Fort Bay* harbour was carried out. The basis of this study was formed by another wave climate study, called "Wave conditions *Oranjestad* breakwater, *Sint Eustatius*" [Lit 11]. The study is carried out by *WL| Delft Hydraulics* in 1988. This study was chosen, because *St. Eustatius* is an island near *Saba* (distance between the islands is approximately 30 [km]) and therefore deep-water wave conditions were assumed identical in both cases.

Description of wave climate study near *St. Eustatius*, WL| Delft Hydraulics [Lit 11]

The research of *WL| Delft Hydraulics* included an examination of "normal" and "extreme" wave conditions in the area near the breakwater of the *Oranje Bay* of *St. Eustatius*. According to the report, first the deep-water wave climate was derived, followed by a translation of this wave climate to shallow water in the area near the breakwater of *Oranje Bay*. The deep-water wave climate has been reconstructed with "normal" and "extreme" wave data from different organisations. The "normal" deep-water wave conditions were derived from a data set of ship based wave observations. The data set was available from the *British Meteorological Office* (*BMO*) and from a document called *Ocean Wave Statistics*, written by *N. Hogben* and *F.E. Lumb* (1967) (Document is not available for the present study). The "extreme" deep-water wave conditions during hurricanes, were obtained from the American organisation, called *Oceanroutes Inc.* (*Marine Weather Science Division*). This organisation

performed a study on these "extreme" wave conditions in December 1987. A complete description of the hurricane hindcast study of *Oceanroutes Inc.* is given in Section 5.2.2. *WL| Delft Hydraulics* summarised the "normal" and "extreme" deep-water wave conditions in a probability of exceedance graph, see Annex II.

Knowing the "normal" and "extreme" deep-water wave conditions, *WL| Delft Hydraulics* translated them to the shallow water area near the *Oranje Bay* breakwater with the wave model *ENDEC* (acronym for *Energy Decay*). The wave model *ENDEC* is one-dimensional and designed primarily to take account of the effect of depth-induced breaking in near shore regions. *ENDEC* uses an energy balance method for random waves on arbitrary bottom topography. Refraction effects due to along shore uniform depth and current variations are also included.

Resuming, the following effects are accounted for in the *ENDEC* model:
- Shoaling;
- Refraction due to bottom and current variations;
- Energy loss due to depth-induced breaking and bottom friction;
- Energy gain due to local wind;
- Water level variation due to radiation stress gradients.

For several return periods the *ENDEC* model derived wave conditions at the 6 and 7 [m] depth contours. These wave conditions were taken as design wave conditions of the breakwater of the *Oranje Bay* at *St. Eustatius*.

Derivation of wave conditions near the *Fort Bay* harbour

In the case of the *Fort Bay* harbour at *Saba*, the deep-water wave conditions were not determined again, but they were copied from the report of *WL| Delft Hydraulics* [Lit 11]. The translation of these deep-water wave conditions towards the *Fort Bay* harbour is again carried out with the wave model *ENDEC*. The *ENDEC* model is applied along two rays, see Figure 4. This resulted in wave conditions at the following water depth contours:
- main breakwater (1): 5 [m]
- main breakwater head (3): 9 [m]

The significant wave heights resulting from the *ENDEC* calculations are listed in Table 4.

Table 4: Results according to ENDEC computations

Deep-water wave height H_s [m]	Ray I (depth= 9 [m]) H_s [m]		Ray II (depth= 5 [m]) H_s [m]	
	T= 10 [sec]	T= 12 [sec]	T= 10 [sec]	T= 12 [sec]
6	5.8	6.1	Not available	Not available
7	6.8	6.9	4.1	Not available
7.5	6.8	7.2	Not available	4.1
8	7.1	7.5	Not available	4.2
8.5	7.4	7.6	Not available	4.2
9	7.6	8.0	4.3	4.3

Source: Fort Bay design paper 1990 [Lit 1]
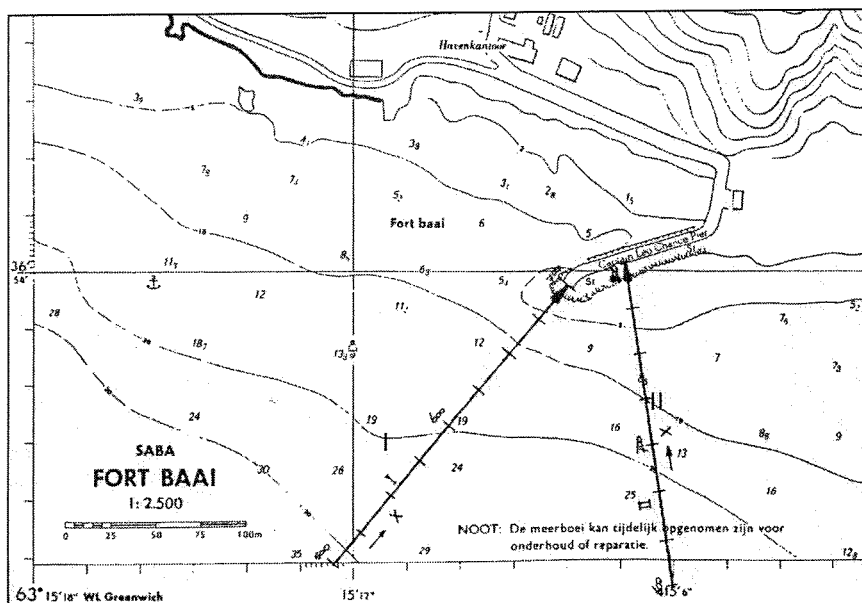
Figure 4: Rays as used by ENDEC

2.3.3. Evaluation of the derived wave conditions

In the next, wave conditions from *ENDEC* will be evaluated by comparing them with wave conditions resulting from two commonly used rules. First the method of *Miche* will be described, secondly the method of *Goda* will be discussed. However, since in the rest of the present study the terms shallow and deep-water will be used frequently, first these terms will be defined for general waves as generated during hurricanes.

Distinction between shallow and deep water

The distinction between shallow and deep water is commonly made, based on the value of the relative water depth, see Equation 1.

Relative water depth = d/L   Equation 1

d = Water depth [m]
L = Deep-water wave length [m]

Shallow water is characterised by d/L<1/20 (0.05); deep-water is characterised by d/L>1/4 (0.25). Generally waves generated by hurricanes have a significant wave height of approximately 10 to 12 [m] and a wave period of approximately 12 [sec] at deep-water. Expressing the deep-water wave period into the deep-water wavelength is done with Equation 2.

$$L = gT^2/2\pi$$ Equation 2

G = Gravitational acceleration [m/s^2]
T = Wave period [s]

Resulting from Equation 2, L $\approx$ 225 [m] for waves at deep-water, during the presence of a hurricane. In this way shallow water is characterised by d<0.05x225= 11.25 [m] and deep-water is characterised by d>0.25x225= 56.25 [m]. The range of water depths between 11.25 [m] and 56.25 [m] is indicated as transitional water.

Determination of wave conditions with Miche

A dimensionless parameter which is of crucial importance to all kinds of problems in shore protection is the so-called *Irribarren* number, see Equation 3. This parameter indicates that the notions "steep" and "gentle" for a slope are relative ones.

$$\xi = \frac{\tan \alpha}{\sqrt{H/L}}$$

Equation 3

α = Slope angle [°]
H = Wave height [m]

The angle of the foreshore near *Fort Bay* harbour is approximately 1:10. With a significant wave height of 12 [m] and a deep-water wavelength of 225 [m], the *Irribarren* number, for hurricane generated waves in this region, becomes ξ= 0.433. This value indicates a *plunging breaker* type. Knowing the type of breaker it is possible to determine the possible wave heights, because they are dependants of ξ. According to [Lit 16] *Miche* gives a general limit to the maximum individual wave height (H_{max}), see Equation 4.

$$H_{max} = 0.142L \tanh\left(\frac{2\pi}{L}d\right)$$

Equation 4

For shallow water, Equation 4 leads to H_{max}/d= 0.88 (d/L < 0.05 → tanh(2πd/L) ≈ 2πd/L). Applied to H_s in irregular waves, values of H_s/d≈0.4-0.5 are usually found. However, it could be possible that this general rule for the combination of large waves (in the case of waves generated by hurricanes) and a steep fore shore (1:10) is not completely valid. This possibility is substantiated with Figure 5.

Source: [Lit 16]
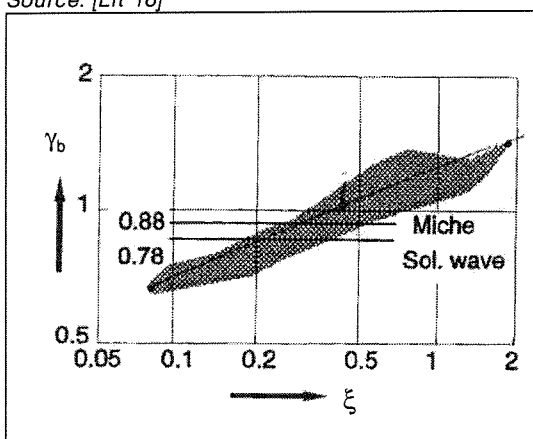
Figure 5: Breaker depth in shallow water

γ_b = Breaker depth ratio (H/d)
ξ_0 = *Irribarren* number defined at deep-water

The *Irribarren* number was determined as ξ= 0.433. Looking to Figure 5, the breaker depth ratio (γ_b) becomes 1.2 or perhaps even larger. A larger breaker depth ratio implicates a larger possible H_{max}. Because H_{max} and H_s are related to each other it is reasonable to assume a larger H_s as well. According to these considerations the value of the breaker depth ratio of H_s is assumed to be 0.6 instead of 0.4 or 0.5, see Equation 5.

$H_s/d \approx 0.6$ Equation 5

The results of the translation of the significant deep-water wave heights into significant wave heights at various water depth contours, according to Equation 5, are given in Table 5.

Table 5: Results according to Miche (Equation 5)

Deep-water wave height H_s [m]	Ray I (depth= 9 [m]) H_s [m]		Ray II (depth= 5 [m]) H_s [m]	
	T= 10 [sec]	T= 12 [sec]	T= 10 [sec]	T= 12 [sec]
6	5.4	5.4	3	3
7	5.4	5.4	3	3
7.5	5.4	5.4	3	3
8	5.4	5.4	3	3
8.5	5.4	5.4	3	3
9	5.4	5.4	3	3

Determination of wave conditions with Goda

According to [Lit 18], *Goda* (1970) has derived an empirical relationship to determine the wave height at breaking (H_b). This relationship depends on the deep-water wave height (H_0), the deep-water wave steepness and the beach slope (m= tanα). Figure 6 and Figure 7 illustrate this relationship. With Figure 6 it is possible to translate the deep-water wave height into the wave height at breaking whereas with Figure 7 it is possible to determine the water depth where the wave will break (d_b).

Source: [Lit 18]
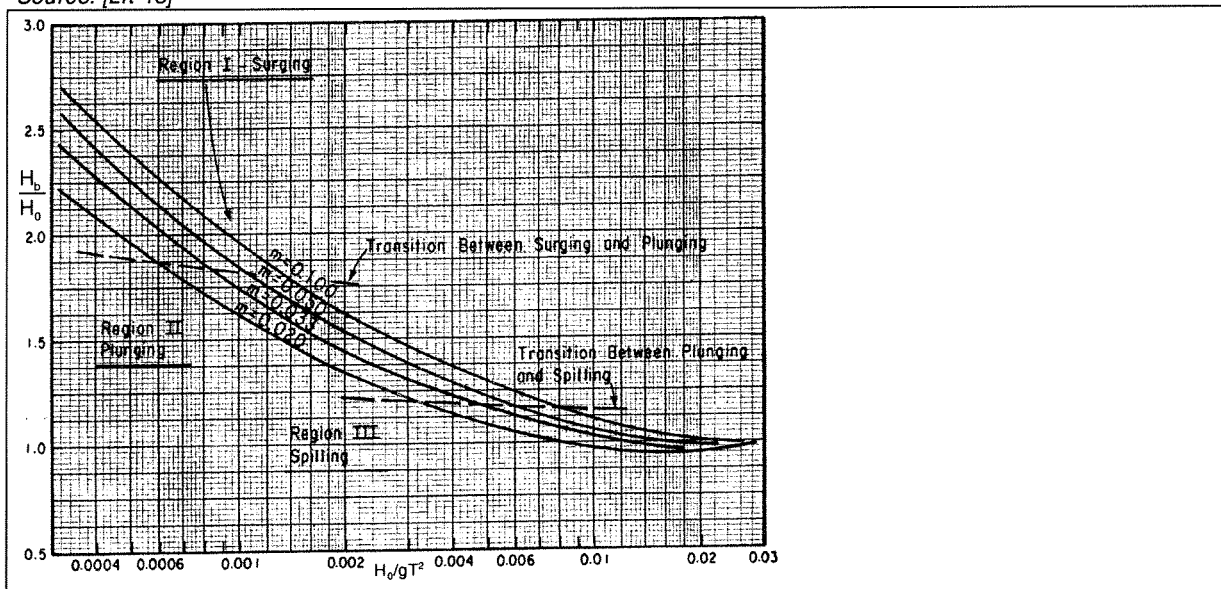
Figure 6: Breaker height index (H_b/H_0) vs. deep-water steepness (H_0/gT^2), from Goda, 1970
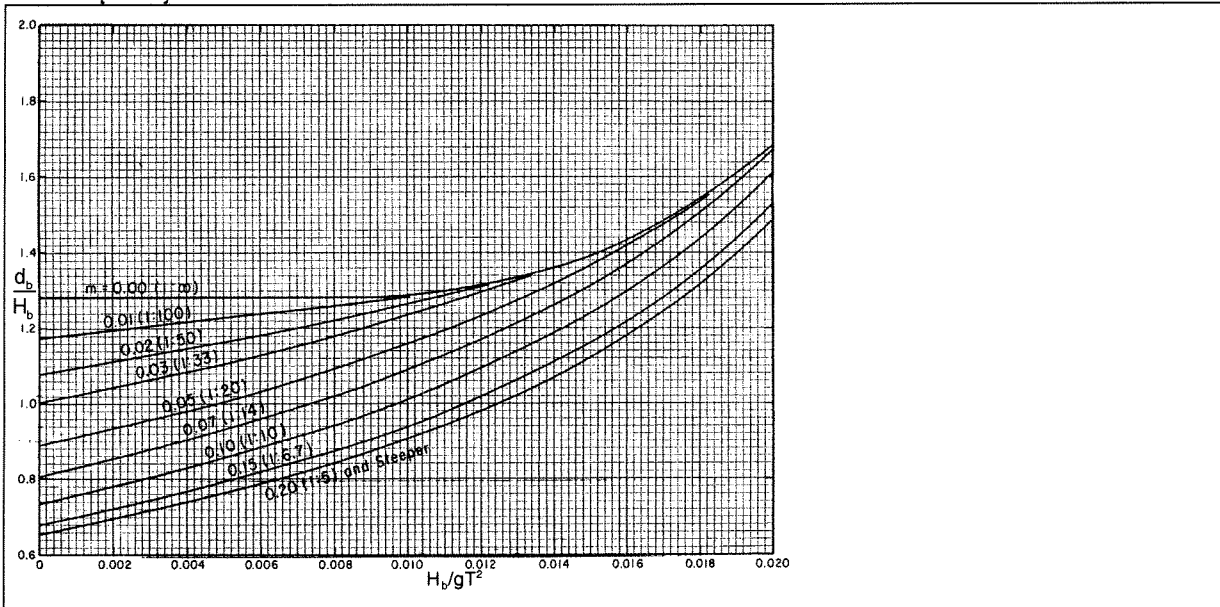
Figure 7: Dimensionless depth at breaking(d_b/H_b) vs. breaker steepness (H_b/gT^2)

According to the approach of *Goda* it is necessary to determine first whether or not the incoming wave has already broken due to the local depth, before it reaches the location of interest. This is done by the determination of the breaker height (H_b) and the water depth at the breaker line (d_b) (for these purposes Figure 6 and Figure 7 need to be used).

When the water depth at the breaker line is larger than the water depth at the location of interest, the wave is already broken. In that case the wave height at the location of interest is assumed to be equal to the breaker height at the location of interest. According to [Lit 18] the curves in Figure 6 are described by Equation 6.

$$\frac{d_b}{H_b} = \frac{1}{a - (aH_b/gT^2)}$$

Equation 6

Where the coefficients a and b are functions of the foreshore slope m, and may be approximated by Equation 7 and Equation 8.

$$a = 43.75(1 - \exp(-19m))$$

Equation 7

$$b = \frac{1.56}{(1 + \exp(-19.5m))}$$

Equation 8

By adjusting Equation 6 to Equation 9 it is possible to determine the breaker height at a given depth.

$$H_b = \frac{d_b bgT^2}{gT^2 + ad_b}$$

Equation 9

When the water depth at the breaker line is smaller than the water depth at the location of interest, the wave is not broken. In that case the wave height at the location of interest can be determined

Fort Bay harbour, Saba. A study on hurricane conditions

12

with the use of the shoaling coefficient (K_s). According to [Lit 18] the shoaling coefficient is given by Equation 10.

$$K_s = \left(\frac{c_{g0}}{c_g} \right)^{1/2}$$

<div style="text-align: right">Equation 10</div>

c_{g0} = Wave group velocity at deep-water [m/s]
c_g = Wave group velocity at the location of interest [m/s]

An example illustrating the estimation of the local (shallow) significant wave height is given in the box hereafter.

Example:
In the case of *Fort Bay* harbour, the foreshore has a slope of approximately 1:10. Because of the steep sloping shore near *Fort Bay*, most likely refraction does not play a significant role. Therefore at this stage refraction is not taken into account. Assume further a deep-water significant wave height (H_0) of 9 [m] and a period of T= 10 [sec]. The question is to find the significant wave height at the depth contour of 9 [m].

Solution:
First it is necessary to find the water depth at which the incoming deep-water wave of 9 [m] will break. Entering H_0/gT^2= 0.00917 in Figure 6 and intersecting the curve for a slope of 1:10 (m= 0.1) results in H_b/H_0= 1.125. Therefore H_b= 1.125x9= 10.125 [m]. To determine the depth at breaking, we need to calculate H_b/gT^2= 0.0103 and enter Figure 7 at the intersection with m= 0.1. This leads to a factor d_b/H_b= 1.02 and the breaker depth becomes d_b= 1.02x10.125= 10.328 [m] (The factor d_b/H_b is the inverse of the breaker depth ratio γ_b).

The location of interest has a water depth of 9 [m]. Since the breaker depth is larger than the water depth at the location of interest, the incoming wave has already broken before it reaches the location of interest. For the determination of the significant wave height at the location of interest the breaker depth ratio γ_b is determined with Equation 9. In this way the local significant wave height becomes H_s= 9.163 [m].

The results of the translation of the significant deep-water wave heights into significant wave heights at various water depth contours, according to *Goda* are given Table 6.

Table 6: Results according to Goda

Deep-water wave height H_s [m]	Ray I (depth= 9 [m]) H_s [m]		Ray II (depth= 5 [m]) H_s [m]	
	T= 10 [sec]	T= 12 [sec]	T= 10 [sec]	T= 12 [sec]
6	6	6.384	5.740	6.034
7	7	7.448	5.740	6.034
7.5	7.5	7.98	5.740	6.034
8	9.163	9.936	5.740	6.034
8.5	9.163	9.936	5.740	6.034
9	9.163	9.936	5.740	6.034

Comparison of the results from ENDEC, Miche and Goda

The comparison of the results from *ENDEC,* Miche and *Goda* in fact boils down to a comparison of the contents of Table 4, Table 5 and Table 6. In Figure 8 the comparison is illustrated.
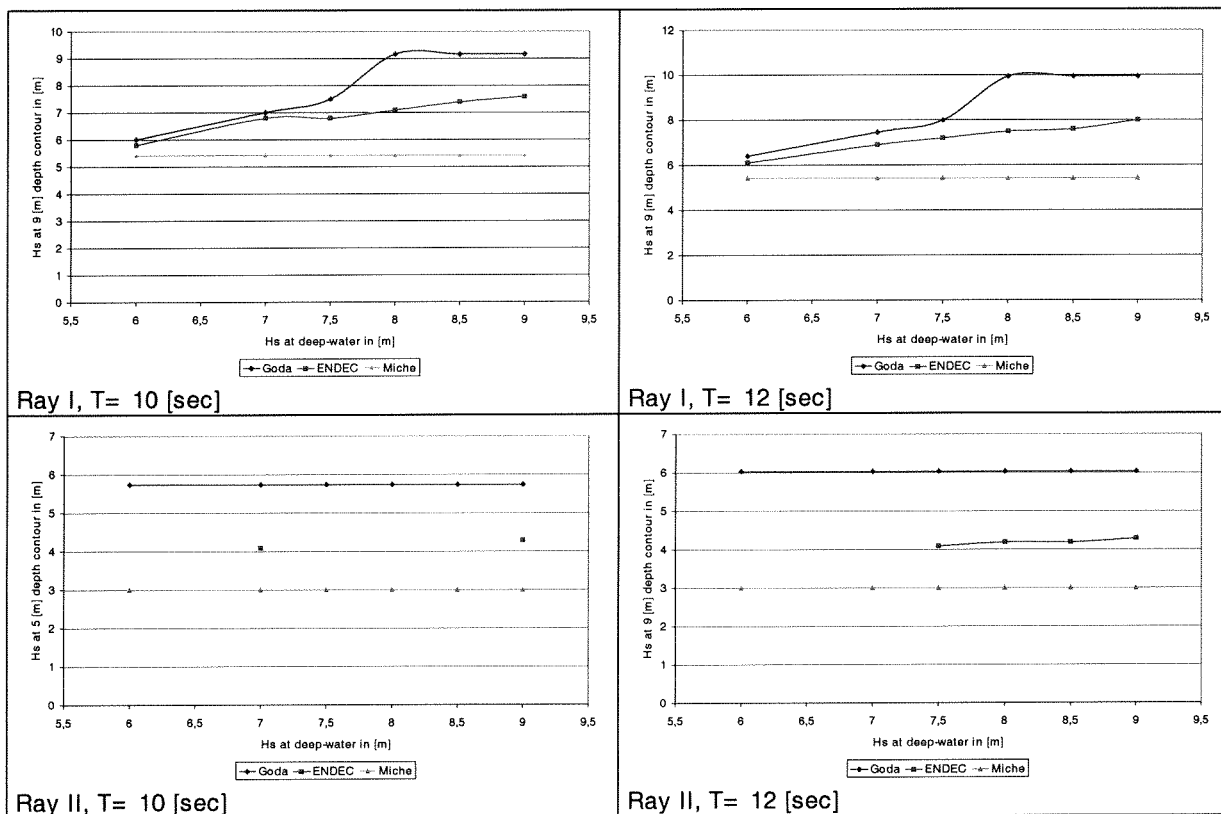
Figure 8: Results from ENDEC, Miche and Goda

Looking at Figure 8, the *ENDEC* computations fall inside the range between the results of *Miche* and *Goda*. However, the differences between the results of the different methods are quite large. *Miche* and *ENDEC* are based on theoretical relationships and valid in cases with gentle slopes. Therefore the behaviour of large waves on a relatively steep sloping shore is probably not presented very well in these relations. The restrictions of *ENDEC* are explained more extensively in the next Section. *Goda* is empirical and tested on a 1:10 slope (scale model). Therefore *Goda* is probably more suitable to estimate shallow wave conditions in the area of *Fort Bay* harbour.

Remarks on the use of ENDEC for locations with a steep sloping shore

Normally waves reduce their wave heights when they travel into a shallow area with decreasing water depth. This is due to the dissipation of wave energy, by wave breaking and bottom friction. However, when deep-water waves generated by hurricanes, with heights of for instance 10 to 12 [m] travel into a shallow area with rapidly decreasing water depth (like the area around *Fort Bay* harbour), they have not enough time to reduce their wave heights. As a result the waves then start to build up a surplus of wave energy, because the dissipation of wave energy can not keep up with the rapidly decreasing water depth.

The wave model *ENDEC* does not account for this phenomenon. *ENDEC* is based on an energy balance and the model assumes that the amount of wave energy at a certain water depth cannot exceed a directly to this water depth related upper limit (wave energy limit). To keep the wave energy below this limit, the model assumes that the dissipation of wave energy keeps up with the decrease of water depth. As a result *ENDEC* underestimates the wave conditions in such cases.

2.3.4. Description reconstruction design (1990)

The following adjustments were made to the harbour:

- Extension of the harbour with a fishery port, by creation of a second breakwater, the so called fishery breakwater (6);
- Use of *Accropodes* on the main breakwater (1) and the new fishery breakwater (6, 9);
- Use of rock penetrated with hydrocrete for the main breakwater head (3) and the new fishery breakwater head (8).

The layout of the reconstruction design is given in Figure 9 and views and cross-sections are available in Annex I; the main harbour structures are given in Table 7. The harbour structures in Table 7 have been assigned by numbers that can be looked up in Figure 9. The changes of the reconstruction design relative to the original design of 1972 are dashed. The applied design wave conditions (from *ENDEC* computations) are given in Table 8

Source: W+ B and CEC,Damage evaluation and restoration plan 2000 [Lit 10]
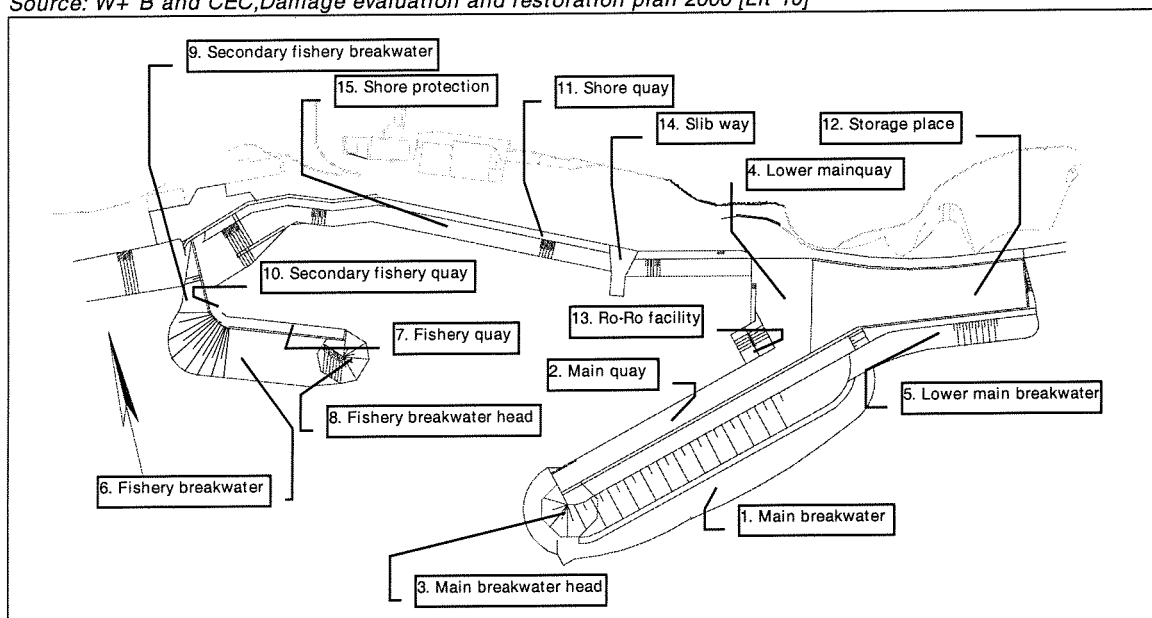
Figure 9: Layout reconstruction design (1990)

Table 7: Main harbour structures (1990)

Structure	Part	Construction material
Main breakwater (1)	Core	Rock 0-500 [kg]
	Secondary armour layer	Rock 500-2000 [kg]
	Primary armour layer	*Accropodes* 6, 9.6 and 15.12 [ton]
	Toe	Rock 6-10 [ton]
Main breakwater head (3)	Foundation	Bags filled with concrete
	Core	Rock 100 [kg]
	Primary armour layer	Rock 500-1000 [kg] penetrated with hydrocrete
Main quay (2, 4)	Foundation	Bags filled with concrete
	Upper structure	Concrete caissons
Fishery breakwater (6)	Core	Rock 500-1000 [kg]
	Primary armour layer	*Accropodes* 6 [ton]
	Toe	Rock 6000-10000 [kg]
Fishery breakwater head (8)	Foundation	Rock, but weights are not available
	Core	Rock 500-1000 [kg] penetrated with hydrocrete
	Primary armour layer	Rock 500-1000 [kg] penetrated with hydrocrete
Fishery quay (7)	Upper structure	Concrete caissons placed on rock
To be continued		

		Continued
Secondary fishery breakwater (9)	Core	Rock 500-1000 [kg]
	Primary armour layer	Rock 2000-5000 [kg]
	Toe	Rock ± 5000 [kg]
Secondary fishery quay (10)	Core	Rock 500-1000 [kg]
	Primary armour layer	Rock 1000-2000 [kg]
	Deck	Concrete road build on the core

Table 8: Applied design significant wave heights (1990)

Structure	H_s [m] (from *ENDEC*)
Main breakwater (1) (depth= 5m)	4-5
Main breakwater head (3) (depth= 9m)	7.5
Fishery breakwater (6) (depth= 7m)	4.5
Fishery breakwater head (8) (depth= 7m)	5
Secondary fishery breakwater (9) (depth= ± 5m)	4-4.5

Remarks on the applied design wave heights in Table 8

Design reports from CEC do not contain information regarding the deep-water wave height that has been used to derive the design wave heights in Table 8. However, looking to Table 4 (see Section 2.3.2) the applied design wave heights in Table 8 seem to originate from a deep-water wave height of approximately 9 [m]. Looking to Annex II the 9 [m] deep-water wave height has a corresponding return period of approximately 5 [years] (when looking to the line representing the hurricane hindcast). An explanation for using the 9 [m] deep-water wave height to derive the design wave heights for the harbour structures is not available for the present study.

Why extending the harbour with a fishery port?

According to the local authorities of *Saba* the need existed for extending the harbour facilities with a fishery port and for creating a more tranquil wave environment in the harbour basin (See the beginning of section 2.3). Both aims were reached simultaneously by constructing an additional breakwater.

Why using Accropodes? [Lit 1]

According to the computations with *ENDEC*, the wave conditions near the *Fort Bay* harbour can become severe, because according to Table 8, the main breakwater (1) has to deal with H_s = 4 to 5 [m] and the main breakwater head (3) with H_s = 7.5 [m]. As seen from the past, when rock was applied in the primarily armour layer of the main breakwater (1), damages did already occur to the breakwater during hurricane wave conditions. It is possible to use heavier rock and/or application of a less steep slope to increase the stability of the breakwater and to reduce damages, but two problems arise. First, the rock will probably be to heavy to handle by the available cranes. Secondly, resulting from the application of a less steep breakwater slope, much more rock material is needed to construct the breakwater, due to the steep fore shore of *Fort Bay* harbour.

A solution to these problems was found in the use of *Accropodes*, patented by the firm *SOGREAH*. A picture of an *Accropode* is given in Annex III. The advantage of *Accropodes* is their higher hook resistance relative to normal rock. Because of the higher hook resistance smaller and lighter *Accropode* units can be used relative to normal rock units. Another advantage of the higher hook resistance is the possibility of placing *Accropodes* on a steeper slope than could be possible with normal rock units. More information about *Accropodes* can be found in the *SOGREAH Accropode* information document [Lit 7].

When going from the main breakwater head (3) to the junction of the lower main breakwater (5), the depth besides the main breakwater reduces from ± 6 to ± 2 [m]. As a result also the design conditions (according to *ENDEC*) decrease from H_s= 5 [m] to H_s= 4 [m]. Therefore the primary armour

layer of the main breakwater (1) consists of three different kinds of *Accropodes*. The location of the *Accropodes* is given in Figure 10.
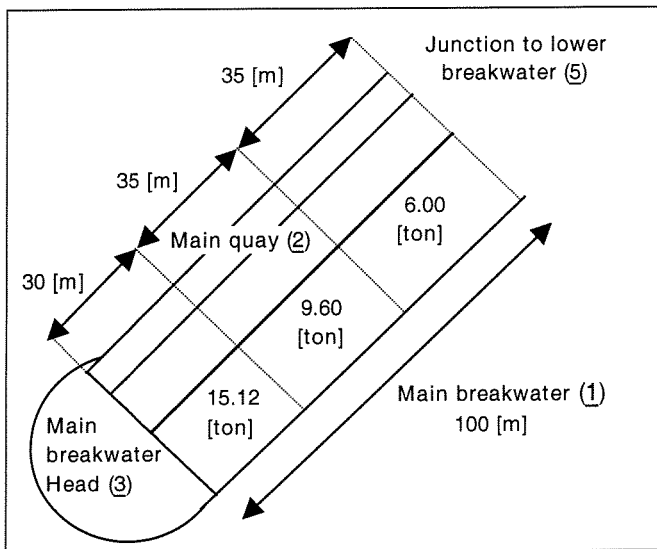
Figure 10: Location of the Accropodes on the main breakwater

Why using rock penetrated with hydrocrete for the breakwater heads? [Lit 1]
According to the computations with *ENDEC*, the design significant wave height near the main breakwater head (3) amounts to H_s= 7.5 [m]. Due to this large H_s, no *Accropode* units were used for the heads. The *Accropode* units would become too large and heavy and as a result too difficult to produce and handle. Instead rock penetrated with hydrocrete was used to construct the breakwater heads. In [Lit 1] this type of structure is called a monolithic structure. However, it is not sure that this kind of structure is really comparable with a monolithic structure, because it is not sure whether or not the penetration with hydrocrete results in a effective and durable bond between the armour units (rock). However, in the rest of the present study these kinds of structures still will be indicated as monolithic structures. See Annex I for more details of the applied breakwater heads.

2.3.5. Stability of reconstruction design (1990)
In this section the reconstruction design of 1990 will be evaluated against the most common breakwater design principles (*Hudson* and *Van der Meer*). These design principles are taken from the *CUR 169* [Lit 12]. Only the stability of the structures with *Accropodes* will be evaluated. An evaluation of the stability of the structures consisting of rock penetrated with hydrocrete has not been carried out. The structural characteristics of these structures are difficult to estimate., because the degree of bound between the rock units and the hydrocrete is not known well enough.

Coastal structures, exposed to direct wave attack, can be classified by the use of the stability number N_s, see Equation 11.

$$N_s = H_s/\Delta D_{n50}$$
<div align="right">Equation 11</div>

Δ = Mass density of armour relative to that of water [-]
D_{n50} = Median diameter of armour unit [m]

Small values of N_s represent structures as caissons or structures with large armour units. Large values correspond to gravel beaches and sand beaches.

Hudson
A widely used formula to determine the size of armour units is the formula of *Hudson* (1953) [Lit 12].
The *Hudson* formula is given in Equation 12.

$$\frac{H_s}{\Delta D_{n50}} = \sqrt[3]{K_D \cot \alpha}$$

Equation 12

K_D = Stability coefficient

K_D values suggested for design correspond to a "no damage" condition (up to 5% of the armour units may be displaced).

The *Hudson* formula has many limitations, they are briefly listed hereafter.
- The formula has been derived from physical model tests with regular waves only. Neither the potential scale effects nor the impact of non-regular waves on the validity of the formula have been evaluated to their full extend;
- The formula gives no description of the damage level;
- The formula has only been tested with non-overtopped and permeable core structures.

According to the general information document of *Accropodes* [Lit 7], the firm *SOGREAH* uses the formula of *Hudson* to determine *Accropode* sizes and weights. In that case the stability coefficient of *Accropode* elements on a 3:4 or a 2:3 (= 1:1.5) slope is $K_D \cong 12$ for breaking waves and $K_D \cong 15$ for non-breaking waves.

Van der Meer
For rocky armour units the *Van der Meer* (1988) [Lit 12] equations are a step forward compared to *Hudson*, because more parameters are included. The *Hudson* formula is only related to the slope angle $\cot\alpha$ of the structure. Apart from the slope angle, the *Van der Meer* formulae takes also into account the wave period (or wave steepness), the permeability of the structure and the storm duration. However, for artificial armour units the standard formulae of *Van der Meer* are not valid. Instead, *Van der Meer* performed a limited number of tests with artificial units. Analysis of the tests have resulted in indicative curves for "no damage" and "failure" for artificial armour units, see Figure 11.
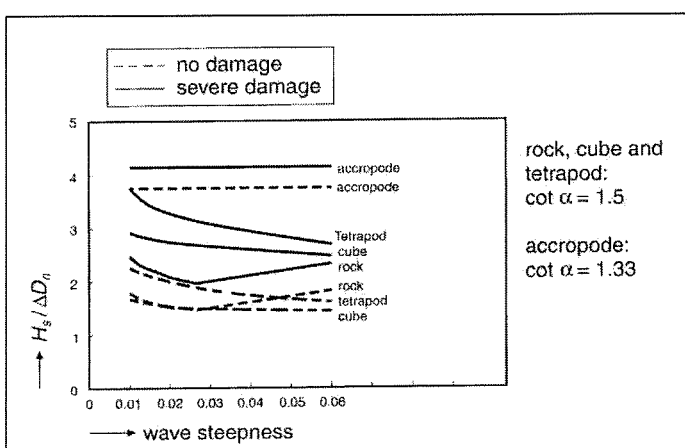
Figure 11:

Looking at Figure 11 the stability number for "no damage" for Accropodes is 3.7.

Hereafter the stability of the *Accropode* revetments will be analysed, according to *Hudson* and *Van der Meer*.

Stability main breakwater (1)

The characteristics of the main breakwater (1) are:

α = 1:1.5 = 33.7 [°]

Δ = 2400/1030-1= 1.33

The stability status of the *Accropodes* on the main breakwater is given in Table 9.

Table 9: Stability of Accropodes on main breakwater

Accropode [ton]	From *ENDEC* H_s [m]	D_{n50} [m]	Hudson			Van der Meer		Status
			K_D	$H_s/\Delta D_{n50}$	Stable till H_s [m]	$H_s/\Delta D_{n50}$	Stable till H_s [m]	
6	4	1.37	12	2.62	4.77	3.7	6.74	Stable
			15	2.82	5.14			Stable
9.6	4.5	1.59	12	2.62	5.54	3.7	7.82	Stable
			15	2.82	5.96			Stable
15.12	5	1.86	12	2.62	6.48	3.7	9.15	Stable
			15	2.82	6.98			Stable

Stability main breakwater head (3) and fishery breakwater head (8)

The available reports from *CEC* do not give any theory of the derivation of the monolithic head structures. Today there are also no commonly used rules for breakwater head design available. According to *Jensen* [Lit 12] a general procedure in the design of heads is to increase the weight of the armour used for the head relatively to the armour used for the trunk section of the breakwater. The required increase is a factor between 1 and 4, depending on the type of armour unit.

In the case of the breakwater heads, the increase of weight is achieved by penetrating the primary armour layer with hydrocrete. However, it is not sure that this kind of structure really provides in the necessarily increase of the weight, because it is not sure whether or not the penetration with hydrocrete results in a effective and durable bond between the armour units (rock).

A probable check of the stability of the breakwater heads could consist of an investigation showing whether the heads could be moved due to wave forces. Another part of such an investigation could consist of taking a closer look at the possibility of the building up of high water pressures, due to the wave attack and impermeability of the heads. However, as mentioned at the beginning of this Section, these stability checks will not be carried out in the present study, instead they need to be investigated in a further study.

Stability fishery breakwater (6)

The characteristics of the fishery breakwater are:

α = 1:2 = 26.6 [°]

Δ = 2400/1030-1= 1.33

The stability status of the *Accropodes* from the fishery breakwater (6) is given in Table 10.

Table 10: Stability status of Accropodes on fishery breakwater

Accropode [ton]	From *ENDEC* H_s [m]	D_{n50} [m]	Hudson			Van der Meer		Status
			K_D	$H_s/\Delta D_{n50}$	Stable till H_s [m]	$H_s/\Delta D_{n50}$	Stable till H_s [m]	
6	4.5	1.37	12	2.62	4.77	3.7	6.74	Stable
			15	2.82	5.14			Stable

2.4. Fort Bay harbour: Present-day design made by CEC (1995)

The present-day design is not a completely new design. In fact only relatively small adjustments were made to the harbour design of 1990. The adjustments were necessary, because hurricanes had caused damages to the revetments of both breakwaters. The applied adjustments and the reported damages are presented in this Section. Finally this Section ends with the present status (year 2000) of the harbour structures.

2.4.1. Inspection of harbour status (1995)

The reconstructed harbour (1990) remained in good shape until 1995. In 1995 hurricanes *Luis* and *Marilyn* passed by and caused severe damage to the harbour structures. In order to mark the damages, a harbour inspection was carried out. In Table 11 the inspection results are listed.

Table 11: Inspection results (1995), after hurricane Luis and Marilyn

Structure	Damage
Main breakwater (1)	Some *Accropodes* have moved up, resulting in a steeper slope. Further no big damages were reported.
Main breakwater head (3)	The monolithic head is damaged and dislocated. During the hurricane an amount of rock units under the monolithic head were removed. Because of this the head has subsided and moved towards the harbour basin.
Fishery breakwater (6)	The monolithic fishery breakwater head (8) is intact. The 6 [ton] *Accropodes* have vanished completely. The *Accropodes* are relocated to some 25-30 meters in front of the fishery breakwater (6).
Secondary fishery (9) breakwater and secondary fishery quay (10)	The concrete deck of the secondary fishery quay (10) has subsided, due to severe settlements of the rock where the deck was placed on.

Source: CEC inspection report 1995 [Lit 4]

Considerations based on inspection report (1995) [Lit 4]

- Factors that could have caused the damage are:
  - the exceptional long duration of hurricane *Luis* (almost two days);
  - the short period between hurricane *Marilyn* and hurricane *Luis* (no time for short-term recoveries);
- Transitions between construction parts need special care. Especially *Accropodes* are sensitive for transition problems. Looking to a transition from rock to *Accropodes*, the loss of some rock near the transition can create instability of the nearest *Accropodes*. When these *Accropodes* disappear a chain reaction is initiated which results in the disappearing of much more *Accropodes*. See Figure 12.
- Penetration of rock with hydrocrete was intended to increase the strength of the breakwater head. However, dealing with wave forces, the use of concrete in the armour layers results in an impervious and a smoothened breakwater head, leading to high water pressures below the armour layers and more wave overtopping.
- The toe needs special care; when the foundation of the toe is not good enough, sliding of the *Accropode* revetment may occur for both breakwaters.

Fort Bay harbour, Saba. A study on hurricane conditions

20
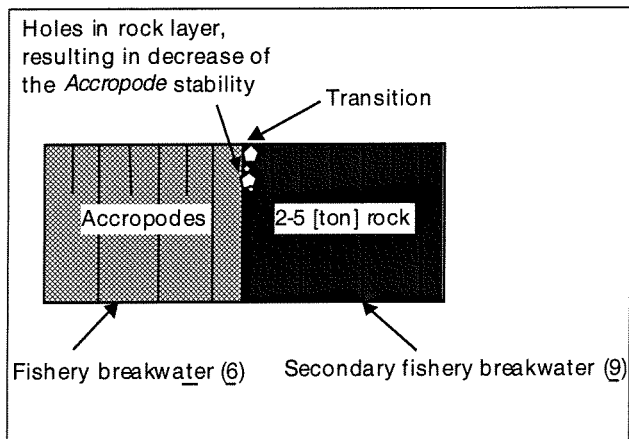
Figure 12: Transition problem

2.4.2. Repair works (1995)

After the inspection carried out in 1995, repair works started under supervision of *CEC*. The repair works are described hereafter.

Repair works to the main breakwater head (3):
- Reconstruction of the monolithic head;
- Recovery of the concrete damage at the caisson next to the break water head.

Repair works of the fishery breakwater (6):

Without any explanation the design significant wave height of the fishery breakwater (6) is increased from 4.5 to 6 [m]. Probably *Accropodes* would become too heavy and too difficult to handle when adapted to the H_s= 6 [m]. Therefore the same monolithic principle is used for the fishery breakwater as has been used earlier for both breakwater heads. The revetment of the fishery breakwater is penetrated with concrete and the revetment is closed up by a toe, consisting of concrete boulders. All together this was supposed to form a monolithic construction. Figure 13 shows a cross-section of the toe. The main harbour structures are listed in Table 12. The changes of the harbour design relative to the reconstruction design from 1990 are dashed.

Source: W+ B and CEC restoration paper (2000) [Lit 10]
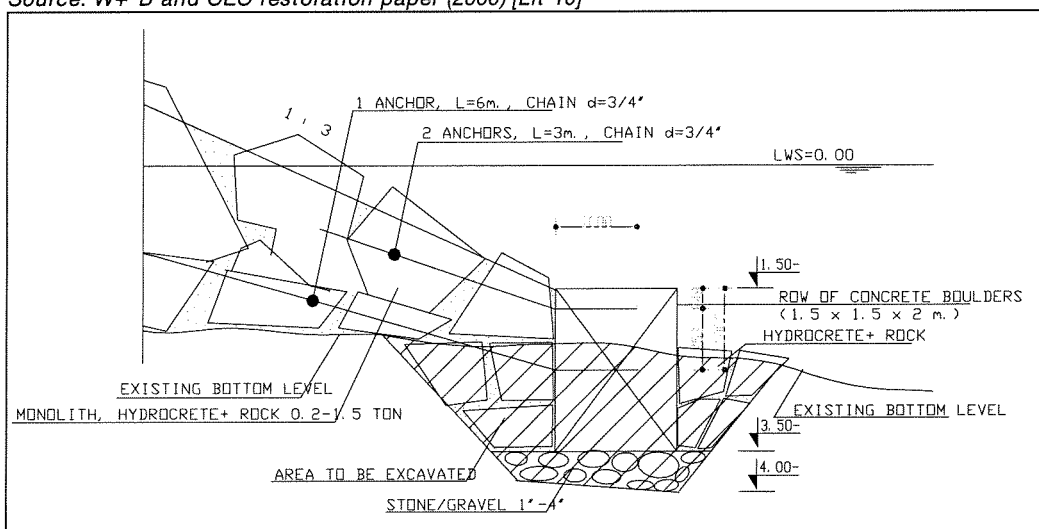
Figure 13: Cross-section of fishery breakwater after repair works (1995)

Table 12: Main harbour structures (1996)

Structure	Part	Construction material
Main breakwater (1)	Core	Rock 0-500 [kg]
	Secondary armour Layer	Rock 500-2000 [kg]
	Primary armour layer	*Accropodes* 6, 9.6 and 15.12 [ton]
	Toe	Rock 6-10 [ton]
Main breakwater head (3)	Foundation	Bags filled with concrete
	Core	Rock 500-1000 [kg]
	Primary armour layer	Rock 500-1000 [kg] penetrated with hydrocrete
Main quay (2, 4)	Foundation	Bags filled with concrete
	Upper structure	Concrete caissons
Fishery breakwater (6)	Core	Rock 200-1500 [kg] penetrated with hydrocrete
	Primary armour layer	Rock 200-1500 [kg] penetrated with hydrocrete
	Toe	Concrete boulders (1.5x1.5x2 [m])
Fishery breakwater head (8)	Foundation	Rock, but weights are not available
	Core	Rock 500-1000 [kg] penetrated with hydrocrete
	Primary armour layer	Rock 500-1000 [kg] penetrated with hydrocrete
Fishery quay (7)	Upper structure	Concrete caissons placed on rock
Secondary fishery breakwater (9)	Core	Rock 500-1000 [kg]
	Primary armour layer	Rock 2000-5000 [kg]
	Toe	Rock ± 5000 [kg]
Secondary fishery quay (10)	Core	Rock 500-1000 [kg]
	Primary armour layer	Rock 1000-2000 [kg]
	Deck	Concrete road build on the core

2.4.3. Inspection of harbour status (2000)

A few years after the repair works carried out in 1995, hurricane *George* passed by in 1998. Hurricane *Georges* caused minor damage to the harbour. The damage was concentrated at a few spots of the fishery breakwater. *CEC* recommended some repair works, but those were not carried out because of lack of funds. However, in 1999 hurricane *Lenny* caused major damage to the harbour. The damage of hurricane *Lenny* is presented in Table 13. An aerial view of the harbour status after hurricane *Lenny* is already given in Figure 1 (See Chapter 1). A closer look to the damages is presented in Figure 14 and Figure 15.

Table 13: Reported damages after hurricane Lenny (2000)

Structure	Damage
Main breakwater head (3)	Head is displaced with 15 [m] to the inside of the harbour basin;
Main quay (2)	Hardly any damage, one hole detected, but most probably not caused by hurricane *Lenny*;
Fishery breakwater (6)	Severe damage; all concrete blocks have been removed, only the anchoring of the blocks is present; the rock and hydrocrete cracked severely;
Fishery breakwater head (8)	Not damaged;
Secondary fishery quay (10)	Hardly any damage under water; some displacement detected, most probably caused during original construction; hole detected in corner, occurred already after hurricane *George*;
Shore protection (15)	Many stones slid down the slope into the harbour basin; a lot of debris in front of the slope;
Lower main breakwater (5)	Sedimentation with pebbles up to above the water level;
Ro-Ro quay (13)	No damage detected;
Slip way (14)	Slabs are displaced, but recoverable;
Harbour basin	Decreased water depth by rock and debris;

Source: W+ B and CEC restoration papers (2000) [Lit 9] and [Lit 10]

Fort Bay harbour, Saba. A study on hurricane conditions

22

Source: W+ B and CEC restoration paper (2000) [Lit 10]
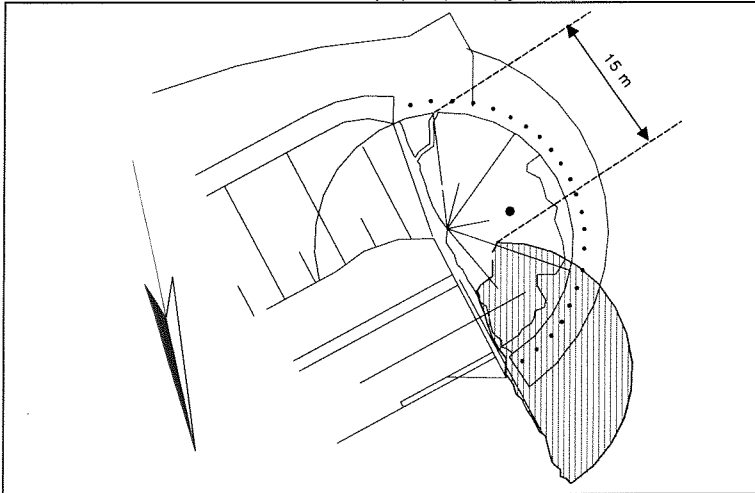
Figure 14: Displacement of main breakwater head

Source: W+ B

A: Fishery port

B: Hole in the armour layer of the fishery breakwater

C: Damaged fishery quay

D: Main quay and heavily damaged main breakwater

Figure 15: Several views of Fort Bay harbour after hurricane Lenny

3. STUDY OBJECTIVES

3.1. Problem definition

According to the stability analysis as given in Section 2.3.5, theoretically the breakwaters protected by *Accropodes* should stay stable during wave conditions generated by hurricanes. Although the stability of the monolithic structures (breakwater heads (3 and 8) and fishery breakwater (6)) has not been evaluated in the present study, *CEC* apparently had enough reason to assume stability of these structures during hurricane wave conditions as well. However, looking to the damages that have been reported by several harbour inspections, both the *Accropodes* and the monolithic structures were not stable during wave conditions generated by some of the hurricanes that hit the area.

For the *Fort Bay* harbour, hurricane wave conditions belong to the extreme load class. The status of the harbour just before failure and caused by these extreme conditions is defined as the *Ultimate Limit State* (*ULS*). Therefore to find an explanation for the instabilities (damages) of the harbour structures, it is necessary to take a closer look to the *ULS* of *Fort Bay* harbour. In this case failure of the harbour means permanent damage to one of the two breakwaters of *Fort Bay* harbour. Failure is the result of a failure mechanism, containing all the events necessary for a construction to fail.

The function describing an *ULS* is called a reliability function. The common shape of a reliability function is given in Equation 13. If Z<0, a structure will fail according to the considered failure mechanism.

$$Z = R - S \hspace{4cm} \text{Equation 13}$$

where:

R = Resistance against failure (<u>R</u>ésistance)

S = Load (<u>S</u>ollicitation)

It is possible to formulate a reliability function of the same type for *Fort Bay* harbour as well. The components of the reliability function are then formulated as:

R = The design wave conditions of the two breakwaters of *Fort Bay* harbour.

S = The wave conditions appearing near the two breakwaters of *Fort Bay* harbour;

In other words, whether or not the structure fails depends in this approach on the relation to one another of the actual (or appearing) and the design wave conditions. This leads to the following two basic questions (also corresponding with the first objective in Chapter 1):

- <u>Basic question 1</u>: Is it possible that wave conditions (near the two breakwaters), generated by hurricanes (S), have become more extreme during the existence of *Fort Bay* harbour?
- <u>Basic question 2</u>: Is it possible that the resistance of the two breakwaters (R) was lower than could be expected?

3.2. Research questions

The research necessary to find an answer on the aforementioned basic questions can be detailed further into research questions. They are given in the following Sections.

3.2.1. Research questions regarding the first basic question (S)

Regarding basic question 1, it is possible to formulate three research questions. The questions are accompanied with an explanation why the questions could be formulated.

1. Have deep-water wave conditions (in the area of *Fort Bay* harbour), generated by hurricanes, become more extreme during the existence of *Fort Bay* harbour (1972-2000)?

    - It seems that after 1994 the harbour is suddenly hit by several strong hurricanes. In the period from 1995 till 2000 even four major hurricanes stroke the harbour (*Luis* and *Marilyn* (1995), *George* (1998) and *Lenny* (1999)).
    - In contrast to the period from 1994 till 2000, no severe damages to the harbour structures were reported in the period from 1972 till 1994. The only reported damages consisted of recurrent loss of armour material from the main breakwater (1) (Rock). However, the amounts of loss of armour material were not alarming.
    - The design wave conditions, used for the reconstruction design (1990), were derived from a wave climate study for the breakwater at the *Oranje Bay* at *St. Eustatius*. The study is carried out by *WL| Delft Hydraulics* in 1988 [Lit 11] and partly based on a hindcast of hurricanes (from *Oceanroutes Inc.*) that have materialised the area in the period from 1900 till 1986. However, after 1994 the reconstructed harbour (design 1990), suffered severe damage to its two breakwaters. It is therefore imaginable that the wave climate study is not representative for the period after 1986.

2. What changes do the deep-water waves experience while propagating towards *Fort Bay* harbour?

    The *ENDEC* wave model has been used to translate deep-water wave conditions to shallow water near the *Fort Bay* harbour. As described in Section 2.3.3, the slope of the shore near *Fort Bay* harbour is very steep (order 1:10) and there is reason to distrust the computations of *ENDEC* since *ENDEC* is known to underestimate wave heights when the model is used in areas with such steep sloping shores.

3. What are the effects on the near shore wave conditions by taking water level variations into account?

    Looking for instance to the wave height at shallow water, the influence of the bottom on the wave height is strongly dependent on the available water depth. The larger the water depth, the less the influence and therefore the larger the possible wave height.

    Phenomena that cause water level variations are:
    3a) Storm surge (z_a)
    3b) Wind set-up
    3c) Wave set-up

Fort Bay harbour, Saba. A study on hurricane conditions

25

Ad 3a: Storm surge (z_a)
Local minima of atmospheric pressures cause a corresponding rise of mean water level. Mean air pressures at sea level are 1013 [mbar] approximately. In tropical storms, like hurricanes, storm pressures may drop to for example 900 [mbar]. From *CUR* Report 169 [Lit 12], the height of the corresponding static rise of the mean water level (z_a in [m]) is as given in Equation 14. Due to dynamic effects however, the rise in water level can be amplified significantly. The coefficient 0.01 in Equation 14 has the dimension of [m/mbar].

$$z_a = 0.01(1013 - P_a) \hspace{5cm} \text{Equation 14}$$

P_a = Atmospheric mean pressure at sea level [mbar]

Ad 3b: Wind set-up
According to [Lit 12] wind set-up is the result of a wind induced gradient (i_w), see Equation 15.

$$i_w = \frac{c_w(\rho_a / \rho_w)U^2}{gd} \hspace{4cm} \text{Equation 15}$$

U = Wind speed [m/s]
d = Water depth [m]
ρ_w, ρ_a = Mass density of sea water and air (1030, 1.21 [kg/m^3])
c_w = Air/water friction coefficient ($0.8.10^{-3}$ to $3.0.10^{-3}$)

According to Equation 15 the wind set-up is most pronounced along relatively shallow waters (small water depths (d)). In the case of *Fort Bay* harbour, the foreshore (with a slope of 1:10) reaches large depths (hundreds of meters) within a short distance. As a result the relatively shallow water area is small. Therefore wind set-up does almost not occur. Furthermore the coast of the island of *Saba* is relatively short and cannot maintain this kind of water level variations. Due to these reasons a further study to this research question is probably not necessary.

Ad 3c: Wave set-up
Wave set-up is caused by energy dissipation due to shoaling of the incoming waves and occurs in the breaker zone. According to [Lit 12], the magnitude of the wave set-up at the shoreline is given by Equation 16.

$$\eta_{max} = 0.3\gamma_{br}H_b \hspace{5cm} \text{Equation 16}$$

Due to again the relative short coast of the island of *Saba*, this kind of water level variation will not become significant.

3.2.2. Research questions regarding the second basic question (R)

Regarding basic question 2, it is possible to formulate two research questions. The questions are again accompanied with an explanation why the questions could be formulated.

4. Is it possible to formulate mechanisms or phenomena that could have been responsible for the damage to the revetments consisting of *Accropode* elements, given the applied design wave conditions?

   According to the considerations of a harbour inspection carried out in 1995 (described in Section 2.4.1), problems with the transitions between the *Accropodes* and other construction parts as well as problems with the foundation of the toes of both breakwaters, could have played a role in the damages. These are only two problems that could have initiated damage to the *Accropode* revetments. It may be possible to identify other problems that could have been responsible for the *Accropode* instability. To evaluate the *Accropode* stability it is necessary to get a complete picture of these problems.

5. Is it possible to formulate mechanisms or phenomena that could have been responsible for the damage to the revetments consisting of rock penetrated with hydrocrete, given the applied design wave conditions.

   According to the same harbour inspection of 1995, an element that could have played a role in the problems with the stability of the monolithic structures, is the building up of high water pressures below the layers consisting of rock penetrated with hydrocrete. As a result extra uplift forces could have been introduced into the structures, during severe wave attack. To evaluate the stability of the monolithic structures it is also necessary to get a complete picture of these problems.

3.2.3. Description of the contents of part 2

In the second part of the present study the first research question, regarding the potential worsening of deep-water wave conditions during hurricanes in the area of *Fort Bay*, will be analysed. This is done by conducting a new hurricane hindcast study.

The basis of that study is formed by a hindcast of hurricane wave conditions for the years between 1972 and 2000 (age of the harbour). This hindcast is carried out with the mathematical physical wave model *DOLPHIN-B1*. First, the principles and schematisations as used in *DOLPHIN-B1* are described. Secondly, it is made clear how from the results of this hindcast changes in both wave heights and wave directions during hurricanes can be identified. This ability is based on the results of a comparison between the *DOLPHIN-B1* computations and other registrations of hurricane wave conditions.

To determine a potential worsening of the deep-water wave conditions, each hindcasted hurricane is characterised by two wave parameters, viz. the maximum significant wave height ($H_{s,max}$) and the corresponding direction of wave propagation (θ) as computed by *DOLPHIN-B1*. Furthermore, the hurricanes selected for the hindcast have occurred between 1972 and 2000 (age of the harbour) and have neared *Fort Bay* harbour to a distance less than 1000 [km] (hurricanes at a greater distance appeared not to generate appreciable waves). Whether or not the wave conditions have worsened significantly has been analysed statistically by the comparison of the values of $H_{s,max}$ and θ before 1986 and after 1986 (the year 1986 has been used as a turning point, because the damages seem to concentrate after this year). Finally in Chapter 7 it is illustrated what a possible worsening of the deep-water wave conditions means for the design conditions of the two breakwaters at *Fort Bay* harbour.

Part 2

Study of the first research question

4. WAVE MODEL SET-UP

4.1. Approach

In a hindcast study, wave conditions are reconstructed from known hurricane tracks and intensities with the use of a physical-mathematical wave model. In the present study the wave model *DOLPHIN-B1* (See [Lit 6]) will be used to perform the hindcast study. The available hurricane information, a description of the theories and schematisations used in *DOLPHIN-B1* and the preparation of the *DOLPHIN-B1* input files, are described in this Chapter.

4.2. Available hurricane information

4.2.1. Format of hurricane information

Hurricane track information of the *Atlantic* basin is available through the databases of *Unisys* [Lit 24]. The *Unisys* hurricane information is available concerning the area (See Figure 16):
- Longitude: 12.5° W till 105° W
- Latitude: 0° N till 60° N.

An example of the format of the hurricane information from the *Unisys* databases is given in Table 14. Based on the maximum sustained wind speeds ($U_{g,max,sust}$) hurricanes generate, they are classified according to the *Saffir-Simpson* scale. The maximum sustained wind speed is equal to the 1-minute maximum surface wind speed at a height of 10 [m] above mean sea level. The *Saffir-Simpson* scale begins for wind speeds exceeding force 12 on the *Beaufort* scale. An explanation of the *Saffir-Simpson* scale is given in Annex IV.
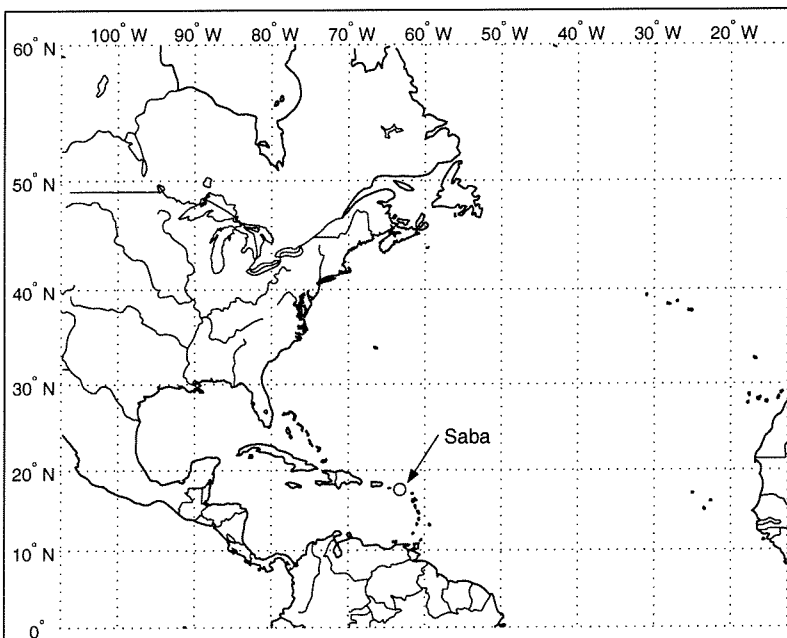
Figure 16: Hurricane track area (*Atlantic* basin)

Table 14: Example of the format of the hurricane information from Unisys

Latitude [°]	Longitude [°]	Time [month/day/time]	Max. sustained wind speed [knts]	Pressure [mbar]	Status [*Saffir-Simpson* scale]
15.40	-53.50	09/19/18Z	125	949	HURRICANE-4
15.70	-54.90	09/20/00Z	130	939	HURRICANE-4
Etc.	Etc.	Etc.	Etc.	Etc.	Etc.

Source: Unisys database [Lit 24]

4.2.2. Restrictions of hurricane information

The *Unisys* databases of hurricane tracks are directly linked with databases of the American *National Hurricane Center* (*NHC*). The *NHC* is a subdivision of the American *National Oceanic and Atmospheric Administration* (*NOAA*). The *NOAA* has published a paper [Lit 22] on their Internet site that deals with a recent revision of the existing hurricane track information, based on new insights into hurricane phenomena. According to this paper the databases of hurricane tracks of the *NHC* are not complete. Mainly in the period 1900 till 1985 some hurricanes that stayed out at sea for their duration and also were not encountered by ships, are not archived for this time period. The *NOAA* estimates the number of "missed" hurricanes for the period between 1900 and 1985 in the order of 0 to 6 per year. Therefore the *Atlantic* basin database of hurricane records should not be considered as complete for either the frequency or intensity of hurricanes for the years between 1900 and 1985. Nevertheless, this database has been used in the present study, because alternative sources of information could not be searched and accessed.

4.3. Wave model DOLPHIN-B1

4.3.1. Overall description *DOLPHIN-B1*

DOLPHIN-B1 [Lit 6] is a physical-mathematical model to estimate the two-dimensional wave spectrum at a number of locations and times in arbitrary wind fields over the ocean. *DOLPHIN-B1* can both deal with defined coastlines as well as with a depth grid at the same time. Wave propagation in the model is achieved with a tracing technique along rays radiating from the prediction location (or in this study, hindcast location). The generation and dissipation of each spectral component is obtained by using the analytical solution of linear and exponential growth or exponential decay per time step. For completeness it must be noted that the model does not account for refraction of the waves. For a further description of the theory behind *DOLPHIN-B1*, see Annex V.

The wave parameters computed in *DOLPHIN-B1* and which are available as output of the model, are the following:
- The two-dimensional spectrum (variance density as function of frequency and direction);
- The one-dimensional spectrum (variance density as function of frequency);
- The mean wave direction as a function of frequency;
- The directional spreading as a function of frequency;
- The significant wave height (H_s), the mean frequency (f_m), the peak frequency (f_p), the overall mean wave direction (θ), and the overall directional spreading.

4.3.2. Wind field used in DOLPHIN-B1

Wind field

A special feature of *DOLPHIN-B1* is the *CYCLONE* tool. This tool creates a wind field in the form of a hurricane defined by the following set of parameters:

X(t)	=	X-co-ordinate (longitude) of the center of the hurricane
Y(t)	=	Y-co-ordinate (latitude) of the center of the hurricane
P_{diff}(t)	=	Pressure difference between infinity and the center of the hurricane
R(t)	=	Radius of the hurricane eye
t	=	Time

The location parameters are explained in Figure 17.
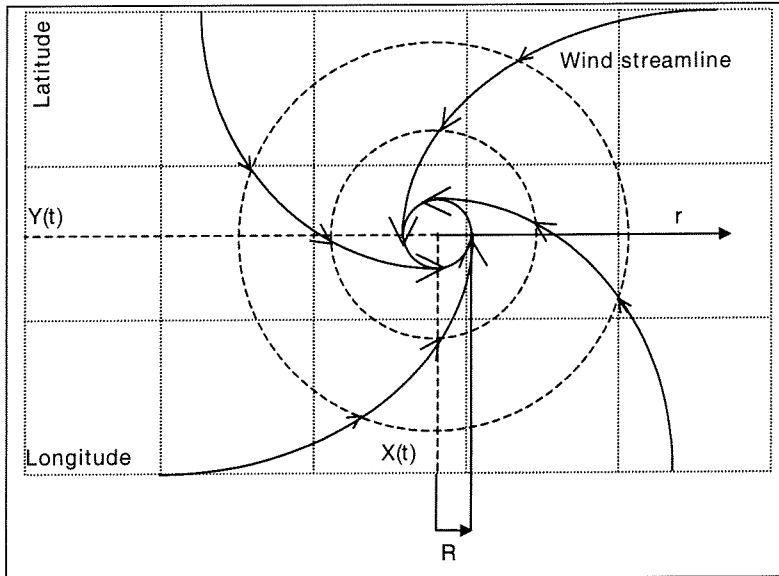
Figure 17: Explanation of CYCLONE parameters

Based on the model of *Myers* (1954) (mathematically described by *Harris* (1958), see the *Shore Protection Manual* (*SPM*) [Lit 18], page 3-56) and the input parameters, the *CYCLONE* tool computes a theoretical hurricane wind field. The model of *Myers* consists of an expression for the pressure difference between the center of a hurricane with infinity (Equation 17 and Equation 18) and an expression for the pressure-wind relation (Equation 19).

$$P_{diff} = P_{inf} - P_{eye}$$

Equation 17

$$P = P_{eye} + P_{diff} \exp(-R/r)$$

Equation 18

$$\frac{dP}{dr} = \rho_a \left(\frac{1}{r} U_g^2 + f_{cor} U_g \right)$$

Equation 19

P   = Pressure of an arbitrary point where one wants to know the pressure
P_{eye} = Pressure in the center of the hurricane
P_{inf} = Environmental pressure at the outer limit of a hurricane where the cyclonic circulation ends
r   = Radius from the center of the hurricane to an arbitrary point where one wants to know the wind velocity
ρ_a = Mass density of air
U_g = Gradient wind speed at an elevation of 10 [m] above mean sea level
f_{cor} = *Coriolis* parameter

In Equation 19, the wind speed is called the gradient wind speed U_g, because the wind does exist due to the resulting centripetal force of an existing pressure gradient and the *Coriolis* effect.

An example of the theoretical pressure profile based on Equation 12 is presented in Figure 18.
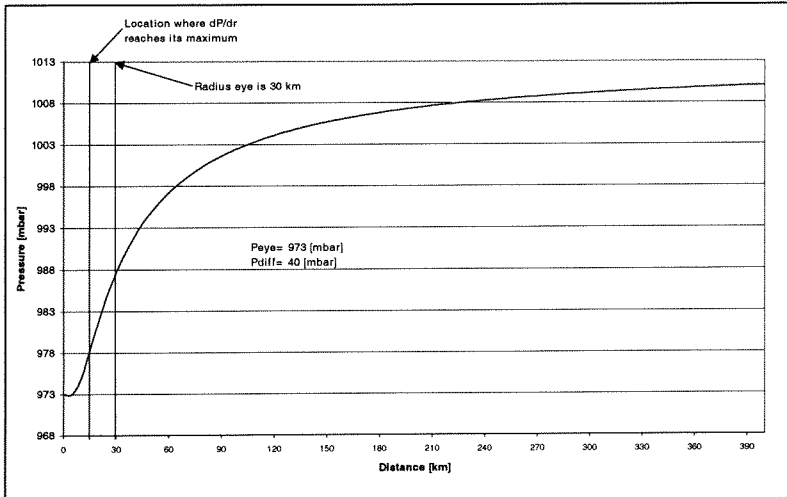
Figure 18: Example of pressure profile from hurricane center to infinity

It must be kept in mind that the wind speed $U_{g,max,sust}$ (maximum sustained wind speed, from Section 4.1) and $U_{g,max}$ (maximum gradient wind speed) are not the same. $U_{g,max,sust}$ represents a peak value of the gust of wind , while $U_{g,max}$ represents an averaged value of the peak gusts of wind.

The distance from the hurricane centre to locations with $U_{g,max}$ is called the radius to maximum wind speed. The distance coincides with the radius of the hurricane eye, because according to information from the *NHC* [Lit 22] the strongest winds during a hurricane are produced at the outskirts of the eye (eye wall). Therefore the radius to maximum wind speed as well as the radius of the hurricane eye are assumed to be equal and indicated by the same parameter (R).

Substituting Equation 18 into Equation 19, results in two expressions for the gradient wind speed (U_g) Only the expression resulting in positive values for U_g is relevant and is given in Equation 20. An example of the profile of U_g based on Equation 20 is given in Figure 19.

$$U_g = -0.5r\left(f_{cor} - \sqrt{f_{cor}^2 + \frac{4RP_{diff}}{\rho_a r^3}\exp(-R/r)}\right)$$

Equation 20
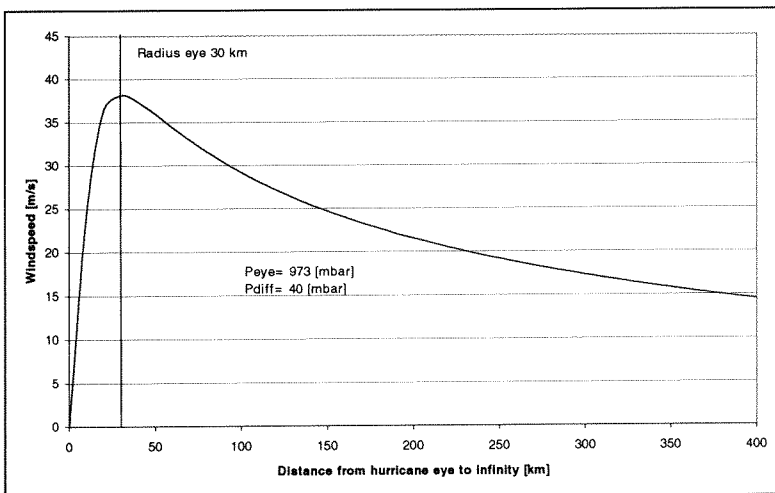
Figure 19: Example of wind speed profile from hurricane center to infinity

One probably should expect that at the location where dP/dr reaches its maximum also the maximum wind speed ($U_{g,max}$) is found. However, looking to see Figure 18 and Figure 19 these locations do not coincide. The maximum dP/dr is found at r= 0.5 x R and $U_{g,max}$ is found at r= R.

4.3.3. Restrictions DOLPHIN-B1

- The model of *Myers* and *Harris* (See Equation 18 and Equation 19) is partly empirical, but according to the *SPM* [Lit 18] it has been used extensively and provides reasonable agreement with observations in many storms. However, the use of the pressure-wind relationships to estimate winds in hurricanes does not account for translational speed of the hurricane itself. In general for hurricanes acting on the Northern Hemisphere, the translational speed is an additive factor on the right side of the storm and a negative factor on the left, when facing to the direction the hurricane is moving. For example, a hurricane moving westwards at 10 [knts] with maximum wind speeds of 90 [knts] on the west and east sides would have approximately wind speeds of 100 [knts] on the north side and 80 [knts] on the south side, see Figure 20.
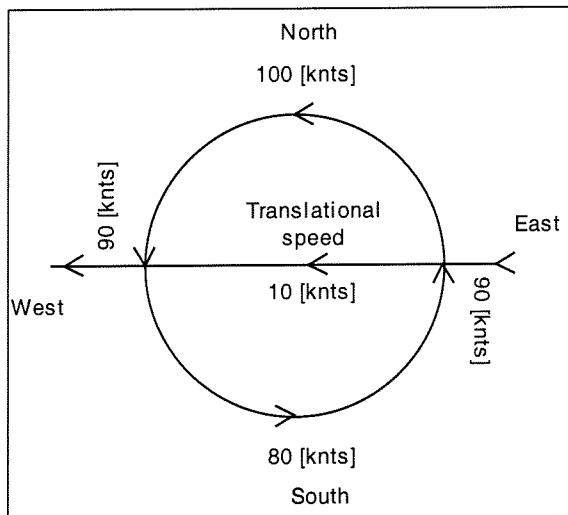
Figure 20: Effects of translational speed on the hurricane wind speeds

The asymmetry of the wind field, due to translational speed of the hurricane itself, has also effects on the wave field that such a wind field creates. The wave field has an even greater degree of asymmetry than the wind field due to the combined influence of the asymmetry of the wind field and the extended fetch, which exists within a translating hurricane. The wind vector in the intense wind region (to the North of the storm centre in Figure 20) is approximately aligned with the direction of forward propagation of the hurricane itself. Hence, waves generated in this region tend to move forward with the hurricane and therefore remain in high wind regions for an extended period of time. In contrast, waves generated on the low wind side of the storm (South side in Figure 20) propagate in the opposite direction to the hurricane translation and rapidly move away from the high wind areas. According to the *SPM* [Lit 18], the asymmetric shape of the wave field is as given in Figure 21.

The synthetic wave field produced by the model *DOLPHIN-B1* is also asymmetric, but the degree of asymmetry is less than the wave field presented in Figure 21, since the model takes into account the extended fetch only and not the asymmetrical wind field.
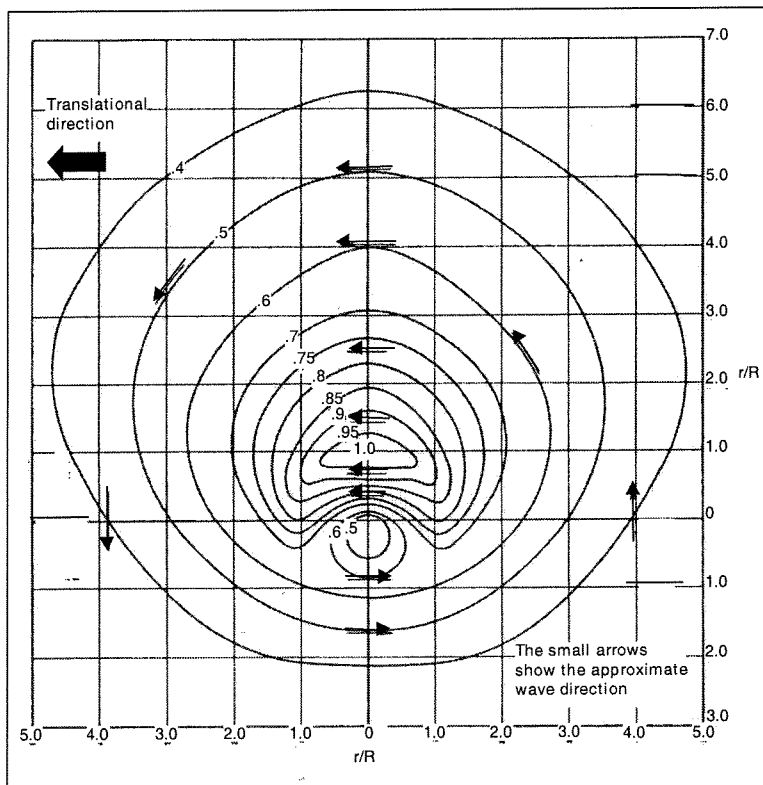
Figure 21: Isolines of the relative H_s for a slow-moving hurricane

- The pressure at infinity P_{inf} , also defined as "the environmental pressure at the outer limit of a hurricane where the cyclonic circulation ends" is assumed to be 1013 [mbar]. This is the mean air pressure at sea level approximately. This is not completely correct, because due to differences in latitude and high or low pressures in the vicinity, P_{inf} might differ from this value. But 1013 [mbar] still gives a reasonable estimate and it is used in a lot of other formulae as reference. See the subject "storm surge" in the *CUR* 169 [Lit 13] and the *NOAA* Internet site [Lit 22].

- Since *DOLPHIN-B1* has not been tested extensively in shallow water areas, in the present study the wave model *DOLPHIN-B1* has only been used to hindcast wave conditions at locations situated on relatively deep-water (See [Lit 27]).

- Using *DOLPHIN-B1* at locations with relatively deep-water does not mean that all the depth information of the surrounding area is disregarded. For example, not taking into account the influence of the *Saba bank*, leads to a too simplified model. Therefore, shoaling effects, energy dissipation by bottom friction and wave breaking (due to limited depth) in these comparatively shallow waters have been taken in account. However, *DOLPHIN-B1* does not take account for refraction of waves.

4.4. Preparation of DOLPHIN-B1 input files

4.4.1. Reconstruction of the hurricane wind field with CYCLONE

In *DOLPHIN-B1* the *CYCLONE* tool is responsible for the reconstruction of a hurricane wind field. However, from the *Unisys* database with hurricane records, the necessary information to reconstruct hurricane wind fields is not available in the right format. For example the *CYCLONE* tool needs to know the radius to maximum wind speed (R) and the pressure difference between the hurricane center and infinity (P_{diff}) both as function of time. However, the *Unisys* database does not contain information regarding the parameter R and for many hurricane records the pressure registration is incomplete. To be able to work with the *CYCLONE* tool, the missing information of R en P_{diff} will be completed by making use of the registration of maximum sustained wind speeds ($U_{g,max,sust}$) from the same *Unisys* database. This registration is complete for each hurricane. The translation of $U_{g,max,sust}$ to R and P_{eye} is carried out with the formulae of *Kraft* (1971) and *Vickery* (2000). These formulae are available from the Internet site of the *NOAA* [Lit 22].

Determination of P_{eye} with formula of Kraft (1971)

A pressure-wind relation has been developed by *Kraft* already in 1971. However, the relation is still used as a rule of thumb for the *Atlantic basin* by the *NHC* to analyse hurricane intensities from satellite images. The relation of *Kraft* is purely empirical, see Equation 21.

$$P_{eye} = 1013 - \frac{U_{g,max,sust}^2}{\mu} \qquad [mbar] \qquad \text{Equation 21}$$

$U_{g,max,sust}$ = in [m/s]
μ = 51.93 [m^2/s^{2}mbar] (empirical coefficient)

The results from the application of Equation 21 in this form showed great resemblance's with a complete pressure registration (P_{eye}) of a hurricane from the *Unisys* database (See Annex VI). In Annex VI the quality of the results from *Kraft* have been expressed in terms of the Root Mean Square difference (RMS) and relative difference. From these differencess it is concluded that the estimations of P_{eye} from *Kraft* are indeed reliable enough.

Determination of R with formula of Vickery (2000)

It is difficult to estimate the radius to maximum wind speed as it is not routinely available. However, to estimate the radius to maximum wind speed (R), *Vickery* gives an expression depending on P_{diff} and the position of the hurricane centre. The expression is given in Equation 22 and valid only for the Northern Hemisphere.

$$\ln\left(\frac{R}{a_1}\right) = -a_2 P_{diff}^2 + a_3 Lat \qquad \text{Equation 22}$$

a_1 = 13.957 [km]
a_2 = 5.086.10^{-5} [mbar^{-2}]
a_3 = 3.94899.10^{-2} [degree^{-1}]
P_{diff} = in [mbar]
Lat = Latitude in [degree]
R = in [km]

Fort Bay harbour, Saba. A study on hurricane conditions

35

The coefficients a in Equation 22 have been determined empirically by *Vickery*. It was not possible to compare results from the formula of *Vickery* with registrations of R, because sources containing these kind of registrations were not available for the present study.

Example of wind field generated with CYCLONE

Based on the position of the hurricane center (latitude and longitude), the central pressures of the hurricane eye (P_{eye}) and the radius to maximum wind speeds (R), the *CYCLONE* tool is able to provide *DOLPIN-B1* with a reconstruction of the hurricane wind field. An example of such a wind field, computed with *CYCLONE* is illustrated in Figure 22.
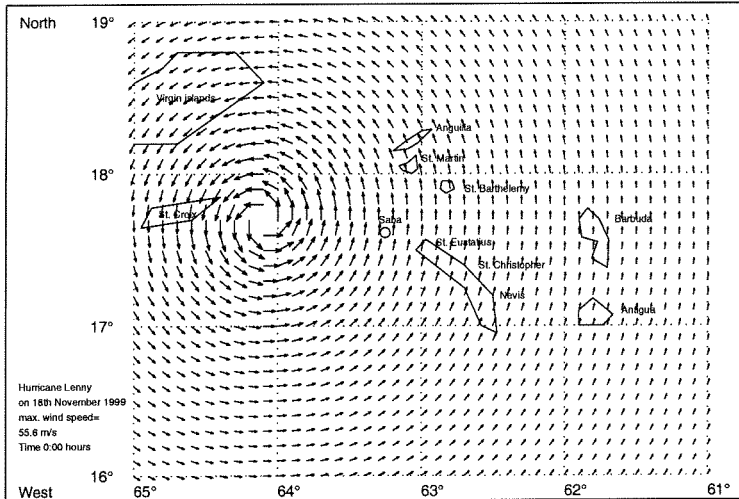
Figure 22: Example of hurricane wind field computed with CYCLONE

4.4.2. Bathymetry

The model area consists of coastlines and a depth grid. The area for which coastlines are defined is chosen in such a way that the island of *Saba* lies in the middle. The position and dimensions of the depth grid are chosen in such a way that the grid covers both *Saba* and the *Saba bank*. Figure 23 shows the coastlines and the position of the depth grid.
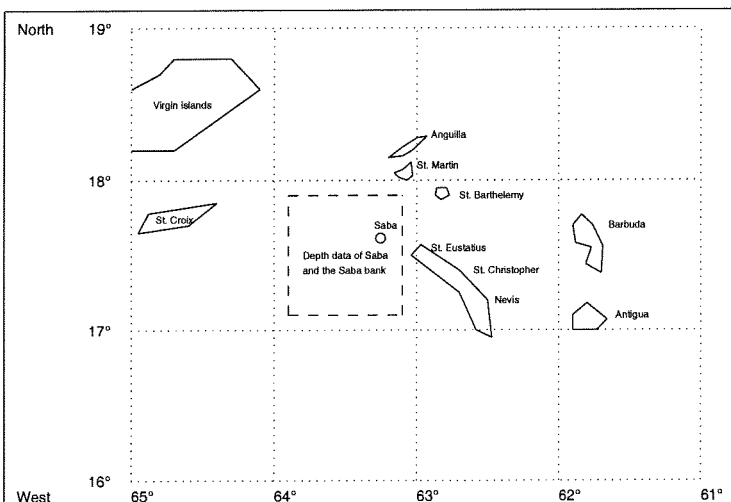
Figure 23: Coastlines and position of depth grid, as used in DOLPHIN-B1

The applied depth grid is based on spherical co-ordinates. The size is 160x160 grid cells. The size of one grid cell is 0.005 [°] x 0.005 [°]; this is equivalent to approximately 532.14 [m] for eastern directions and 553.37 [m] for northern directions. In this way the total grid size is: 532.14*160 = 85.024 [km] by 553.37*160 = 88.540 [km]. The bathymetry of the concerned area is obtained from sea maps of the *Caribbean Sea*, see [Lit 25] and [Lit 26]. First the water depths were sampled on a grid with a size of 0.05 [°] x 0.05 [°]. Locally in the area of *Saba* the depths were sampled on the 0.005 [°] x 0.005 [°] grid. With the use of the computer tool *Surfer*, a triangular interpolation technique is used to calculate depth values on all grid points of the 0.005 [°] x 0.005 [°] grid. Annex VII contains two figures showing the bathymetry as it is used in *DOLPHIN-B1*.

5. VERIFICATION AND APPLICATION OF THE WAVE MODEL

5.1. Approach

The wave model *DOLPHIN-B1* has its limitations, because due to several assumptions and schematisations it provides only a restricted presentation of the reality. This chapter illustrates these restrictions and describes in what way the results of a hurricane study carried out with this model can contribute in defining new or changed harbour design wave conditions. Against this background, first the degree to which *DOLPHIN-B1* is able to estimate the "real" wave conditions is verified. In the present study this ability is called the reliability. The reliability of the *DOLPHIN-B1* model has been verified by comparing the model results with two available registrations of hurricane wave conditions, being:

- A hurricane study, see [Lit 11], performed by the American organisation *Oceanroutes Inc.* in 1987. This study was part of a general study on wave conditions in the area of *St. Eustatius*, carried out by *WL| Delft Hydraulics* in 1988. These studies have previously been used by *CEC* for the derivation of design wave conditions as applied to the *Fort Bay* harbour design of 1990 (See Section 2.3.2).
- Satellite observations of wave conditions during hurricanes, available from *ARGOSS*, see [Lit 19].

Unfortunately, it proved to be impossible to estimate the reliability of *DOLPHIN-B1* with these two registrations, due to the following reasons:

- For their hindcast study, *Oceanroutes Inc.* schematised the reality as well. However, the degree of schematisation is unknown. Therefore the reliability of this study is unknown as well.
- Only three satellite observations with wave conditions during hurricanes were available. This amount of observations is too less to derive a proper estimation of the reliability of *DOLPHIN-B1*.

Although the reliability of the *DOLPHIN-B1* model could not be estimated, the aforementioned comparison indicated that some part of the differences between the results of *DOLPHIN-B1* and both registrations of hurricane wave conditions is of a systematic nature. Against this background it has been reasoned that there is a systematic difference between the *DOLPHIN-B1* results and the "real" wave conditions as well. In this way the hindcast computations from *DOLPHIN-B1* could be used to identify changes in hurricane wave conditions. The assumption of a systematic difference between wave heights as computed by *DOLPHIN-B1* and the wave heights occurring in reality is illustrated in Figure 24.
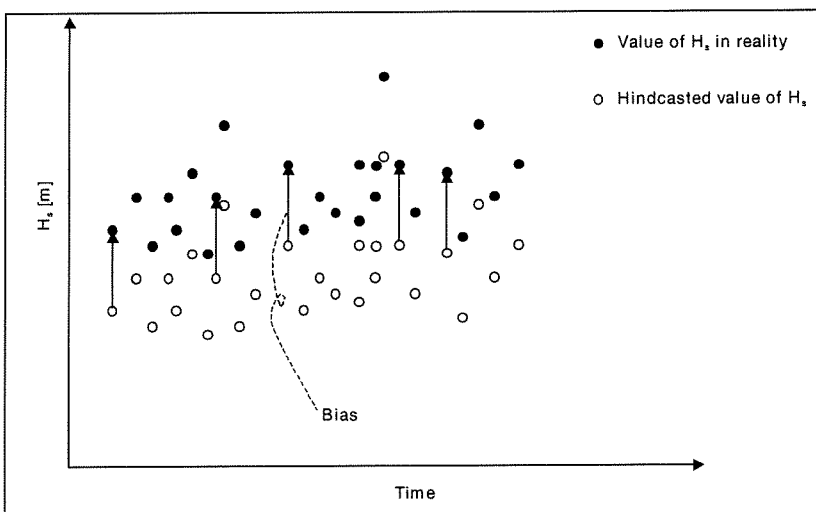
Figure 24: Explanation of the absolute difference between the "real" H$_s$ and the ones from DOLPHIN-B1

Since, at this stage it was clear what kind of information could be withdrawn from a hurricane hindcast carried out with *DOLPHIN-B1* model, the actual hindcast computations could be carried out. A description of these computations is given at the end of this Chapter.

5.2. Comparison of DOLPHIN-B1 results with hurricane study from Oceanroutes Inc.

Back in 1987 the American organisation *Oceanroutes Inc.* performed a hurricane hindcast study in the area of *St. Eustatius*. This study was part of a general study on wave conditions under supervision of *WL Delft Hydraulics*. Hereafter, first the methodology of the American study is discussed briefly, secondly a few remarks are made concerning the applied methodologies. Finally the *DOLPHIN-B1* model will be compared with the results of the American hindcast study.

5.2.1. Methodology of hurricane hindcast study performed by Oceanroutes Inc.

Ocean routes Inc. hindcasted waves for the most severe storms acting in the area near *Oranje Bay, (St. Eustatius)* for the period between 1900 till 1986. They selected the hurricanes based on two selection criteria, namely:

- A first criterion defining a selection of hurricanes with tracks passing through a 5 [°] x 5 [°] square centred at the location: 17.5 [°] N and 63.0 [°] W. This location lies in the vicinity of the *Oranje Bay*. The water depth at this location is approximately 50 [m]. This first selection contained a group of 49 hurricanes.

- A second criterion selecting 20 hurricanes with the largest wind speeds, from the group of 49 hurricanes.

Oceanroutes Inc. have determined the wave conditions during these 20 most severe hurricanes using *Bretschneider* wave diagrams and *Pierson, Neumann and James* techniques, see [Lit 15]. *Oceanroutes Inc.* does not give a further explanation on how these different techniques have been applied in the case of the *Oranje Bay* of *St. Eustatius*. Instead, they restricted themselves by giving only the computed wave conditions at six-hour intervals together with the hurricane track information used to derive these wave conditions. The wave conditions are expressed in terms of the significant wave height (H_s), the corresponding mean direction of wave propagation (θ) and significant wave period (T_s).

5.2.2. Remarks on the hurricane study of Oceanroutes Inc.

- *WL Delft Hydraulics* assumed that the wave conditions, resulting from the hurricane hindcast study of *Oceanroutes Inc.* apply to relatively deep-water. However, it is not clear whether *Oceanroutes Inc.* hindcasted waves on either deep or shallow water, because their hindcast location is unclear. First they mention the location of 17.5 [°] N and 63.0 [°] W, where the square of 5 [°] x 5 [°] (first hurricane selection criterion, see Section 5.2.1) is centred at. Secondly, they mention the tip of the breakwater of the *Oranje Bay* as hindcast location. However, these two locations do not coincide with each other and are characterised by different water depths. The water depth at the first location is approximately 50 [m]; at the second location this is approximately 9 [m]. According to Equation 1 and Equation 2 (see Section 2.3.3), waves generated by hurricanes, experience a water depth of 50 [m] almost as deep water and a water depth of 9 [m] as shallow water.

Not knowing the hindcast location of the study from *Oceanroutes Inc.* forms an obstruction for the comparison of the results from *DOLPHIN-B1* with the ones from *Oceanroutes Inc.*, as will be carried out in Section 5.2.3. Because it was not possible to clear this obstruction within the present study, the interpretation of *WL Delft Hydraulics* is assumed to be correct. Therefore wave conditions from the *Oceanroutes Inc.* study are assumed to be deep-water wave conditions, hindcasted at the location 17.5 [°] N and 63.0 [°] W.

- As mentioned in Section 5.2.1, *Oceanroutes Inc.* does not give an explanation of the schematisations and assumptions they applied for their hurricane hindcast study. As a result differences between the hindcasted wave conditions from *Oceanroutes Inc.* and *DOLPHIN-B1* cannot be explained.

5.2.3. Results of the comparison between DOLPHIN-B1 and Oceanroutes Inc.

To be able to compare results from *DOLPHIN-B1* with the results from *Oceanroutes Inc.*, the 20 hurricanes that have been hindcasted by *Oceanroutes Inc.* will be hindcasted as well by *DOLPHIN-B1*. According to Section 5.2.2, the hurricane hindcast study of *Oceanroutes Inc.* is performed at the following location:

- Position: 17.5 [°] N and 63.0 [°] W
- Water depth: 50 [m]

The hindcast location used in *DOLPHIN-B1* could not be exactly the same. One of the demands when using a depth grid in *DOLPHIN-B1* (See [Lit 6) is that the hindcast location has to fit within the limits of the depth grid. However, the depth grid (Composed in Section 4.4.2) did not cover the hindcast location used by *Oceanroutes Inc.* Therefore in *DOLPHIN-B1* a slightly different location is chosen, positioned at the boundary of the depth grid and with a minimum distance to the hindcast location as used by *Oceanroutes Inc.* The characteristics of the hindcast location used in *DOLPHIN-B1* are:

- Position: 17.5 [°] N and 63.1 [°] W
- Water depth: 400 [m]

Annex VIII contains the hindcasted significant wave heights and the corresponding directions of wave propagation for the 20 hurricanes according to *Oceanroutes Inc.* and according to *DOLPHIN-B1*. Looking at Annex VIII, *DOLPHIN-B1* gives lower values of H_s than *Oceanroutes Inc.* Especially, the largest H_s during a hurricane ($H_{s,max}$) are significant lower according to *DOLPHIN-B1* than according to *Oceanroutes Inc.* Looking at the hindcasted directions of wave propagation, no significant differences between both hindcasts can be observed.

Hereafter, the observed differences between the wave heights of both hindcasts (*DOLPHIN-B1* and *Oceanroutes Inc.*) will be quantified. Further it will be determined to what extend these differences are of a systematic nature. As mentioned in Section 5.1 a certain degree of systematic difference between both hindcasts contributes to the assumption of a systematic difference between the wave conditions as computed by *DOLPHIN-B1* and the wave conditions in reality.

Theory to determine the degree of systematic difference

In Figure 25A an example is given of two registrations of wave heights. As can be observed the difference (ε) between both registrations is significant, but a large part of this difference seems to be systematically. The theory to determine the degree of systematic difference is given hereafter.
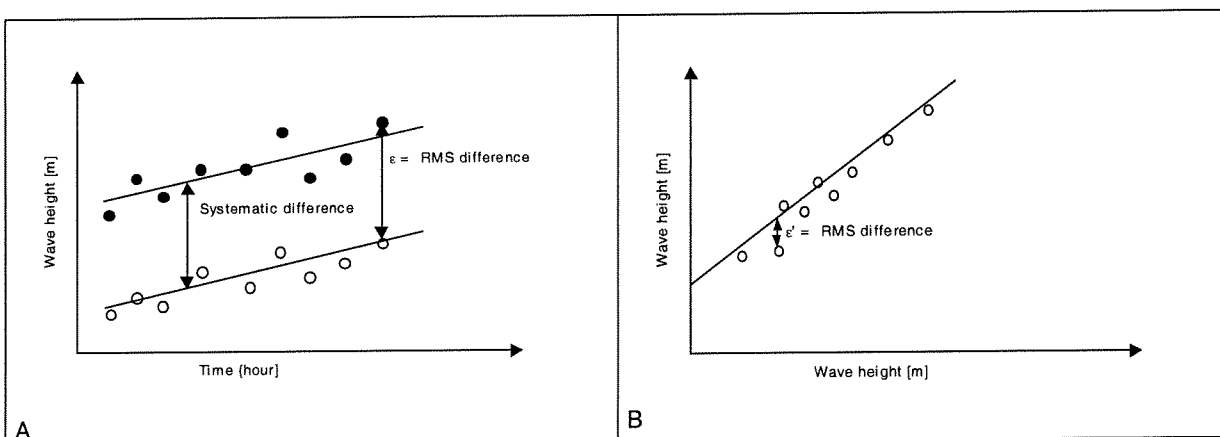
Figure 25: Explanation of the RMS

The difference between both registrations in Figure 25A can be expressed in terms of the Root-Mean-Square difference (RMS), indicated by the symbol ε. The formula of the RMS difference is given in Equation 23.

$$RMS = \sqrt{\frac{1}{N}\sum_{i=1}^{N}\left(D_{T,i} - D_{R,i}\right)^2}$$

<div align="right">Equation 23</div>

$D_{T,i}$	=	Data sample from the test data set
$D_{R,i}$	=	Data sample from the reference data set
i	=	Sample number
N	=	Number of samples in D_T or D_R

In general, the RMS difference (ε) is either systematic, non-systematic or a combination of both. To identify the nature of the RMS difference (ε), first in Figure 25B the wave heights of the two registrations have been plotted versus each other. A measure for the degree of non-systematic difference is formed by the vertical distance between the straight line in Figure 25B and the plotted points. The straight line has been fitted to the points with the least squares method, see [Lit 17]. Quantification of the vertical distances is done by the calculation of a new RMS difference (ε'), see Figure 25B. In the case of $\varepsilon \gg \varepsilon$', the non-systematic difference is relative small compared to the systematic difference.

Quantification of the differences between the values of H_s from DOLPHIN-B1 and Oceanroutes Inc.
In Figure 26 the wave heights (H_s) according to *DOLPHIN-B1* and *Oceanroutes Inc.* are plotted versus each other. Although there is a large variation of the data, a certain degree of linearity can be observed. This linearity is indicated by the straight line, which has been fitted to the data by the method of the least squares.
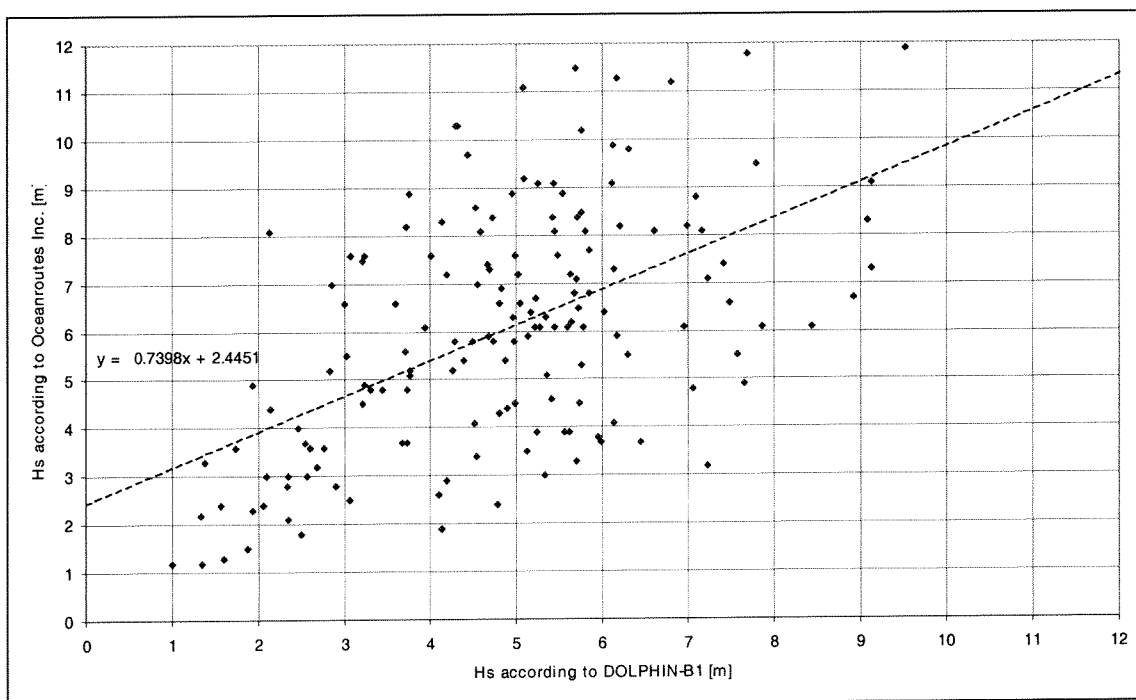
Figure 26: H_s (DOLPHIN-B1) versus H_s (Oceanroutes Inc.)

Using the values of H_s from *Oceanroutes Inc.* as reference, $D_T = H_s$ *(DOLPHIN-B1)* and $D_R = H_s$ *(Oceanroutes Inc.)*, the differences between both hindcasts are:

- RMS difference ε = 2.43 [m]
- RMS difference ε' = 1.088 [m]

Since $\varepsilon > \varepsilon$' a significant part of the difference between the hindcasts is systematic. However, a large part of the difference is also non-systematically.

Quantification of the differences between the values of $H_{s,max}$ from DOLPHIN-B1 and Oceanroutes Inc.
At the beginning of Section 5.2.3 it was noted that in particular the largest H_s during a hurricane ($H_{s,max}$) were estimated significantly lower by *DOLPHIN-B1* than by *Oceanroutes Inc.* Since, in the present study we are most interested in the extreme loads that may occur, it is useful to take a closer look to the values of $H_{s,max}$. In Figure 27 the values of $H_{s,max}$ according to both hindcasts are plotted versus each other.
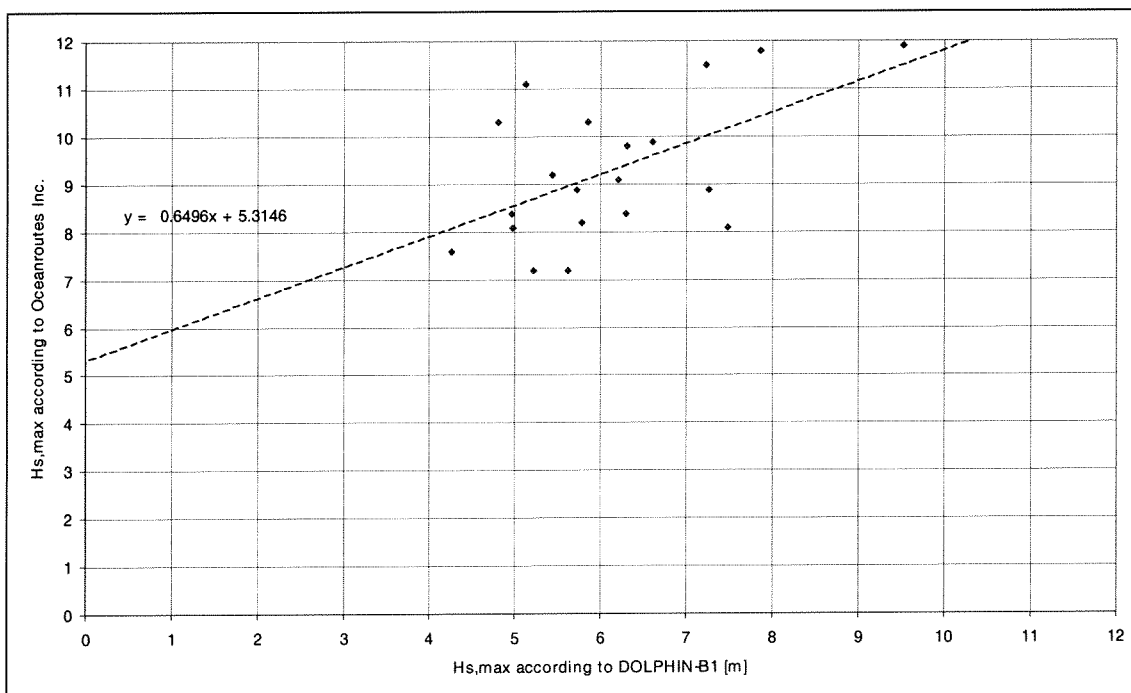
Figure 27: $H_{s,mx}$ (DOLPHIN-B1) versus $H_{s,max}$ (Oceanroutes Inc.)

Although the variation of the data, a certain degree of linearity can be observed. This linearity is indicated again by the straight line. Using the values of $H_{s,max}$ from *Oceanroutes Inc.* as reference, $D_T = H_{s,max}$ *(DOLPHIN-B1)* and $D_R = H_{s,max}$ *(Oceanroutes Inc.)*, the differences between both hindcasts are:

- RMS difference ε = 3.41 [m]
- RMS difference ε' = 1.20 [m]

Since $\varepsilon > \varepsilon$' a significant part of the difference between the hindcasts is systematic. However, the non-systematic difference is cannot be neglected.

Conclusions

- The significant wave heights are estimated significantly lower by *DOLPHIN-B1* than by *Oceanroutes Inc.* In particular, this yields for the estimations of the largest significant wave heights during hurricanes.

- The differences between the wave heights from *DOLPHIN-B1* and *Oceanroutes Inc.* is for a significant part systematically. However, the non-systematic part is large as well and certainly not negligible.

- The comparison of the mean wave directions between *Oceanroutes Inc.* and *DOLPHIN-B1* is not expressed in terms of a RMS difference. Instead, visual observation of the graphs in Annex VIII concluded that wave directions in most cases show a reasonable resemblance without a systematic difference.

5.3. Comparison of DOLPHIN-B1 results with satellite observations

For the comparison three time series with satellite observations of wind speeds and wave heights during hurricane conditions were available. The observations are all centred at the position 17.5° N and 63.5° W. Each series is a registration of satellite passes covering a period of 14 days, available from the *ARGOSS* databases [Lit 19]. A satellite pass is defined as a set of satellite observations resulting from one pass of the satellite over the area under investigation (in this case an area of 100 x 100 [km²]). This set of satellite observations are expressed in terms of a maximum, a median and a minimum value. See Figure 28.
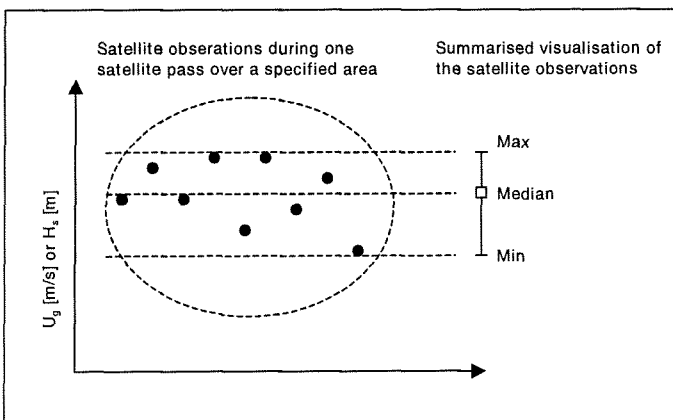
Figure 28: Rendering of the satellite observations during one satellite pass

According to *ARGOSS*, the observed wind speeds are equal with the 1-hour averaged wind speeds at an elevation of 10 [m] above mean sea level. Therefore these wind speeds can be compared with the hindcasted gradient wind speeds (U_g) from *DOLPHIN-B1* (see Section 4.3.2 for the definition of the gradient wind speed (U_g)). The observed wave heights are equal to the significant wave heights (H_s). A brief explanation on how satellite observations are translated into several kinds of data is given in Annex IX.

5.3.1. Remarks of satellite observations

According to *ARGOSS*, some satellite observations have been compared with wave buoy data in the *Atlantic* basin. The differences between the satellite observations and the wave buoy data is expressed in terms of the RMS difference and the relative difference (See Section 5.2.3 for an explanation of the RMS difference). In this case D_R= data from buoys, and D_T= data from satellite. *ARGOSS* only gives RMS differences and does not indicate the composition of this difference.

Table 15: Comparison of satellite observations with wave buoy data

Kind of data	Buoy mean	RMS difference	Relative difference [%]
Wind speed	7.68 [m/s]	1.435 [m/s]	17
Sig. Wave height	1.97 [m]	0.48 [m]	22
Mean period	6.99 [s]	1.01 [s]	14
Zero cross. Period	5.84 [s]	0.72 [s]	12

Source: ARGOSS Internet site [Lit 19]

5.3.2. Results of the comparison between DOLPHIN-B1 and the satellite observations

Verification of *DOLPHIN-B1* is performed by comparing model results to the satellite data. In the present study, this comparison is focussed on the three hurricanes mentioned in Table 16. In terms of number of wind and wave observations these three hurricanes have been monitored relatively well by satellites and they passed *Saba* at a distance sufficiently small to generate wave conditions within our range of interest (near *Fort Bay* harbour).

Table 16: Available satellite observations during the presence of a hurricane

Hurricane number	Hurricane name	Number of satellite passes with wind speed observations	Number of satellite passes with sign. wave height observations
72	Marilyn (1995)	9	5
80	Hortense (1996)	9	2
87	Georges (1998)	6	3

In the intended comparison of model results with satellite data we need to take into account that satellite data are actually averages over an area of 100 x 100 [km^2]. It is therefore hardly possible to associate a satellite observation to a specific point on the map. This complicates the intended comparison, because to verify wave conditions with *DOLPHIN-B1* results, a hindcast location must be known. Furthermore it is unclear whether we have to verify *DOLPHIN-B1* results against the maximum, median or minimum values of the satellite observations.

Because of the difficulties concerning the determination of a hindcast location for *DOLPHIN-B1*, it has been decided to choose a hindcast location within the square of 100 x 100 [km^2] (is equal to the satellite observation area), near *Fort Bay* harbour and at relatively deep-water (because of shallow water restrictions, see Section 4.3.3). The location is characterised by:
- Position: 17.6 [°] N and 63.25 [°] W
- Water depth: 420 [m]

The satellite observations together with the hindcasted wave conditions of *DOLPHIN-B1* are given in the second part of Annex VIII. Looking to the graphs in the second part of Annex VIII, in most cases *DOLPHIN-B1* overestimates wind speeds as well as significant wave heights. The graphs also show that the difference between the maximum satellite observations and the results of *DOLPHIN-B1* in most cases is the smallest. Therefore it has been decided to verify *DOLPHIN-B1* with the maximum satellite observations of wind speed and significant wave height.

Differences between the wind speeds from DOLPHIN-B1 and satellite observations

In Figure 29 the wind speeds according to *DOLPHIN-B1* and the satellite observations are plotted versus each other. Although there is variation of the data, a certain degree of linearity can be observed. This linearity is indicated by the straight line, which has been fitted to the data by the method of the least squares.
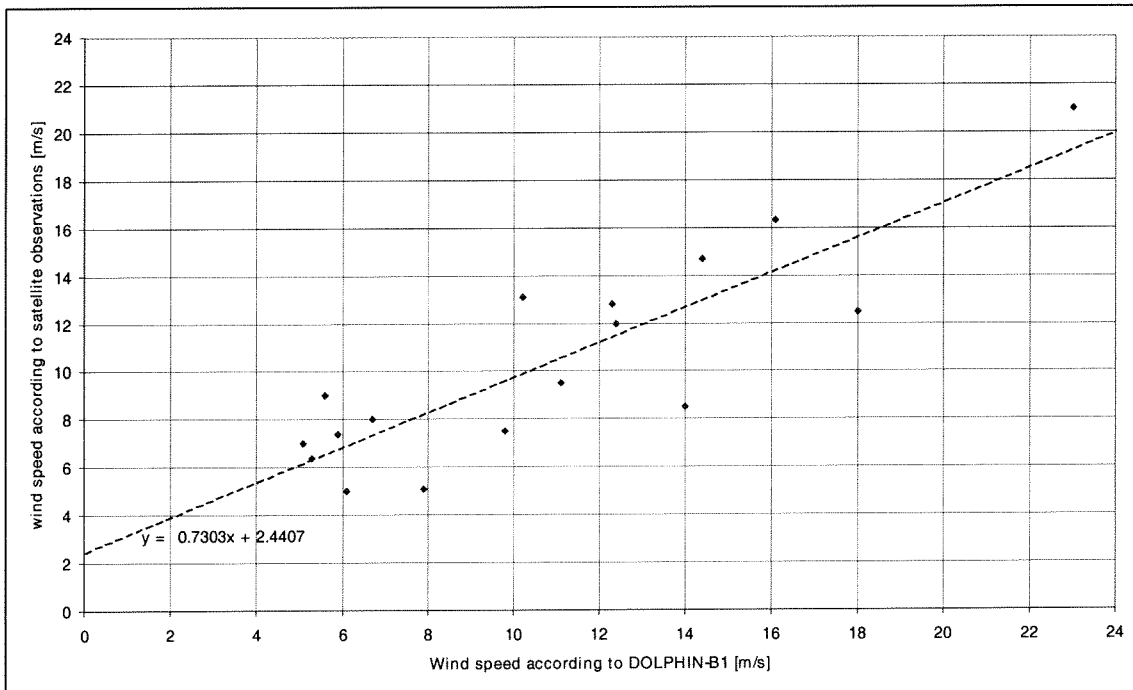

Figure 29: Wind speed (DOLPHIN-B1) versus wind speed (Satellite observations)

Using the wind speeds from the satellite observations as reference, $D_T = U_g$ (*DOLPHIN-B1*) and $D_R = U_g$ (Satellite observations), the differences between the wind speeds are:

- RMS difference $\varepsilon = 2.55$ [m/s]
- RMS difference $\varepsilon' = 1.19$ [m/s]

Since $\varepsilon > \varepsilon'$ a significant part of the difference between the hindcasts is systematic. However, the portion of non-systematic difference can not be neglected.

Differences between the wave heights from DOLPHIN-B1 and satellite observations

In Figure 30 the significant wave heights according to *DOLPHIN-B1* and the satellite observations are plotted versus each other. Although there is variation of the data, a certain degree of linearity can be observed. This linearity is again indicated by the straight line, which has been fitted to the data by the method of the least squares.

Fort Bay harbour, Saba. A study on hurricane conditions

45
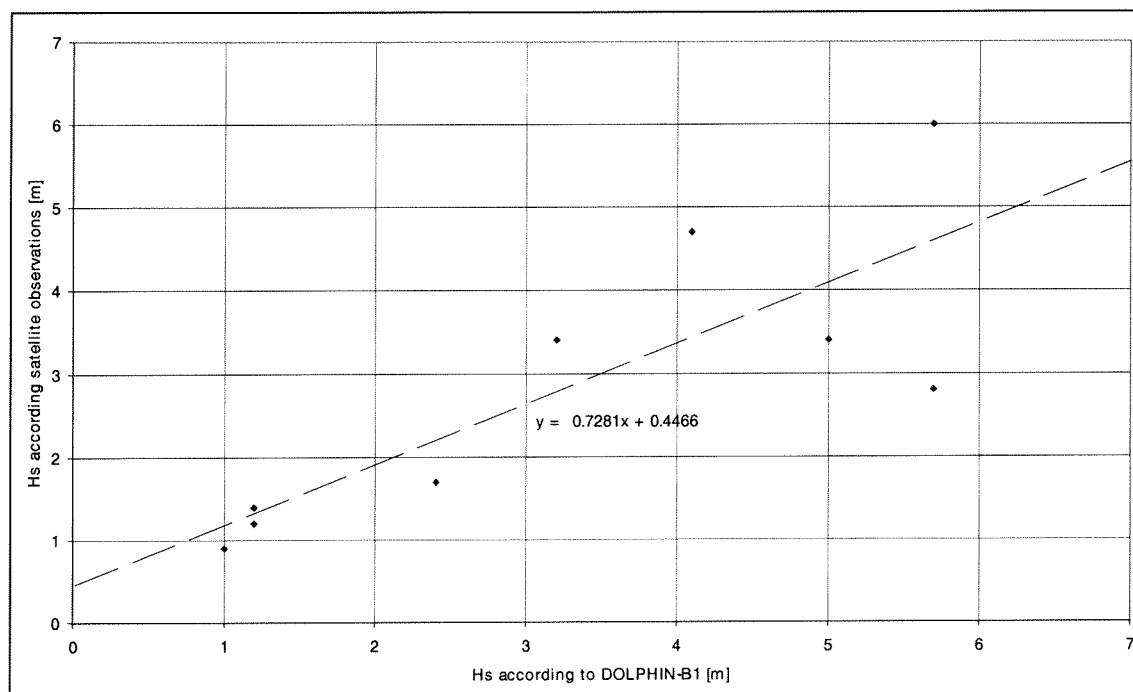
Figure 30: H_s (DOLPHIN-B1) versus Hs (Satellite observations)

Using the wave heights according to the satellite observations as reference, $D_T=$ H_s *(DOLPHIN-B1)* and $D_R=$ H_s (Satellite observations), the differences between the wind speeds are:
- RMS difference ε = 1.154 [m]
- RMS difference ε' = 0.549 [m]

Conclusions
- In general, *DOLPHIN-B1* seems to over-estimate the maximum satellite observations of wind speed and significant wave height.
- The largest maximum satellite observation (is equal to $H_{s,max}$ and $U_{g,max}$) during hurricanes *Marilyn* and *Hortense* show reasonable resemblance's with the ones resulting from *DOLPHIN-B1*. The $H_{s,max}$ and $U_{g,max}$ during hurricane *Georges* however, differ significantly from the *DOLPHIN-B1* results.
- Because of the two matches of the $H_{s,max}$ and $U_{g,max}$ (from hurricanes *Marilyn* and *Hortense*) it may be possible that *DOLPHIN-B1* is able to hindcast proper values of $H_{s,max}$ and $U_{g,max}$. and consequently is able to identify a tendency in $H_{s,max}$ and $U_{g,max}$ as well. However, this theory is based on only two matches between *DOLPHIN-B1* results and satellite observations and therefore indicative only.

5.4. Ability of DOLPHIN-B1 to identify changes in wave conditions
As already mentioned in Section 5.1, the reliability of *DOLPHIN-B1* could not be estimated. Instead, another ability of *DOLPHIN-B1* was verified, namely the identification of changes in wave conditions. The observed differences between *DOLPHIN-B1* and the two registrations with hurricane wave conditions (*Oceanroutes Inc.* and the satellite observations, see Sections 5.2 and 5.3) were to some degree systematically. Furthermore, *DOLPHIN-B1* seemed to approximate the satellite observations during hurricanes *Hortense* and *Marilyn* reasonably well. Therefore it is assumed that *DOLPHIN-B1* is able to identify changes in wave conditions. (this means changes in H_s and θ).

5.5. Hurricane hindcast for the area near Fort Bay and carried out with DOLPHIN-B1

Since at this stage it is known that *DOLPHIN-B1* is able to identify a tendency of changing wave conditions ($H_{s,max}$ and θ), it is possible to carry out the actual hindcast of wave conditions in the area of *Fort Bay* harbour for the period between 1972 and 2000 (age of the harbour). First the choice of the hindcast location will be made clear. Secondly, it is explained which hurricanes have been used for the hindcast.

Choice of hindcast location

The hindcast location has been chosen on deep-water and in the vicinity of *Fort Bay* harbour. Annex VII shows the hindcast location in more detail. The characteristics of the hindcast location are:
- Position: 63.25° W, 17.6° N
- Distance to *Fort Bay* harbour: 1714 [m]
- Water depth: 420 [m] (Deep water for waves generated by hurricanes, see Section 2.3.3)

Hurricane selection

The hurricane hindcast will be carried out with hurricanes which have been selected by two selection criteria. The criteria are:
- A first criterion defining for which period hurricane information will be taken into account. Since the main interest of the present study goes to the changes of wave conditions during the existence of the harbour, the period between 1972 till 2000 (age of the harbour) has been chosen. Based on this first selection criterion, <u>298 hurricanes</u> have been identified.
- A second criterion selecting hurricanes depending on the minimum distance between the hurricane track and the location of *Fort Bay* harbour. This second selection criterion gives a limit to the distance between *Fort Bay* harbour and the track of the hurricane. Only hurricanes with tracks within this limit of distance become part of the selection. This selection criterion is based on the assumption that the further a hurricane is acting from *Fort Bay* harbour, the smaller the waves at *Fort Bay* harbour will be. Choosing the maximum distance between *Fort Bay* harbour and a hurricane track at 1000 [km], <u>98 hurricanes</u> remain from the first selection of 298 hurricanes. In fact the second selection criterion can be interpreted as a circle of 1000 [km] around the *Fort Bay* harbour, see Figure 31.

The explanation for taking the 1000 [km] as radius is substantiated with Figure 78 of Annex X. In advance of Chapter 6, in Figure 78 for each of the 98 hindcasted hurricanes the highest significant wave height ($H_{s,max}$) is plotted against the distance from *Fort Bay* harbour. According to this Figure, hurricanes with tracks outside the radius of 1000 [km] will probably generate waves with negligible heights in the area of *Fort Bay* harbour.
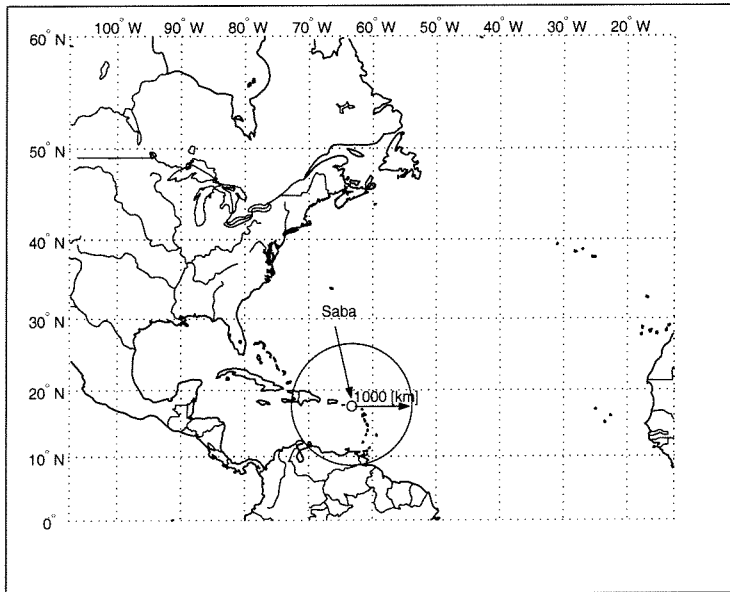
Figure 31: Explanation of the second hurricane selection

A total of 98 hurricanes (resulting from the aforementioned second selection criterion) have been hindcasted with *DOLPHIN-B1*. As it is not clear beforehand at what time wave conditions during a hurricane at the hindcast location reach their maximum or their most unfavourable values, wave conditions have been hindcasted for time intervals of 6 hours, for the entire duration of each hurricane. The hindcast consists of the 6-hourly significant wave heights (H_s), main directions of wave propagation (θ) and wave peak frequencies (f_p). The *DOLPHIN-B1* hindcast together with the used *DOLPHIN-B1* input files and the track information of the 98 hindcasted hurricanes are available on CD-ROM and enclosed within this report.

6. STATISTICAL ANALYSIS OF HINDCASTED DEEP-WATER WAVE CONDITIONS

6.1. Approach

Chapter 5 ends with the actual *DOLPHIN-B1* hindcast of hurricane wave conditions in the area of *Fort Bay* harbour. In that Chapter it was further concluded that if the hindcasted wave conditions show a tendency to increase, a similar phenomenon is likely to have occurred in reality. This Chapter describes the analysis to determine such a tendency objectively.

Characterisation of hurricanes

For the analysis not all of the hindcasted hurricane wave conditions will be taken in account. Instead, we have chosen to characterise each of the 98 hurricanes by two wave parameters, viz. the maximum significant wave height ($H_{s,max}$) and the corresponding direction of wave propagation (θ) as they were hindcasted by *DOLPHIN-B1* at the location near *Fort Bay* harbour. Characterising hurricanes in this way practically means that from all of the 6-hourly hindcasted significant wave heights, the highest significant wave height ($H_{s,max}$) and the corresponding θ of each hurricane are selected. Selecting these two wave parameters is straightforward in the sense that they occur in commonly used basic design rules for breakwaters and similar harbour structures. Information and plots of $H_{s,max}$ and θ can be found in Annex X.

Identification of two separated periods of wave conditions

The design wave conditions of the reconstruction design of *Fort Bay* harbour (1990) were derived from a hurricane hindcast carried out by *Oceanroutes Inc.* in 1987 (part of the wave climate study of *WL| Delft Hydraulics*, 1988 [Lit 11]). This hurricane hindcast is based on hurricane track information from the period 1900 till 1986. However, a couple of years after completion of the reconstruction design (1990), some hurricanes were responsible for severe damage to the harbour structures. Therefore there is a possibility that the hurricane hindcast from *Oceanroutes Inc.* is not representative for the period after 1986. To find evidence for this possibility, it has been decided to divide the period from 1972 till 2000 (age of the harbour) into two periods, namely:

- Period A from 1972 till 1986
- Period B from 1987 till 2000

In this way, the analysis necessary to determine a tendency in wave conditions during the existence of the harbour, is reduced to a comparison between the values of $H_{s,max}$ and θ from two periods. The whole idea of the hurricane selection and the distinction of two periods with values of $H_{s,max}$ and θ is visualised in Figure 32. In the same Figure the two hurricane selection criteria as described in Section 5.5 are given as well.
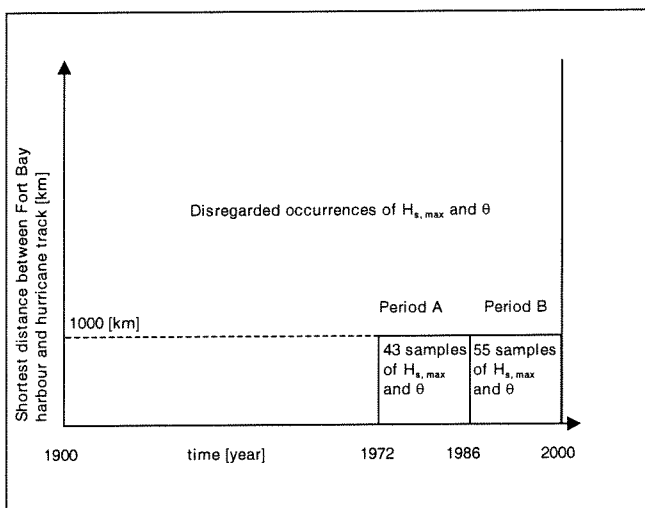
Figure 32: Selections of wave conditions

The distinction of two periods as explained in Figure 32, results in 4 data sets, see Table 17.

Table 17: Definition of the data sets with wave conditions

Period	Data sets		
Period A (1972-1986)	D_I	=	Data set I with $H_{s, max}(1)$, $H_{s, max}(2)$, ...$H_{s, max}(43)$
	D_{II}	=	Data set II with $\theta(1)$, $\theta(2)$, ...$\theta(43)$
Period B (1987-2000)	D_{III}	=	Data set III with $H_{s, max}(44)$, $H_{s, max}(45)$, ...$H_{s, max}(98)$
	D_{IV}	=	Data set IV with $\theta(44)$, $\theta(45)$, ...$\theta(98)$

With these four data sets, the aforementioned analysis is reduced to two comparisons, being:
- A comparison between the data sets of $H_{s,max}$ (data sets I and III)
- A comparison between the data sets of θ (data sets II and IV).

Looking to Figure 77 in Annex X the $H_{s,max}$ in period B (data set III (1987-2000)) have probably increased compared to the $H_{s,max}$ in period A (data set I (1972-1986)). In other words, visually an increasing tendency of the $H_{s,max}$ can be observed. However, whether or not this increasing tendency is statistically significant, will be investigated with the use of a statistical test. The present study is focussed on the comparison of $H_{s,max}$. For this reason, the directions of wave propagation (θ) (data sets II and IV) will not be subjected to a statistical test. Instead, they will be assessed qualitatively (See Section 6.4).

Statistical test
The aforementioned statistical test, assesses the correctness of a hypothesis. The main hypothesis (Z_0) is defined as follows:

Z_0 = The values of $H_{s,max}$ before 1986 (period A) are not significantly different from the ones after 1986 (Period B).

For this hypothesis there are two options, namely:
N1: The hypothesis is correct; there is no significant difference between both periods
N2: The hypothesis is incorrect; there is a significant difference between both periods

To decide which of the aforementioned options appear, there are two decisions possible:
B1: The hypothesis is rejected.
B2: The hypothesis is accepted.

In this way a total of four possible decision situations are possible, see Table 18:

Table 18: Possible decissions

	N1: Z_0 is correct	N2: Z_0 is incorrect
B1: Z_0 is rejected	Wrong decision	Proper decision
B2: Z_0 is accepted	Proper decision	Wrong decision

Because we are looking for evidence of a significantly increasing tendency of $H_{s,max}$, the decision corresponding with B1 and N2 is the most interesting one. In the present study it is further assumed that decisions based on a statistical test are proper ones. However, it must be noted that a decision based on a statistical test does not always have to results in proper decisions. As given in Table 18 there are two kinds of wrong decisions possible. A "wrong" decision corresponding with N1 and B1 is called an error of the first order. A "wrong" decision corresponding with N2 and B2 is called an error of the second order.

6.2. Background information of statistical test

Whether or not the observed increasing tendency of $H_{s,max}$ is really significant, in fact boils down to an investigation of the difference between the $H_{s,max}$ from data sets I and III. In this way, a significant difference between these two data sets implicates a significant increasing tendency of $H_{s,max}$. The statistical test is used to identify a significant difference between both data sets. For this purpose the test investigates whether or not the $H_{s,max}$ in data set III are likely to originate from the same population as the $H_{s,max}$ in data set I. If this is not the case, it is likely to assume a significant difference between both data sets.

As mentioned earlier, the statistical test assesses the correctness of a hypothesis. The hypothesis (Z_0) is already mentioned in Section 6.1. However, for the statistical test the hypothesis Z_0 needs to be expressed in a mathematical form. The hypothesis Z_0 assumed no significant difference between the values of $H_{s,max}$ from period A and period B. In fact this means the same as assuming no significant difference between the two mean values of the $H_{s,max}$ in period A and period B. Therefore the hypothesis Z_0 can be expressed as in Equation 24 and Equation 25.

$$Z_1: \overline{D}_{III} = \overline{D}_I \qquad\qquad\qquad \text{Equation 24}$$

$$Z_2: \overline{D}_I = \overline{D}_{III} \qquad\qquad\qquad \text{Equation 25}$$

$\overline{D}_i$ = Mean value of data set i

The hypothesis Z_0 is translated into two hypotheses, because both data sets can function as reference data set. First in Equation 24 data set III is compared with data set I, where data set I functions as the reference data set and data set III as the test data set. Secondly in Equation 25 the same comparison is made, but instead data set III functions as the reference data set and data set I as the test data set. In this way the hypothesis Z_0 is translated into two mathematical hypotheses Z_1 and Z_2 and the statistical test needs therefore to be carried out twice.

6.2.1. Student's t-Test

The statistical test meant in Section 6.2 is better known as the *Student's t-Test* (see [Lit 17]). The *Student's t-Test* uses the means ($\overline{D}_R$ and $\overline{D}_T$) and the standard deviation $s(D_T)$ of the data sets to evaluate whether or not the data sets originate from the same underlying population. $\overline{D}_R$ represents the mean of the samples in the reference data set, whereas $\overline{D}_T$ represents the mean of the samples in the test data set. To perform a standard *Student's t-Test*, the samples in D_R and D_T must be taken from a normally distributed population. The standard deviations of the data sets (I and III) in relation to the difference between their means, is a measure for the degree to which the underlying populations can be distinguished. This is illustrated in Figure 33. The degree of distinction increases from graph A to B to C.
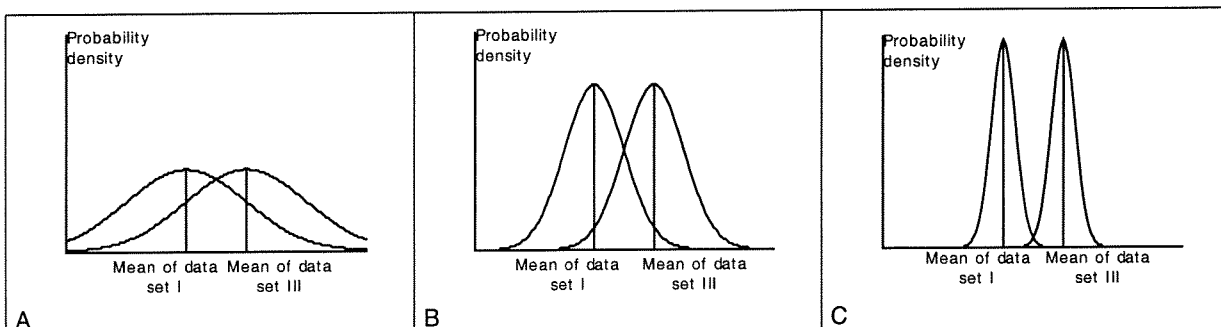
Figure 33: Possible means and standard deviations of the two data sets

The figures in Figure 33 could be for instance the probability density distributions of $H_{s,\,max}$ in periods A and B (data set I and III). Clearly, we would conclude that the two data sets appear most different or distinct in Figure 33C, because there is relatively little overlap between the two curves. With the *Student's t-Test* it is possible to quantify this overlap and make a quantitative decision whether the two data sets are significantly different. To find out if two data sets are significantly different, the *Student's t-Test* tests (to a certain level of reliability) for the correctness of a hypothesis (for example Z_1 and Z_2). When the test rejects these hypotheses, it is assumed that the samples in both data sets are significantly different and therefore do not originate from the same underlying population.

To asses the correctness of the hypothesis, the *Student's t-Test* uses a parameter, the so-called test parameter t. The parameter is given in Equation 26.

$$t = \frac{\bar{D}_T - \bar{D}_R}{s(D_T)/\sqrt{N_T}}$$

Equation 26

t	=	*Student's t-Test* parameter
$\bar{D}_R$	=	Mean of the samples in the reference data set
$\bar{D}_T$	=	Mean of the samples in the test data set
s( )	=	Standard deviation of the samples in a data set
N_T	=	Number of independent samples in the test data set

The testing parameter t gives an indication of the correctness of the hypothesis. Values of t far from zero indicate the incorrectness of the hypothesis, while values close to zero indicate its correctness. The remaining question is however, how far t may differ from zero before the hypothesis will be rejected. The answer to this question is found by defining an interval around t= 0. When the parameter t lies within this interval, the hypothesis is excepted, otherwise the hypothesis is rejected. Such an interval is called a confidence interval. First one has to assume a certain relative confidence interval (for instance a 95 or 90% confidence interval). Secondly this relative interval has to be translated to a confidence interval in terms of t.

It is possible to determine such a confidence interval by the assumption that the values of the testing parameter t can be described with the stochastical value (t̲). In the case of normally distributed data, t̲ is described with the so-called t-function. In other words, in that case t̲ is t-distributed. The shape of the t-function is symmetrical around t= 0 and has a similar shape as a normal probability density function. Knowing the probability density function of t̲ it is possible to find the boundaries of the confidence interval in terms of t.

6.2.2. Studentized bootstrap
In cases where data sets of for example $H_{s,\,max}$ cannot be described with a normal distribution, the standard *Student's t-Test* can not be carried out. However, for data sets described by other distributions, it is possible to perform a slightly more complicated test. The test is called the *Studentized bootstrap* and is a variant of the normal *Student's t-Test* (see [Lit 17] for a complete description of the *Studentized bootstrap*).

The *Studentized bootstrap* uses the test data set (D_T) for creating new data sets. The new data sets are created by taking and returning (bootstrapping) of the samples from the test data set. In this way an arbitrary amount of new data sets can be created. For every new (bootstrapped) data set, the value of the testing parameter t* is determined. The t* parameter is the same parameter as the t parameter in Equation 26, except the subscript * indicates that t is derived from a bootstrapped data set. It is further assumed that the values of t* represent the probability density function of t̲. Assuming for instance a confidence interval of 90% and an amount of 1000 bootstrapped data sets, the confidence interval in terms of t* is given in Equation 27. A scheme with the exact strategy to perform a *Studentized bootstrap* is given in Annex XI.

$t^{50} < t_1$ and $t_2 < t^{951}$

<div align="right">Equation 27</div>

t^{50} = the 50th value of the bootstrapped t in order of magnitude

t^{951} = the 951st value of the bootstrapped t in order of magnitude

6.3. Application of the statistical test

In this Section the statistical test as described in the previous Section will be applied to data sets I and III containing the samples of $H_{s,max}$. It was possible to see each sample (each $H_{s,\ max}$ during a particular hurricane) as a realisation of a stochastic value. The dependency between the samples (or stochastic values) is unknown. But it is very unlikely to assume a relation between the $H_{s,\ max}$ from a hurricane, acting at this present moment and the $H_{s,\ max}$ from a previous hurricane. Therefore the samples in the data sets are assumed to be realisations of independent stochastic values. Commonly, confidence intervals of 90 or 95 % are used for statistical tests. Within the present study the statistical test is based on a <u>confidence interval of 90%</u>.

Influence of hurricane Lenny on the test result

The ability of the statistical test to identify a significant difference between the values of $H_{s,max}$ from data sets I and III can be disturbed by the presence of an unusual large value of $H_{s,max}$ (for instance a $H_{s,max}$ corresponding with a return period of 500, 1000 or 10000 years). In the case of the presence of such an unusual $H_{s,max}$ it may be possible that the hypotheses Z_1 and Z_2 are rejected in a wrong way, resulting in a decision error of the first order (see Table 18).

Looking to Figure 77 in Annex X, hurricane *Lenny* generated the largest value of $H_{s,max}$. Whether or not this $H_{s,max}$ disturbs the statistical test, will be investigated by carrying out the statistical test twice. The first test takes in account all of the 98 samples of $H_{s,max}$. The second test takes in account the same samples of $H_{s,max}$, except without the presence of the $H_{s,max}$ from hurricane *Lenny*. In this way 97 samples of $H_{s,max}$ are taken in account for the second test. In the case that both tests reject their hypotheses Z_1 and Z_2, or in other words conclude that the values of $H_{s,max}$ in data set III are significant larger than the ones in data set I, the $H_{s,max}$ from hurricane *Lenny* is assumed not to disturb the statistical test. It must be noted that performing the tests in this way does not tell anything of the return period corresponding with the $H_{s,max}$ from hurricane *Lenny*. The statistical tests only evaluate the influence of the $H_{s,max}$ from hurricane *Lenny* on the statistical test results. For convenience a scheme of the structure of the different statistical tests is given in Figure 34.

Test 1: Including the $H_{s,max}$ from hurrican Lenny
- 1a: data set I is used as reference
- 1b: data set III is used as reference

Test 2: Without the $H_{s,max}$ from hurrican Lenny
- 2a: data set I is used as reference
- 2b: data set III is used as reference
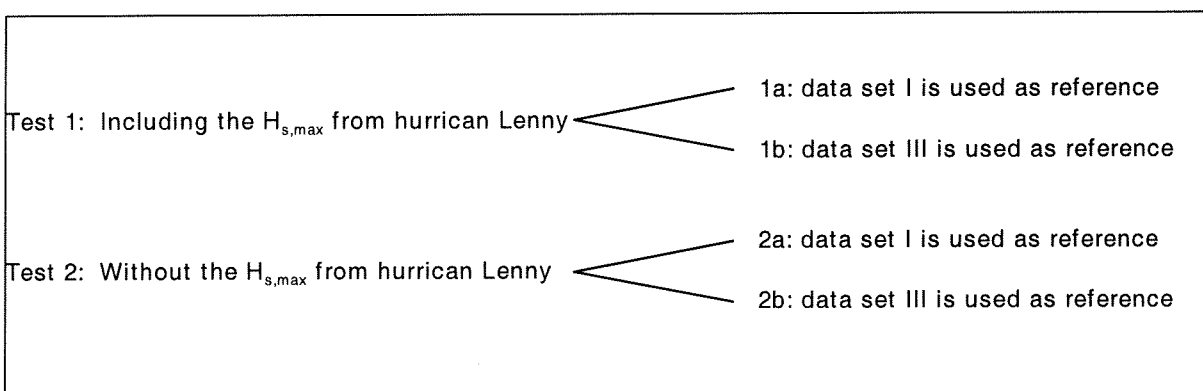
Figure 34: Explanation of the structure of the statistical tests

6.3.1. Test 1, including the sample of $H_{s,max}$ from hurricane Lenny

This section describes the statistical test by taking in account all of the 98 samples of $H_{s,max}$, including the $H_{s,max}$ from hurricane *Lenny*. The characteristics of both data sets with $H_{s,max}$ (data sets I and III) are given in Table 19. The samples of $H_{s,max}$ from both data sets can be approximated with an exponential probability density function, see Equation 28 and Figure 35.

Table 19: Characteristics of the data sets with $H_{s,max}$ (including hurricane Lenny)

Period	Data set	Number of samples	$\bar{D}_i = \bar{H}_{s,max}$	$s(D_i) = s(H_{s,max})$
A) 1972-1986	I	43	1.721	1.865
B) 1987-2000	III	55	2.444	2.345

Exponential probability density function:

$$f_{\underline{x}}(x) = \begin{cases} \dfrac{1}{\mu_{\underline{x}}} \exp\left(-\dfrac{(x-\beta)}{\mu_{\underline{x}}} \right) & , x \geq \beta \\ 0 & , x < \beta \end{cases}$$

Equation 28

x = The actual value of $H_{s,max}$

$\underline{x}$ = Stochastic value of $H_{s,max}$ ($\underline{H}_{s,max}$)

$\mu_{\underline{x}}$ = Mean value of the stochastical value $\underline{H}_{s,max}$ ($\mu_{\underline{H}s,max}$)

β = Threshold. The threshold coincides with $H_{s,max}= 0$, and $\beta= 0$. Defining the threshold is necessary because exponential distributions do not exist where $H_{s,max}$ becomes negative.

Data set I

Distribution of $H_{s,max}$ during period A (1972-1986), 43 samples

A

Data set III (Including $H_{s,max}$ of hurricane Lenny)

Distribution of $H_{s,max}$ during period B (1987-2000), 55 samples

B
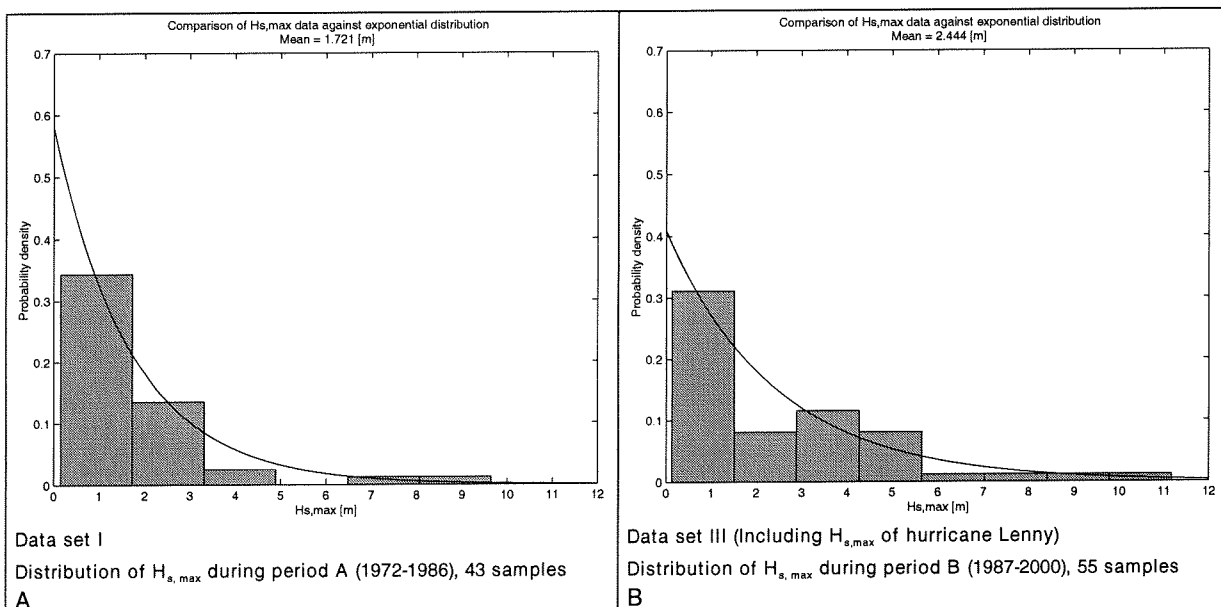
Figure 35: Distributions of $H_{s,max}$ in data set I and III (including hurricane Lenny)

Because of the two hypotheses Z_1 and Z_2 (See beginning of Section 6.2), the testing parameter t has two values as well, namely:

$$Z_1: \quad t_1 = \frac{\bar{D}_{III} - \bar{D}_I}{s(D_{III})/\sqrt{N_{III}}} = \frac{2.444 - 1.721}{2.345/\sqrt{55}} = 2.288 \qquad \text{Equation 29}$$

$$Z_2: \quad t_2 = \frac{\bar{D}_I - \bar{D}_{III}}{s(D_I)/\sqrt{N_I}} = \frac{1.721 - 2.444}{1.865/\sqrt{43}} = -2.544 \qquad \text{Equation 30}$$

The bootstrapped values of t* are presented in histograms. These histograms are assumed to approximate the probability densities of $\underline{t}_1$ and $\underline{t}_2$. See Figure 36.
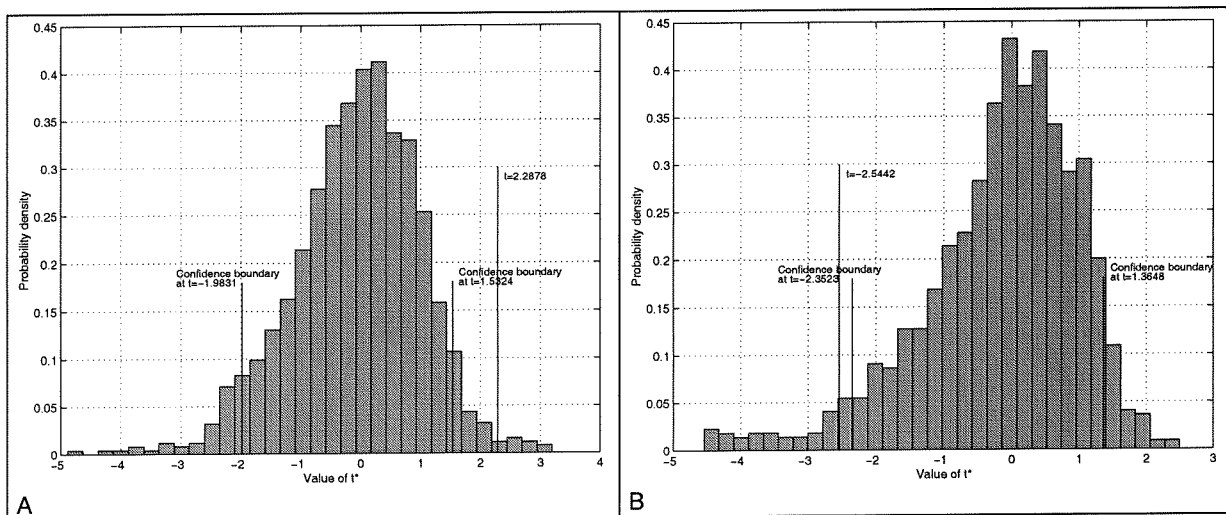
Figure 36: Approximated probability density functions of $\underline{t}_1$ (A) and $\underline{t}_2$ (B) (including hurricane Lenny)

The 90% confidence intervals for t_1 and t_2 become (see Equation 27 at the end of Section 6.2 for an explanation of the confidence intervals):

- Confidence interval 1 $-1.9831 < t_1 < 1.5324$ (Figure 36A)
- Confidence interval 2 $-2.3523 < t_2 < 1.3648$ (Figure 36B)

Conclusion

The test parameters t_1 and t_2 lie outside the 90% confidence interval. Therefore based on these test results both hypotheses Z_1 and Z_2 are rejected. In other words, there is a significant difference between the values of $H_{s,max}$ in period A and period B. In period B the values of $H_{s,max}$ are significantly larger.

6.3.2. Test 2, without sample of $H_{s,max}$ from hurricane Lenny

In this Section the statistical test is carried out without the sample of $H_{s,max}$ from hurricane *Lenny*. Data set I stays unchanged, but data set III is reduced by one sample and contains 54 instead of 55 samples. The characteristics of both data sets are given in Table 20. Disregarding the sample of $H_{s,max}$ from hurricane *Lenny* results in a slightly different probability density function of data set III. See Figure 37.

Table 20: Characteristics of the data sets wit $H_{s,max}$ (without hurricane Lenny)

Period	Data set	Number of samples	$\bar{D}_i = \bar{H}_{s,max}$	$s(D_i) = s(H_{s,max})$
A) 1972-1986	I	43	1.721	1.865
B) 1987-2000	III	54	2.283	2.035

Data set III (Without hurricane Leny)

Distribution of $H_{s,max}$ during period B (1987-2000), 54 samples
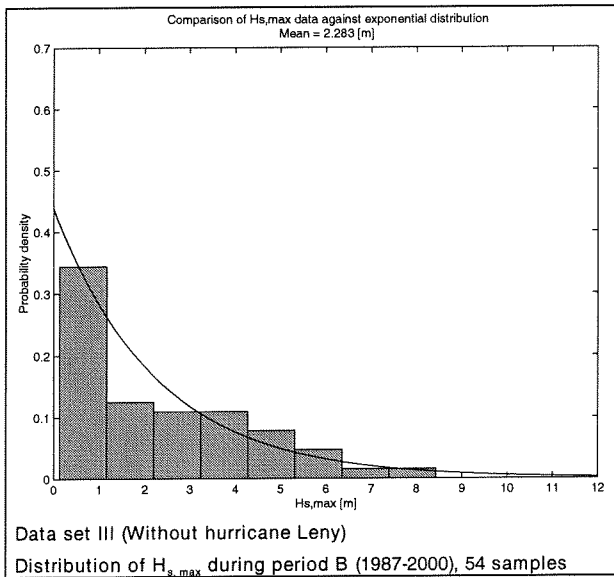
Figure 37: Distribution of $H_{s,max}$ in data set III (without hurricane Lenny)

The testing parameter t has again two values, namely:

$$Z_1: t_1 = \frac{\bar{D}_{III} - \bar{D}_I}{s(D_{III})/\sqrt{N_{III}}} = \frac{2.283 - 1.721}{2.035/\sqrt{54}} = 2.029$$

Equation 31

$$Z_2: t_2 = \frac{\bar{D}_I - \bar{D}_{III}}{s(D_I)/\sqrt{N_I}} = \frac{1.721 - 2.283}{1.865/\sqrt{43}} = -1.976$$

Equation 32

The bootstrapped values of t* are presented in histograms. These histograms are again assumed to approximate the probability density of $\underline{t}_1$ and $\underline{t}_2$. See Figure 38.
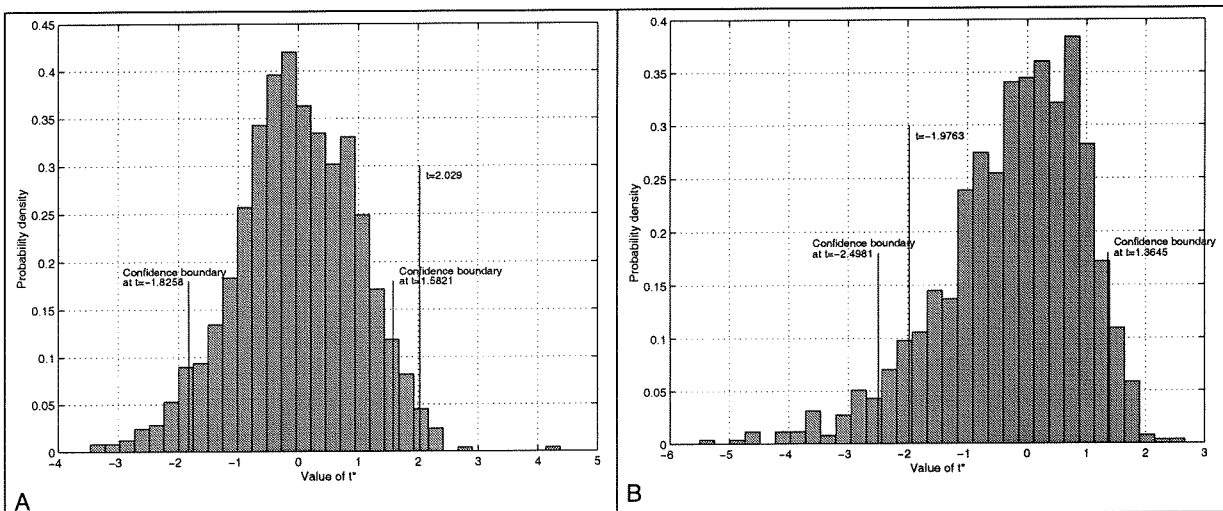
Figure 38: Approximated probability density functions of $\underline{t}_1$ (A) and $\underline{t}_2$ (B) (without hurricane Lenny)

The 90% confidence intervals for t_1 and t_2 become (see Equation 27 at the end of Section 6.2 for an explanation of the confidence intervals)::
- Confidence interval 1 $-1.8258 < t_1 < 1.5821$ (Figure 38A)
- Confidence interval 2 $-2.4981 < t_2 < 1.3645$ (Figure 38B)

Conclusion

The test parameter t_1 lies outside confidence interval 1, leading to rejection of the hypothesis Z_1, see Figure 38A. The test parameter t_2 lies within confidence interval 2, leading to acceptation of the hypothesis Z_2, see Figure 38B. The problem is that both tests (2a and 2b) lead to different decisions regarding the acceptation and/or rejection of the hypotheses. This makes it more difficult to verify whether or not the values of $H_{s,max}$ in period B (or data set III) are significantly larger than the ones in period A (or data set I). However, looking to Figure 38B, the test parameter t_2 is positioned far from zero, but close to the left boundary of the confidence interval (thus in other words, almost leading to rejection of the hypothesis). By taking in account the rejection of Z_1 the overall decision of both statistical tests is that the $H_{s,max}$ in period B are significantly larger than the ones in period B.

6.3.3. Interpretation of test results

According to Test 1 and Test 2 as described in the Sections 6.3.1 and 6.3.2, both hypotheses Z_1 and Z_2 are rejected. These rejections indicate that the values of $H_{s,max}$ in period B were significantly larger than the ones in period A. As mentioned in Section 6.1 with the rejections of both hypotheses it is likely that wave heights have significantly increased during the existence of the harbour (1972 till 2000).

6.4. Application qualitative test on the wave directions (θ)

This Section describes the differences in wave directions (corresponding with the $H_{s,max}$) between data sets II and IV (see Section 6.1). It is again possible to see each sample of θ in the two data sets (data set II and IV) as realisations of stochastic values. Assuming independence between the wave directions, the probability density function of both periods (A and B) can be estimated with a normal probability density function, see Equation 33.

Normal probability density function:

$$f_{\underline{x}}(x) = \frac{1}{\sigma_x \sqrt{2\pi}} \exp\left(-\frac{1}{2}\left(\frac{x - \mu_x}{\sigma_x}\right)^2\right), \; x \in \Re \qquad \text{Equation 33}$$

where:
- x = The actual value of θ
- $\underline{x}$ = Stochastic value of θ ($\underline{\theta}$)
- μ_x = Mean value of the stochastical value $\underline{\theta}$ (μ_θ)
- $\sigma_{\underline{x}}$ = Standard deviation of $\underline{\theta}$

The normal probability density functions of the wave directions can be approximated with histograms. In Figure 39 the histograms for both periods are given. According to Figure 39, the mean wave directions show a difference of approximately 10 [°].
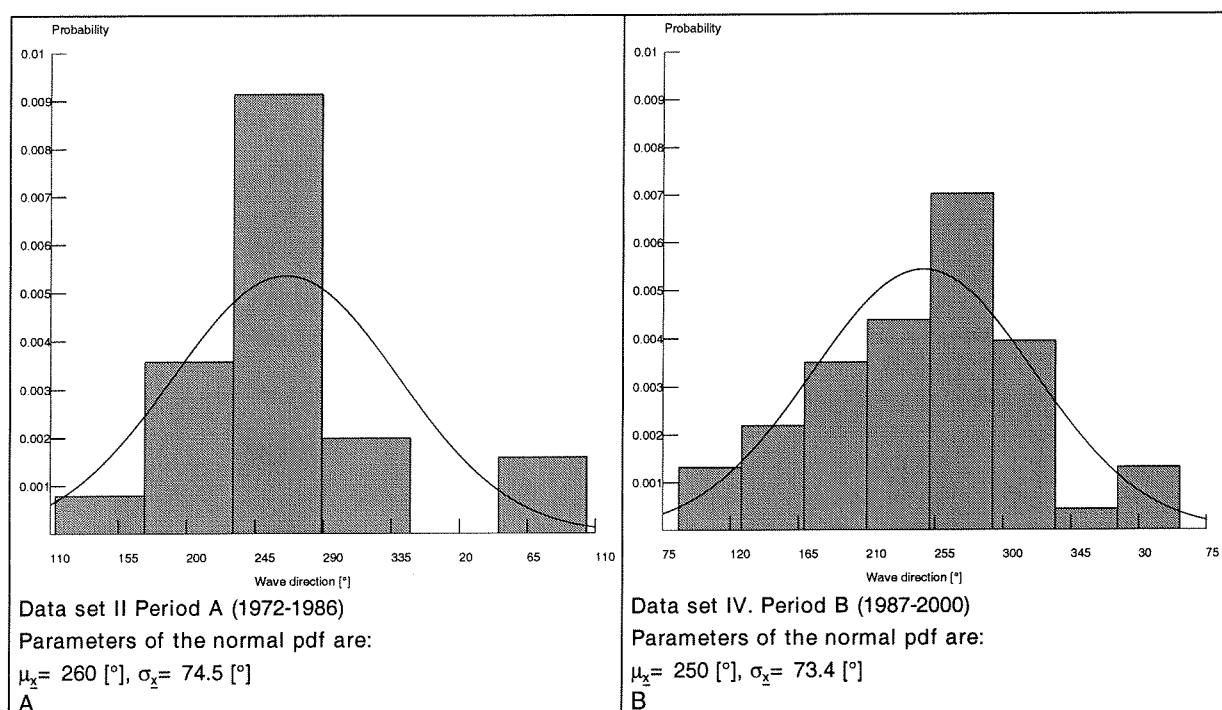
Figure 39: Comparison of wave directions with a normal density function

The hurricanes corresponding to the largest values of $H_{s,max}$ in data set III (period B: 1987 till 2000) were probably responsible for the damage to the harbour structures. Therefore it is more useful to determine the differences between the wave directions corresponding to the largest $H_{s,max}$ from both data sets. In Table 21 the differences are given.

Table 21: Hurricanes responsible for the highest $H_{s,max}$ and their corresponding θ in period A and B

Hurricane	Number	$H_{s,max}$ [m]	θ [°]	$\bar{\theta}$ [°]
Period A (1972-1986)				
David (1979)	22	9.645	172.56	174.93
Allen (1980)	24	7.533	177.29	
Klaus (1984)	36	4.285	270.96	250.14
Gloria (1985)	39	4.107	229.31	
Period B (1987-2000)				
Lenny (1999)	93	11.164	189.15	189.10
Hugo (1989)	52	8.426	189.05	
Luis (1995)	71	7.217	267.85	239.67
Marilyn (1995)	72	6.146	211.49	
Difference			**14.17**	**10.47**

In period A the "two" largest waves came from a direction coinciding with the opening between the *Saba bank* and the island of *St. Eustatius*. It is indeed most likely that the largest waves come from this direction, because there is a small corridor to deep-water without any obstacles. However, in period B the largest waves (even higher waves than in period A) did not come from the small corridor, but came from a direction coinciding with a relatively shallow area of the *Saba bank*. One should expect waves travelling from this direction to be hindered by the relatively shallow area of the *Saba bank* and therefore be reduced. The differences between the wave directions corresponding to the most extreme hurricanes (according to Table 21) are visualised in Figure 40.
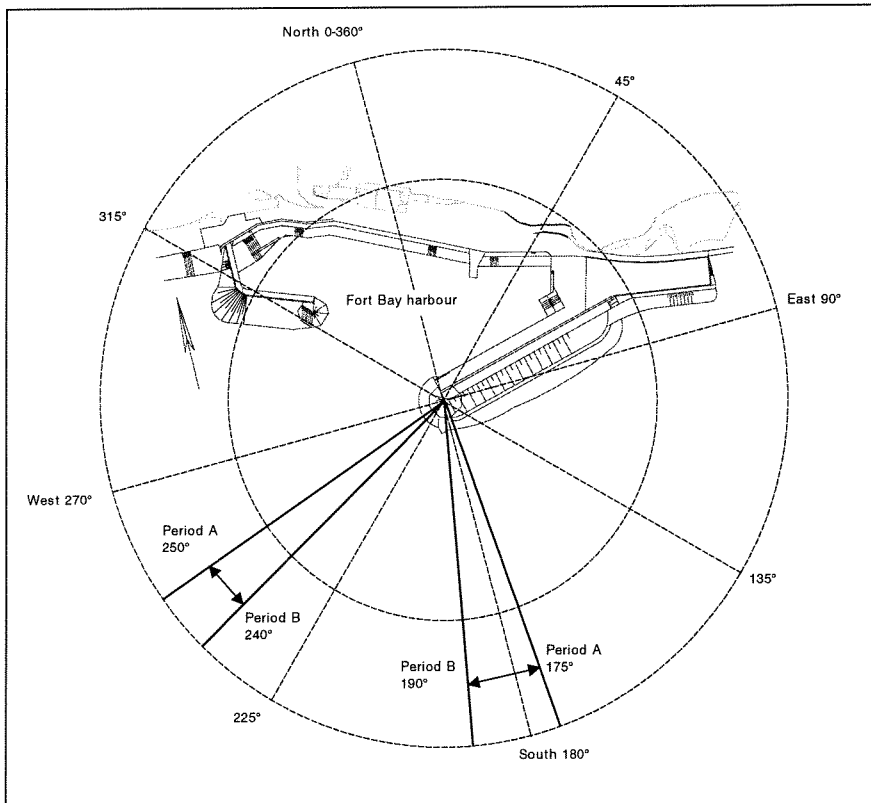
Figure 40: Differences in wave directions corresponding to the largest wave attack

Figure 40 is only valid when refraction due to water depth variations is disregarded. Probably refraction does not play a significant role, due to the steep sloping shore in the area around *Fort Bay* harbour. Therefore the deep-water wave directions do not change much when they arrive at *Fort Bay* harbour and are the straight lines in Figure 40 justified. Looking at Figure 40 the differences in wave directions do not result in a completely different attack on the harbour structures. Therefore it is assumed that the wave directions did not change significantly.

Conclusion
The mean wave directions of waves during hurricanes changed from 260 [°] to 250 [°]. The directions of the waves generated by the largest hurricanes in both periods, differed from each other by approximately 10 to 14 degrees. The differences between the directions of the mean and extreme hurricane waves are not significant, because they do not result in a completely different direction of wave attack on the harbour structures.

7. QUANTIFICATION OF DIFFERENCES BETWEEN WAVE CONDITIONS

7.1. Approach
Among others, Chapter 6 concluded a significant increase of the deep-water wave heights during hurricanes. However, the amount of increase still has to be determined. Furthermore the test concluded that hurricane *Lenny* (or at least the sample of $H_{s,max}$ from hurricane *Lenny*) did not have a significant influence on the statistical test result. However, it was noted that this conclusion gave no reliable information regarding whether or not *Lenny* was an unusual event (with return periods of for instance 500, 1000 or 10000 years). Therefore there remain two questions:
1. Were wave conditions during hurricane *Lenny* accidental with a return period of for instance 500, 1000 or 10000 [year]?
2. To what extend needs the deep-water design wave height, as used by *CEC* for their latest restoration design (1995), to be adjusted?

To find an answer to these questions, the samples of $H_{s,max}$ in data sets I (period before 1986) and III (period after 1986) will be statistically extrapolated to an exceedance level that is commonly used for the design of "rubble mound" breakwaters. The difference between these two extrapolations is a measure of the increase of the $H_{s,max}$ during the years 1972 till 2000 (age of the harbour). By the determination of the return period corresponding to the $H_{s,max}$ of hurricane *Lenny*, it is judged whether or not wave conditions during hurricane *Lenny* were accidental. Finally design wave heights resulting from these extrapolations will be compared with the design wave height as used by *CEC* for their latest design (restoration design, year 1995).

First the extrapolation techniques are discussed, secondly the extrapolations will be carried out and the difference in values of $H_{s,max}$ from both data sets (I and III) will be quantified. Finally the comparison is made between the extrapolations and the used design wave height as used by *CEC*.

7.2. Extreme value estimation

7.2.1. Theory
In the present study, extreme hurricane conditions ($H_{s,max}$) are estimated from statistical extrapolation of available hindcast data. In particular, we will fit the *Weibull* probability distribution to the *DOLPHIN-B1* results gathered in data sets I and III. The probability distribution (F) and the probability density function ($f = dF / dH_{s,max}$) are given in Equation 34 and Equation 35.

$$F(H_{s,max}) = 1 - \exp\left(-\left(\frac{H_{s,max} - \beta}{\sigma}\right)^{\alpha}\right)$$

Equation 34

$$f(H_{s,max}) = \frac{\alpha}{\sigma} * (H_{s,max})^{\alpha-1} * \exp(-(H_{s,max})^{\alpha})$$

Equation 35

where:
F   =   Non-exceedance probability
f   =   Probability density
β   =   Threshold parameter
σ   =   Scale parameter
α   =   Shape parameter

For the parameters σ and α, maximum likelihood estimates are used and the parameter β is chosen in such a way that the RMS difference between fit and data reaches its minimum. In most applications,

the threshold is used to discriminate presumably *Weibull* distributed data from other data. In the present study however, we assume that the $H_{s,max}$ corresponding to all selected hurricanes follow this type of distribution. As it is not possible to estimate the threshold (β) with the maximum likelihood technique, its value is determined by minimising the aforementioned RMS difference.

The described technique requires that a non-exceedance probability is associated to each $H_{s,max}$ in the data set. The plotting rule from [Lit 14] is used for this purpose. It is given by:

$$F(H_{s,max}) = 1 - \frac{m - a}{N + b}$$

<div align="right">Equation 36</div>

F   = Non-exceedance probability
m   = Rank of data sample; in this case, m= 1 refers to the highest value of $H_{s,max}$ in the data set
N   = Number of samples in data set
a, b   = Coefficients depending on the shape parameter α, see Equation 37 and Equation 38

$$a = 0.30 + \frac{0.18}{\alpha}$$

<div align="right">Equation 37</div>

$$b = 0.21 + \frac{0.32}{\alpha}$$

<div align="right">Equation 38</div>

Further the expression of the likelihood function L (in this case the log-likelihood function) to determine α and σ, is given in Equation 39.

$$\ln(L) = N * \ln\left(\frac{\alpha}{\sigma}\right) + (\alpha - 1) * \sum_{j=1}^{N} \ln(H_{s,max,j}) - \sum_{j=1}^{N} \exp(\alpha \ln(H_{s,max,j}))$$

<div align="right">Equation 39</div>

Equalling the derivatives of Equation 39 to zero ($\partial L/\partial \alpha = \partial L/\partial \sigma = 0$) will result in an estimation of the parameters α and σ. The RMS difference ε between the fit and the data samples $H_{s,max}$ to determine the threshold parameter β is given in Equation 40.

$$RMS = \sqrt{\frac{1}{N} \sum_{i=1}^{N} \varepsilon^2}$$

<div align="right">Equation 40</div>

in which $\varepsilon = \left(1 - \frac{m - a}{N + b}\right) - F(H_{s,max})$.

Two steps in the process of fitting the *Weibull* probability distribution to a data set is visualised in Figure 41.
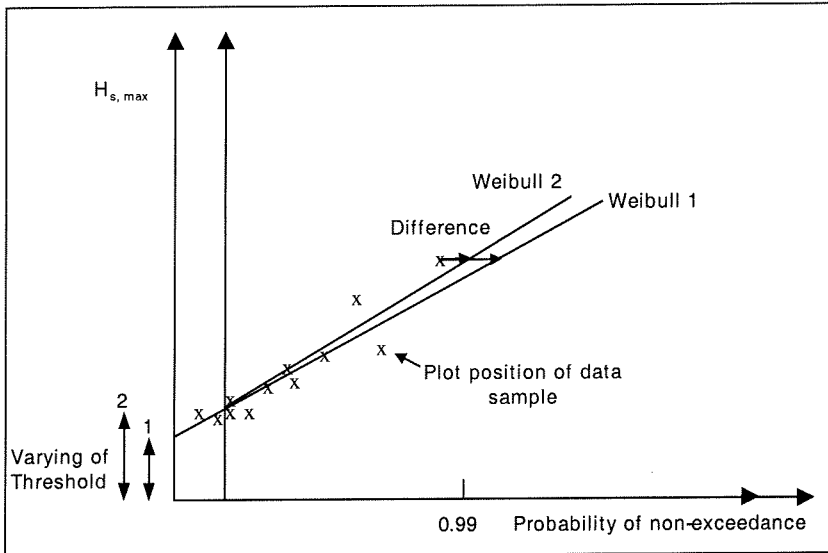
Figure 41: Process of fitting the Weibull distribution to a data set

7.2.2. Application

To determine the threshold β corresponding to the *Weibull* fit, for both data sets (I and III) with $H_{s,max}$, the development of the RMS probability difference vs. the choice of the threshold is given in Figure 42. The *Weibull* fit parameters are given in

Table 22 and the *Weibull* fit distributions to both data sets are given in Figure 43 and Figure 44.
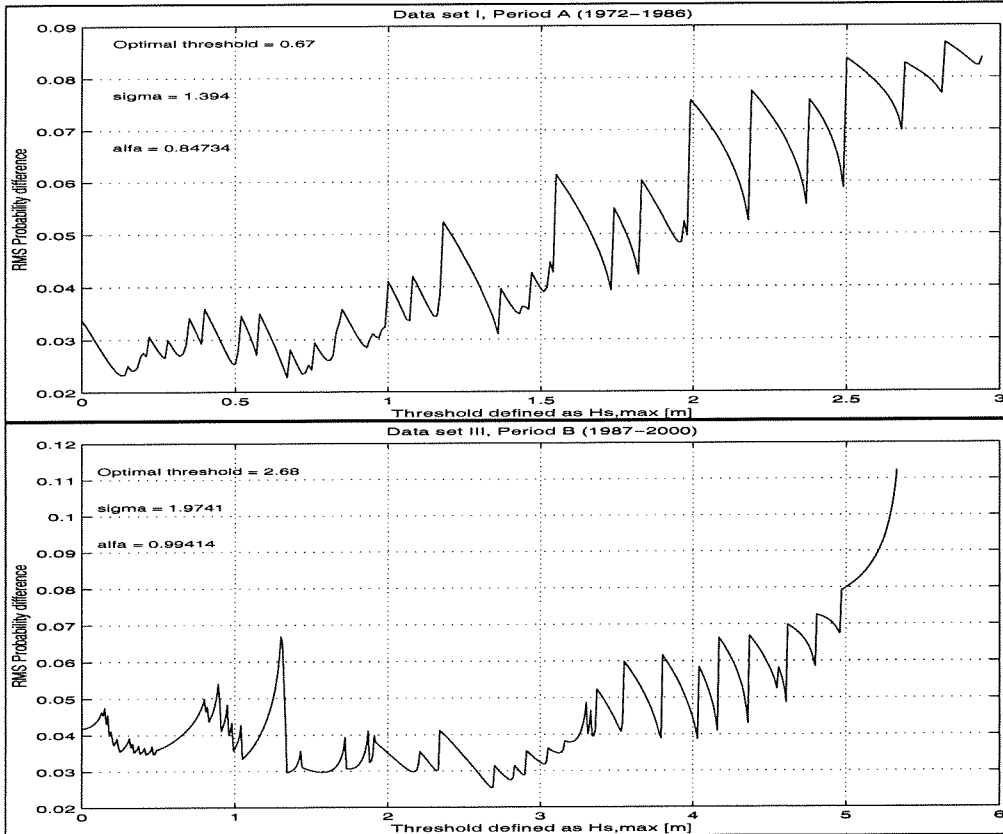
Figure 42: Development of the RMS difference of the probability vs. the choice of the threshold

Table 22: Parameters of the best Weibull fits

Period	Data set	Weibull fit parameters			Original number of samples	Sample size after adjustment to the threshold
		Threshold				
		β [m]	σ [m]	α		
A) 1972-1986	I	0.67	1.394	0.847	43	32
B) 1987-2000	III	2.68	1.974	0.994	55	23
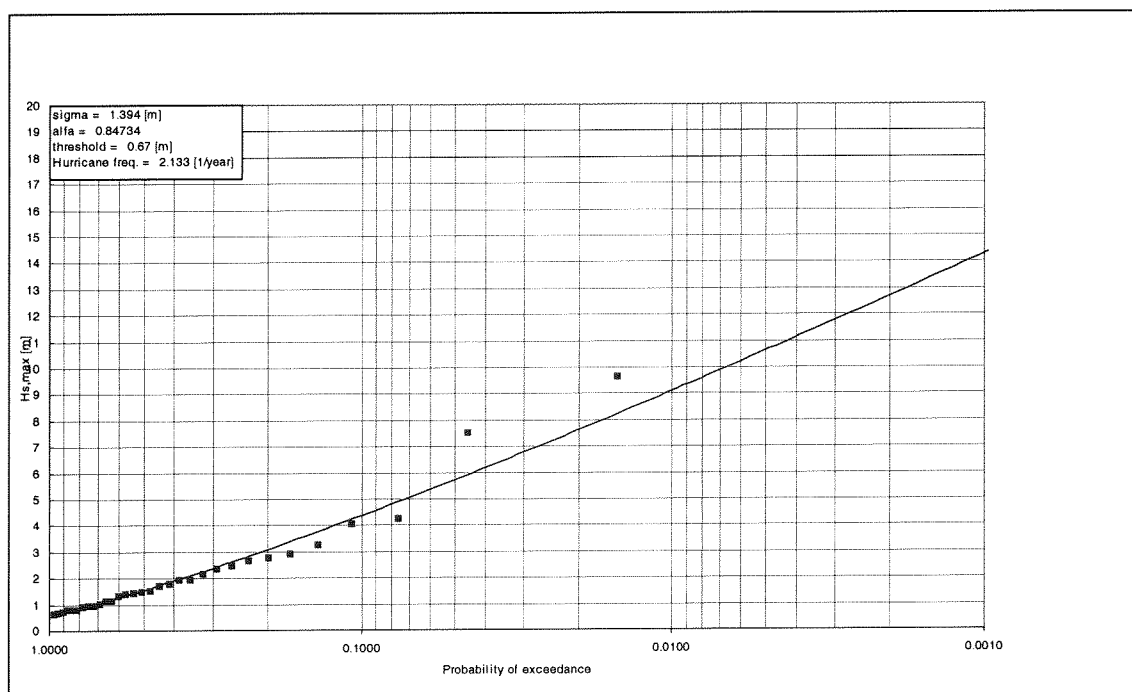
Figure 43: Weibull fit to data set I ($H_{s,max}$, in period 1972-1986)
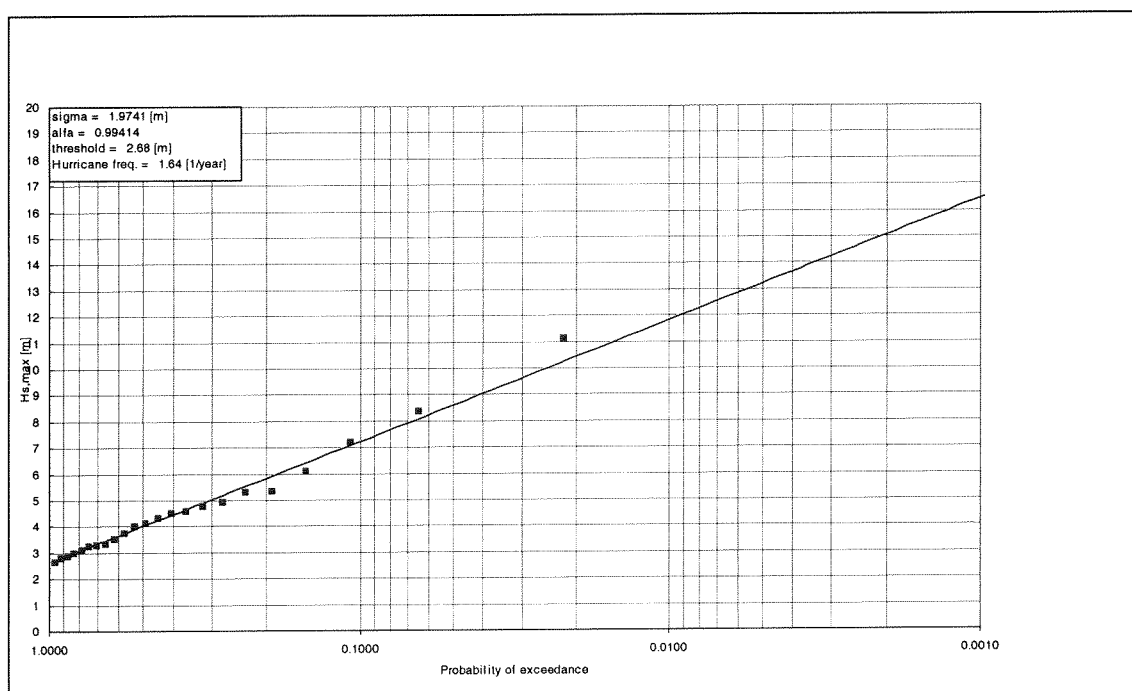
Figure 44: Weibull fit to data set III ($H_{s,max}$, in period 1987-2000)

7.3. Quantification of differences between the Weibull fits

The *Weibull* distributions (Figure 43 and Figure 44) do not give information about the interval of time between occurrences of various $H_{s,max}$. The interval of time of interest is the return period (R_p). It is defined as the average interval, in years, between the occurrences of an $H_{s,max}$ equal to or greater than a certain amount of meters. The $H_{s,max}$ vs. return-period relationship is obtained by transforming the horizontal scale of both best *Weibull* fit distributions to a return-period scale. This is done through Equation 41.

$$R_p = \frac{1}{\lambda(1 - F)}$$

Equation 41

λ = Average number of hurricanes per year; λ is estimated by the ratio N/T

N   = Number of hurricanes in T years

T   = Period of time [year]

F   = Non-exceedance probability

Translating the horizontal scale of Figure 43 and Figure 44 into a scale of return periods, it is possible to plot both *Weibull* distributions in Figure 45. The differences between the $H_{s,max}$ in both data sets are quantified in Table 23. Looking to Figure 45, we see that both lines converge to each other.
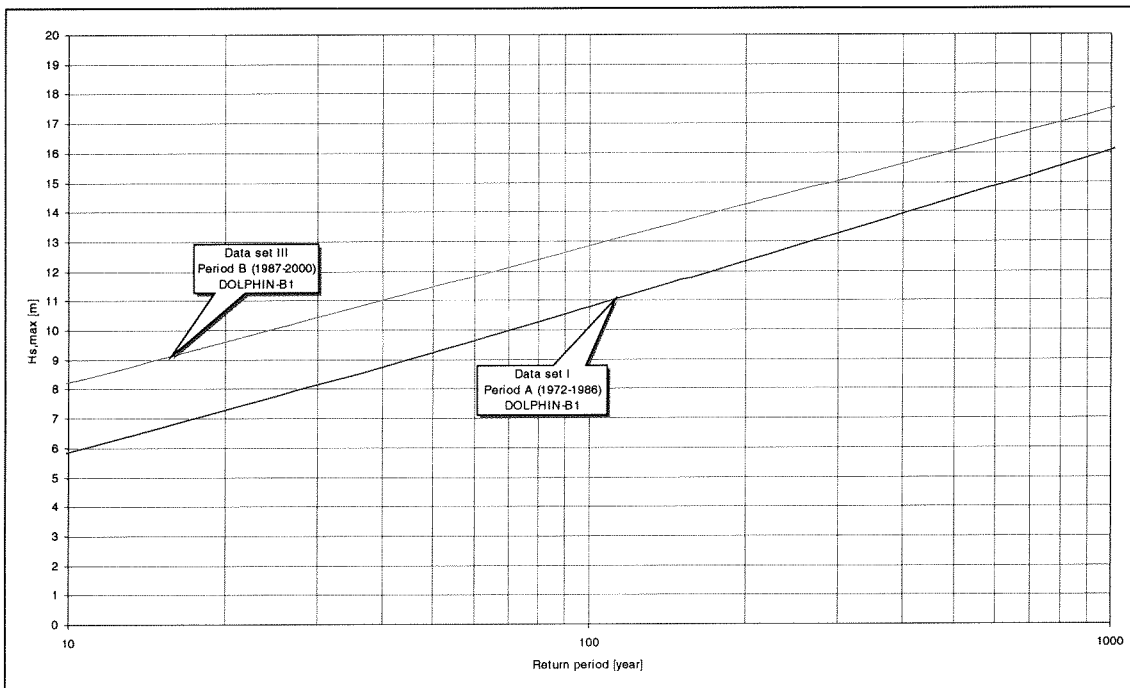
Figure 45: Weibull fits to data sets I and III

Table 23: Differences between the extrapolated values of $H_{s,max}$ in data sets I and III

Return-period	Data set I $H_{s,max}$ [m]	Data set III $H_{s,max}$ [m]	Difference in [m]
10	5.9	8.2	2.3
25	7.9	10.2	2.3
50	9.3	11.5	2.2
100	10.8	12.9	2.1

For deriving design conditions for "rubble mound" breakwaters commonly design conditions are applied corresponding with a return period in the range of 10 to 100 years. Overlooking this period it is clear that data set III contains significant larger wave heights than period I. In this way one must conclude that the tendency (as concluded in Chapter 6) of wave heights during the years 1972 till 2000 results in significant increased wave heights. In other words, there is reason to assume that the situation at *Fort Bay* harbour during hurricane conditions has become worse after 1986.

7.4. Comparison of wave conditions with the design conditions from CEC

To be able to answer the first question described at the beginning of Section 6.1 it has to be evaluated whether the design condition from *CEC* still corresponds with the increased wave conditions resulting from the extrapolations. However, a few remarks to this evaluation can be made, namely:

- The reliability of *DOLPHIN-B1* is unknown (or the ability of *DOLPHIN-B1* to estimate the "real" wave conditions is not known). Therefore this evaluation is only indicative.
- The extrapolations are made including hurricane *Lenny*. However, in the case that hurricane *Lenny* was indeed an unusual extreme event it probably should have been excluded from the extrapolations. Instead, it already has affected the results of the extrapolations in an increasing way and has therefore less chance to be identified as an unusual event.

The first remark forms a large obstruction for the verification of the design conditions from *CEC*. Therefore the *DOLPHIN-B1* results can only be used in a comparative (or indicative) way. In the present study the *DOLPHIN-B1* results are used in the following way:

1. Assume that *DOLPHIN-B1* gives accurate results.

   It is immediately possible to compare the design conditions from *CEC* with the results from *DOLPHIN-B1*, see Figure 45.

2. Assume that *Oceanroutes Inc.* gives accurate results and *DOLPHIN-B1* not.

   We assume the absolute differences between both extrapolations of the *DOLPHIN-B1* results (see Table 23) to be correct. After the determination of the systematic difference between *Oceanroutes Inc.* and *DOLPHIN-B1* as well it is possible to derive design conditions with the assumption that *Oceanroutes Inc.* gives correct results.

3. Assume that neither *DOLPHIN-B1* nor *Oceanroutes Inc.* give accurate results

   There is no estimation of design conditions possible.

Only in the first two cases it is possible to compare the design conditions from *CEC* with the ones from the extrapolations.

Assume that DOLPHIN-B1 gives accurate results

A commonly used return period for the design wave height of "rubble mound" breakwaters is 50 [years]. Looking to Figure 45 the wave height corresponding to a return period of 50 year has been increased from 9.3 [m] (period before 1986) to 11.5 [m] (period after 1986). The deep-water design wave height, as used by *CEC* for the latest harbour design, amounts to 9 [m] and is therefore not representative anymore for the period after 1986.

According to the *DOLPHIN-B1* computations hurricane *Lenny* generated a $H_{s,max}$ of 11.164 [m]. Looking to Figure 45 again, this value is smaller than the new design wave height of 11.5[m]. Therefore the maximum significant wave height during hurricane *Lenny* was not very unusual. Instead, it is likely to be the result of the general increase of $H_{s,max}$.

Assuming the hurricane hindcast of Oceanroutes Inc. as correct

For using *Oceanroutes Inc.* as reference, we first need to know the differences between wave heights resulting from *Oceanroutes Inc.* and from *DOLPHIN-B1*. Section 5.2 contains the comparison of *DOLPHIN-B1* with the results of a hindcast study from *Oceanroutes Inc.* For the comparison the same hurricanes were hindcasted by *DOLPHIN-B1* as were hindcased by *Oceanroutes Inc.* Differences between both hindcasts were already obtained in that Section. However, these differences were not based on extrapolations. To obtain the differences between *DOLPHIN-B1* and *Oceanroutes Inc.* from both hindcasts the values of $H_{s,max}$ will be extrapolated with *Weibull* fits. The differences between both *Weibull* fits represent the difference between wave heights resulting from *Oceanroutes Inc.* and from *DOLPHIN-B1*.

To determine the threshold β corresponding to the *Weibull* fit, for both hindcasts, the development of the RMS probability difference vs. the choice of the threshold is given in Figure 46. The *Weibull* fit parameters are given in Table 24 and the *Weibull* fit distributions to both hindcasts are given in Figure 47 and Figure 48.
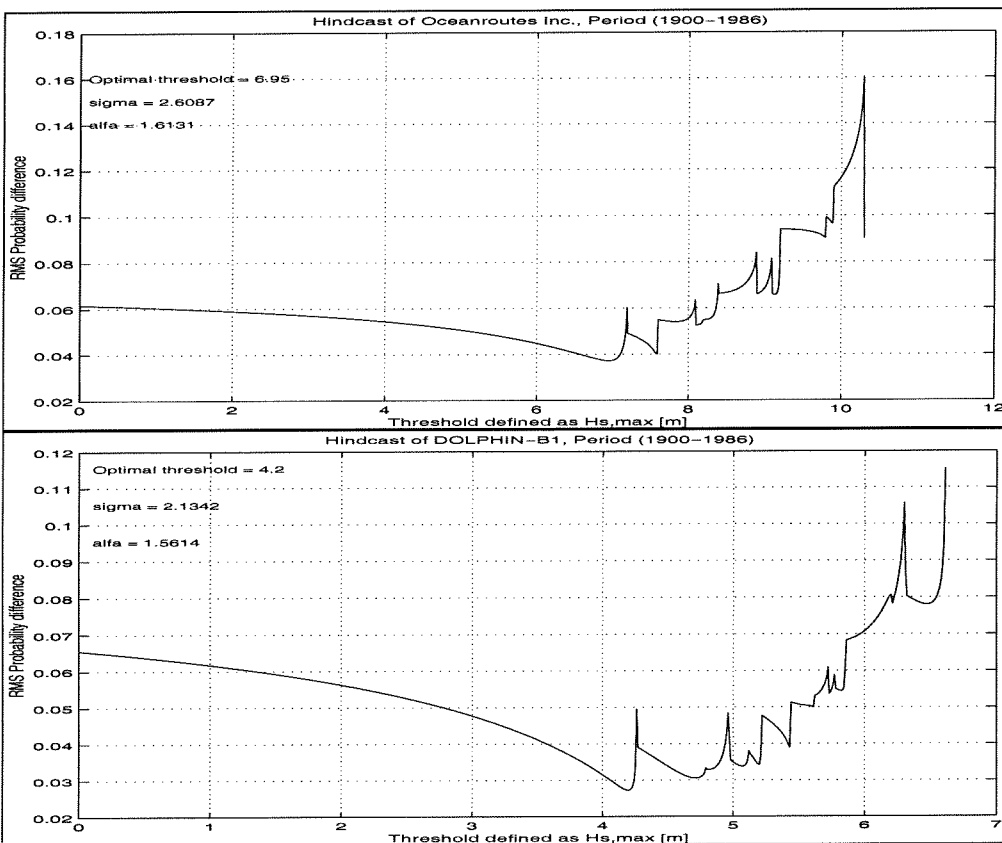
Figure 46: Development of the RMS difference of the probability vs. the choice of the threshold

Table 24: Parameters of the best Weibull fits

Period	Data set	Weibull fit parameters			Original number of samples	Sample size after adjustment to the threshold
		Threshold				
		β [m]	σ [m]	α		
1900-1986	*Oceanroutes Inc.*	6.95	2.6087	1.6131	20	20
1900-1986	*DOLPHIN-B1*	4.2	2.1342	1.5614	20	20
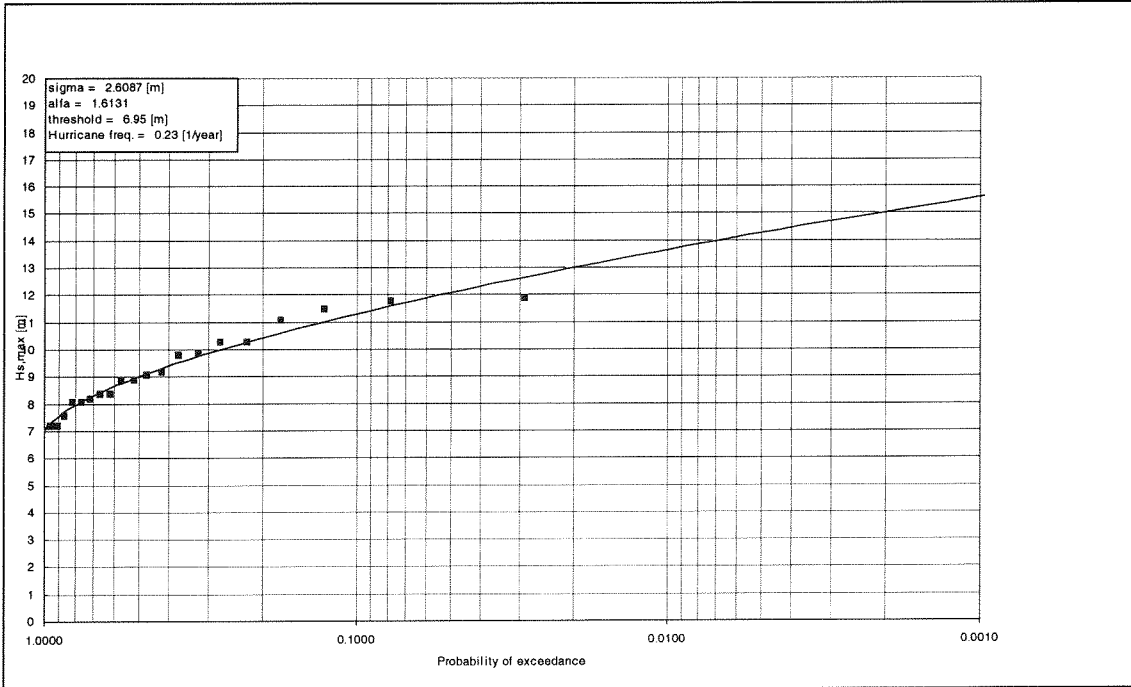
Figure 47: Weibull fit to hindcast from Oceanroutes Inc. (period 1900-1986)
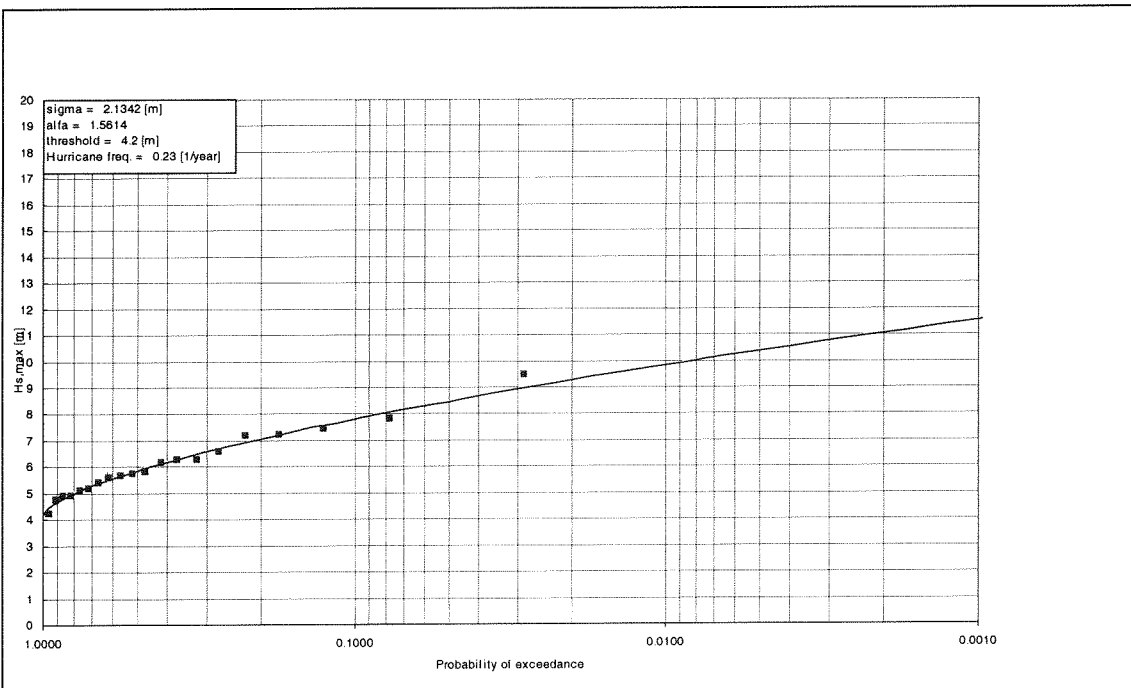
Figure 48: Weibull fit to hindcast from DOLPHIN-B1 (period 1900-1986)

Translating the horizontal scales into a scale of return periods, the *Weibull* fits to both hindcasts are given in Figure 49.
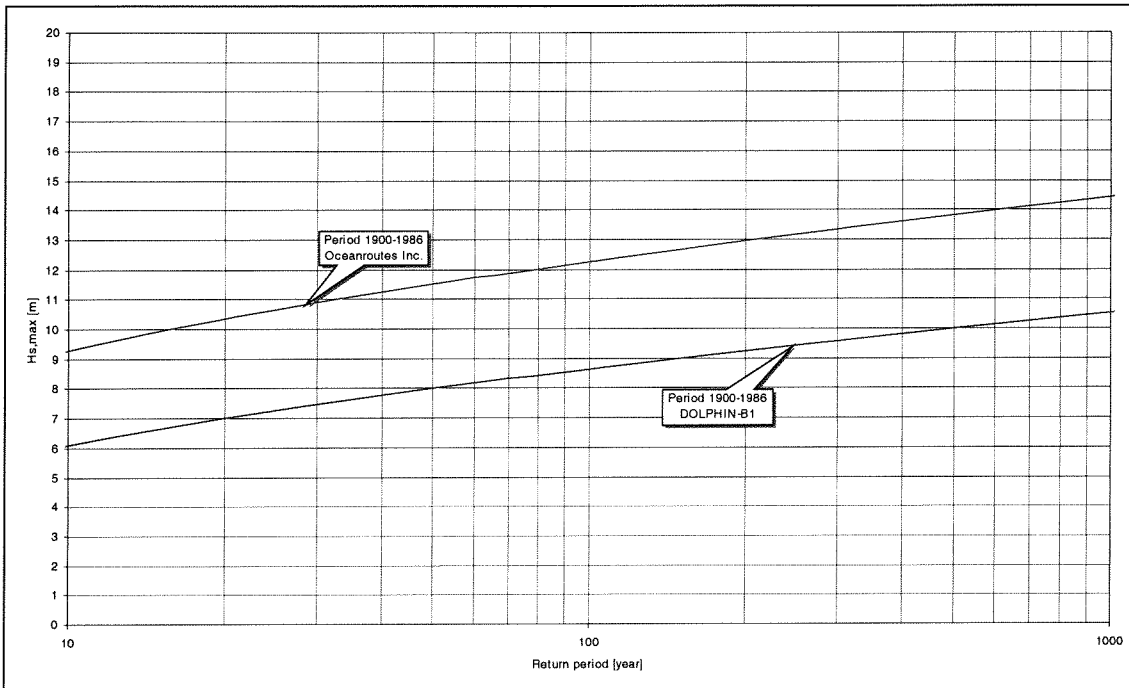
Figure 49: Differences between the Weibull fits to Oceanroutes Inc. and to DOLPHIN-B1

Both lines diverge from each other. In fact one tends to think that the blue line in Figure 49 represents the same line as the hurricane hindcast line in Annex II. However, the graphs can not be compared with each other, because the graphs have been constructed with different statistical tools.

The differences between *Oceanroutes Inc.* and *DOLPHIN-B1* are indicated in Table 25.

Table 25: Differences between the extrapolated values of $H_{s,max}$ from Oceanroutes Inc. and DOLPIN-B1

Return-period	Oceanroutes Inc. $H_{s,max}$ [m]	DOLPHIN-B1 $H_{s,max}$ [m]	Difference in [m]
10	9.3	6.1	3.2
25	10.7	7.4	3.3
50	11.5	8	3.5
100	12.3	8.6	3.7

For the range of return periods between 10 and 100 [year], the difference between *DOLPHIN-B1* and *Oceanroutes Inc.* amounts to ± 3.5 [m]. Therefore by adding 3.5 [m] to the wave heights from *DOLPHIN-B1*, the wave heights are adjusted to wave heights according to *Oceanroutes Inc.* For example: The design condition according to *Oceanroutes Inc.* (with a return period of 50 [year]) becomes 11.5 +3.5= 15 [m].

By taking *Oceanroutes Inc.* as reference the design wave height from *CEC* (9 [m]) is significantly lower than 15 [m] and adjustment of the design wave height is strongly recommended.

According to *DOLPHIN-B1* hurricane *Lenny* generated a $H_{s,max}$ of 11.164 [m]. Adjusting this wave height according to *Oceanroutes Inc.* hurricane *Lenny* generated a $H_{s,max}$ of 11.164+3.5= 14.664 [m]. Therefore the maximum significant wave height during hurricane *Lenny* was not very unusual. Instead, it is likely to be the result of the general increase of $H_{s,max}$.

8. CONCLUSIONS AND RECOMMENDATIONS

8.1. Conclusions

Fort Bay harbour is a small harbour, located at the South of the island of *Saba*. Since its construction in 1972, it has been exposed to several hurricanes. Unfortunately some of these hurricanes were responsible for damage to the harbour structures (mostly to the breakwaters). Especially hurricane *Lenny* (1999) left the harbour in the poor condition it still is in at present. About 9 years before *Lenny*, implementation of an extensive re-design of the harbour was completed. As in this re-design, special attention had been paid to the potentially devastating effects of hurricanes, questions have arisen about 'what went wrong?' In the first of the two parts of the present study, this type of question has been assessed in a general and qualitative manner. It has lead to an inventory of phenomena and mechanisms that may have caused that the re-design was not able to withstand the conditions that some hurricanes brought about. One of them is that the frequency and intensity of hurricanes may have increased over the years. Whether this has actually occurred, has been analysed in detail in the second part of the study. Conclusions and recommendations regarding both parts of the study are given hereafter.

Conclusions regarding PART 1

Looking at the history of *Fort Bay* harbour and at the evaluations regarding the applied design wave conditions and the stability of the harbour structures of the harbour reconstruction design (1990), several phenomena and mechanisms that may have caused the damage to the re-design of *Fort Bay* harbour were identified. These phenomena and mechanisms have been translated into several research questions. The questions have been divided into questions regarding the wave conditions (loads on the harbour structures) and into questions regarding the strength of the harbour structures. The research questions are:

Questions regarding the loads on the structures
The breakwaters are exposed primarily to hydrodynamic loads of which the worst are generated by hurricanes. In particular, it concerns wave attack in combinations with water level changes driven by waves, wind and spatial variations in atmospheric pressure. In the determination of design wave conditions, distinction has been made between generation of waves in comparatively deep-water in front of *Fort Bay* harbour and propagation of waves from deep-water to the breakwaters. With respect to the first of these two steps, the following question could be put forward:
1. Did deep-water wave conditions (in the area of *Fort Bay* harbour), generated during hurricanes, worsen significantly (higher waves and changed directions of wave propagation) during the existence of *Fort Bay* harbour (1972-2000)?

and with respect to the second step the following two other questions could be formulated:

2. What changes do the deep-water waves experience while propagating at a relatively steep sloping shore towards *Fort Bay* harbour?
3. What are the effects on the near shore wave conditions by taking water level variations into account?

Questions regarding the strength of the structures
The damages to the breakwaters that have occurred till so far were concentrated mostly to the *Accropode* revetments and the revetments made of rock penetrated with hydrocrete. Besides the aforementioned phenomena, which were related to the loads, other phenomena related to the strength of the harbour structures could have been responsible for the damages. In the case that some of these phenomena were not foreseen in previous harbour designs, unwillingly the strength of the breakwaters could have been overestimated. The following two questions are dealing with this possibility.

4. Is it possible to formulate mechanisms or phenomena that could have been responsible for the damage to the revetments consisting of *Accropode* elements, given the applied design wave conditions.

5. Is it possible to formulate mechanisms or phenomena that could have been responsible for the failure of the revetments consisting of rock penetrated with, given the applied design wave conditions.

Conclusions regarding PART 2

The second part of the present study deals with the possibility of hurricane conditions having worsened over the past decades to a level not foreseen in the latest breakwater designs of 1990 and 1995 (See research question 1). This possibility has been assessed with an extensive hindcasting exercise of hurricane conditions in the area around *Saba* with the physical mathematical wave model *DOLPHIN-B1*. Hereafter the results of this exercise have been subjected to a statistical analysis. Concluded was that deep-water wave conditions, occurred after 1986, were significantly worse than those encountered before that time.

Unfortunately, the described exercise could not be performed to its full potential, because hardly any field data were available for the present study. A proper verification of the hindcast results was therefore impossible. However, it appeared that differences between the results of this hindcast and the scarcely available field data are to some extend of a systematic nature. This was substantiated by a comparison of the hindcastresults with a hindcast study, performed by the American organisation *Oceanroutes Inc.* in support of the latest harbour design. A certain systematic difference between these hindcasts could be observed as well. Against this background, it has been reasoned that the *DOLPHIN-B1* hindcast computations can be used to identify changes in hurricane conditions encountered before and after 1986. The changes are listed in Table 26.

Table 26: Indication of the worsening of the deep-water wave height

Return period [year]	Period: 1972-1986 H_s [m]	Period: 1987-2000 H_s [m]	Worsening [%]
10	5.9	8.2	39
25	7.9	10.2	29
50	9.3	11.5	24
100	10.8	12.9	19

Quantification of the consequences of these changes in terms of breakwater design conditions was possible under the assumption of either the correctness of the hindcast study of *DOLPHIN-B1* or the correctness of the hindcast study of *Oceanroutes Inc.* Given these two assumptions, the deep-water design wave conditions are listed in Table 27.

Table 27: New deep-water design wave heights

Return period [year]	According to *DOLPHIN-B1* H_s [m]	According to *Oceanroutes Inc.* H_s [m]
10	8.2	11.7
25	10.2	13.7
50	11.5	15
100	12.9	16.4

Looking at the values in Table 27 the design deep-water wave condition of 9 [m] (as used for the harbour re-designs by *CEC*) is not representative anymore for the near future and needs to be increased. In this respect, the damages to the harbour could have been caused by the exceedance of the deep-water design wave conditions. However, in a further study it still must be investigated till what extend the exceedance of the deep-water design wave condition resulted in the exceedance of the shallow water design wave conditions.

According to the hindcast exercise with *DOLPHIN-B1*, hurricane *Lenny* (November 1999) generated the most severe wave conditions within the considered period of time (from 1972 till 2000). However, the wave conditions during this hurricane were not identified as an unusual extreme event. Instead, they were indicated as a result of the general increase of the hurricane wave conditions.

It must be noted that only the largest wave height and the corresponding direction of wave propagation during each hindcasted hurricane have been subjected to a statistic analysis. No attention has been paid to a phenomenon like the hurricane duration. Particularly hurricane *Lenny* stayed in the vicinity of the island of *Saba* for a relatively long period of time. As a result the breakwaters of *Fort Bay* harbour have been exposed to severe wave attack for a longer duration than on average.

8.2. Recommendations

Recommendations regarding PART 1

The present study has come a long way in finding an answer to the question "what has caused the damage to the *Fort Bay* harbour breakwaters". Possible phenomena and mechanisms that could have been responsible for these damages have been identified and the phenomenon of a potential worsening of the deep-water wave conditions over the years, has been analysed extensively. However, not all of the identified phenomena have been analysed in the present study. Therefore it is necessary to perform a further study to the other identified phenomena. Especially a study to the translation of the deep-water wave conditions towards the shore deserves a strong recommendation. In that study the determination of the behaviour of the hurricane generated waves at a steep sloping shore forms a large challenge.

Recommendations regarding PART 2

The wave model *DOLPHIN-B1* played a significant role in the hindcast of the deep-water wave conditions during hurricanes. Besides a systematic difference, it has been reasoned that from the results of a hindcast with *DOLPHIN-B1* changes in wave conditions can be identified. However, certain recommendations can be made for using this model. They are listed hereafter.

- In the present study verification of the model results could not be performed to its full potential. Its recommended to gather more field data in order to make a proper verification possible.
- *DOLPHIN-B1* does not account for wave refraction. Especially at the shallow *Saba-bank*, situated at some distance next to the *Fort Bay* harbour, refraction may play a significant role. Therefore the effects of neglecting this phenomenon need to be evaluated.
- An important input parameter of *DOLPHIN-B1* is the radius to maximum wind speed. This parameter represents the distance between the centre of a hurricane and the location where the maximum wind speed occurs. In the present study, this parameter has been estimated with a relationship that takes into account the pressure drop and the position of the hurricane centre. Unfortunately, the outcomes of this relationship could not be verified, due to the lack of registrations containing values of this radius.
- Based on two parameters, namely the radius to maximum wind speed and the pressure drop in the hurricane centre, *DOLPHIN-B1* generates a synthetic hurricane wind field. This synthetic wind field is symmetric. However, due to translational speed of the hurricane itself the wind field is asymmetric in reality. An investigation of neglecting this asymmetry is recommended.

From the present analysis it can be concluded that since the construction of *Fort Bay* harbour in 1972, hurricane wave conditions show a tendency to increase. It cannot be excluded beforehand that this tendency will continue into the future. This hampers proper determination of design conditions for the *Fort Bay* harbour. For the reconstruction plan to be delivered by *CEC*, it is recommended that *CEC* takes into account a continuation of the apparent worsening of conditions and that a monitoring strategy is developed, focused on a further substantiation of this worsening.

REFERENCES

Reports:
Lit 1   Civil Engineering Caribbean CEC, *Fort Baai Haven Saba, Definitief ontwerp*, January 1990.
Lit 2   Civil Engineering Caribbean CEC, *Fort Baai Haven Saba, Ontwerpnotitie: Golfbreker*, Annex to: *Fort Baai Haven Saba, Definitief ontwerp* [Lit 1], January 1990.
Lit 3   Civil Engineering Caribbean CEC, *Haven faciliteiten Saba, Projectdossier*, april 1988 (Developed for: Regering van de Nederlandse Antillen, Departement voor Ontwikkelingssamenwerking).
Lit 4   Civil Engineering Caribbean CEC, *Inspektierapport Haven Saba 778/0*, September 1995.
Lit 5   Civil Engineering Caribbean, *Herstel Stormschade Haven Saba, vooronderzoek (concept)*, February 1996 code: ANT777.1
Lit 6   DIGITAL HYDRAULICS HOLLAND B.V., *DOLPHIN-B1 version 30.27, User Manual*, 1988.
Lit 7   SOGREAH Ingenierie, *Accropode ® General information document*, October 1996
Lit 8   Steinmetz, R.O., *Visserijgolfbreker*, Letter of TU Delft to Albert Treffers (W+B), November 1995.
Lit 9   Witteveen+Bos and Civil Engineering Caribbean CEC, *Fort Bay Harbour, Saba. Damage evaluation and restoration plan*, March 23rd 2000 (Developed for: Departement van Financiën Sector Interne Deskundige).
Lit 10   Witteveen+Bos and Civil Engineering Caribbean CEC, *Fort Bay Harbour, Saba. Damage evaluation and restoration of damage due to hurricane Lenny*, March 3rd 2000 (Developed for: Departement van Financiën Sector Interne Deskundige).
Lit 11   WL|Delft Hydraulics, *Wave conditions Orjanjestad breakwater, Sint Eustatius*, January 1988 code: 777.

Literature:
Lit 12   CUR Report 169, Centre for Civil Engineering Research and Codes, Directorate-General for Public Works and Water Management, *Manual on the use of Rock in Hydraulic Engineering*, November 1994
Lit 13   CUR Report 190, Centre for Civil Engineering Research and Codes, Directorate-General for Public Works and Water Management, *Kansen in de civiele techniek, Deel 1*, March 1997
Lit 14   Petruaskas, C. and Aagaard, P. M., *Extrapolation of historical storm data for estimating design wave heights*, 1970, Offshore Technology Conference, Paper number OTC 1190.
Lit 15   Pierson, W.J. Jr., G. Neumann and R.W. James, *H.O. Pub No. 603 Practical Methods for Observing and Forecasting Ocean Waves by Means of Wave Spectra and Statistics*, 1971
Lit 16   Schiereck, G.J., TU Delft, Faculty of Civil Engineering and Geosciences, *Introduction to Bed, Bank and Shore Protection*, December 1998
Lit 17   TU Delft, Faculty of Information Technology and Systems, *Mathematics part 4*, October 1997
Lit 18   US Army Corps of Engineers, Department of the Army, *Shore Protection Manual*, Second printing 1984.

Internet:
Lit 19   ARGOSS homepage, http://www.argoss.nl/index.html including http://www.waveclimate.com/
Lit 20   AVISO Internet site (Radar altimetry), http://www.jason.oceanobs.com/html/portail/actu/actu_ welcome_ uk.php3
Lit 21   Lonely Planet Word Guide, destination Saba, http://www.lonelyplanet.com/destinations/caribbean/saba/
Lit 22   NOAA, The Atlantic Hurricane Database Re-analysis Project, http://www.aoml.noaa.gov/hrd/hurdat/Documentation.html, 2001
Lit 23   The Saffir-Simpson Hurricane Intensity Scale, http://www.citi-net.com/george/ss-scale.html, Adapted from Simpson, R.H. and Riehl, H. The Hurricane and its Impact. L.S.U. Press
Lit 24   Unisys homepage, http://weather.unisys.com/hurricane/index.html

Maps:
Lit 25   Leeward islands, St. Eustatius, St. Christopher, Nevis, Montserrat & Saba, Imray-Iolaire no. A25, June 2000
Lit 26   Mona Passage to Dominica, Admiralty chart no. 2600, year 1999

Meetings:
Lit 27   Personal communication with Dr. ir. L.H. Holthuijsen (TU Delft) and Dr. ir. N. Booij (TU Delft), date: 13th February 2001

ANNEX I   CROSS-SECTIONS HARBOUR DESIGNS

Source: CEC project file 1988 [Lit 3]
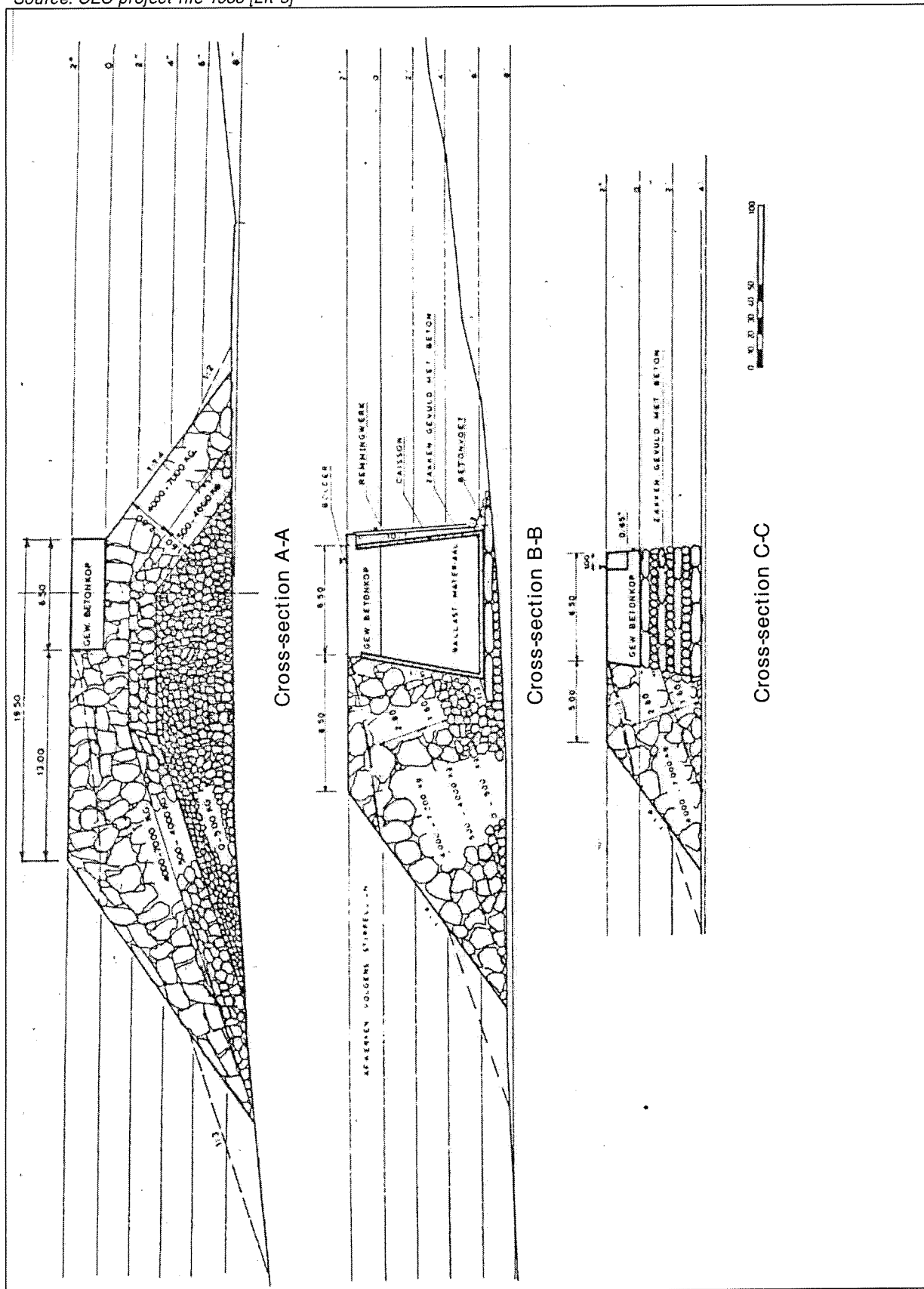
Figure 50: Cross-sections from NACO (design 1972)

Fort Bay harbour, Saba. A study on hurricane conditions

74

Source: CEC Design paper (1990) [Lit 2]

Cross-section breakwater trunk
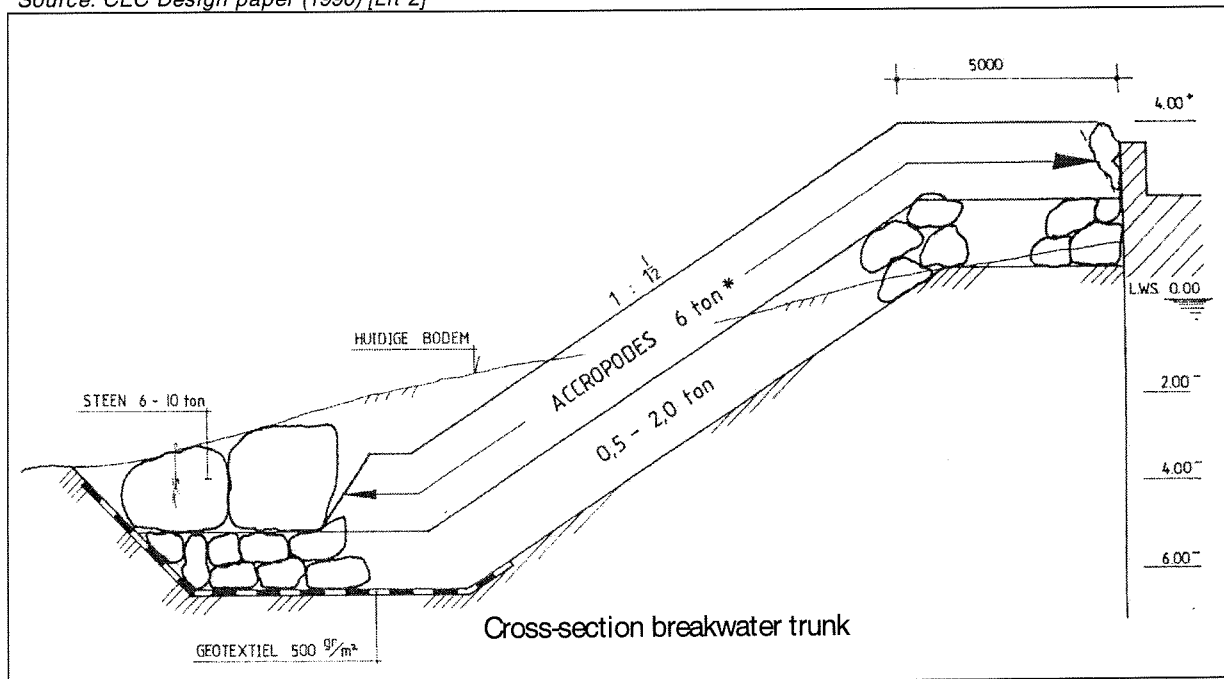
Figure 51: Cross-section from CEC (design 1990)
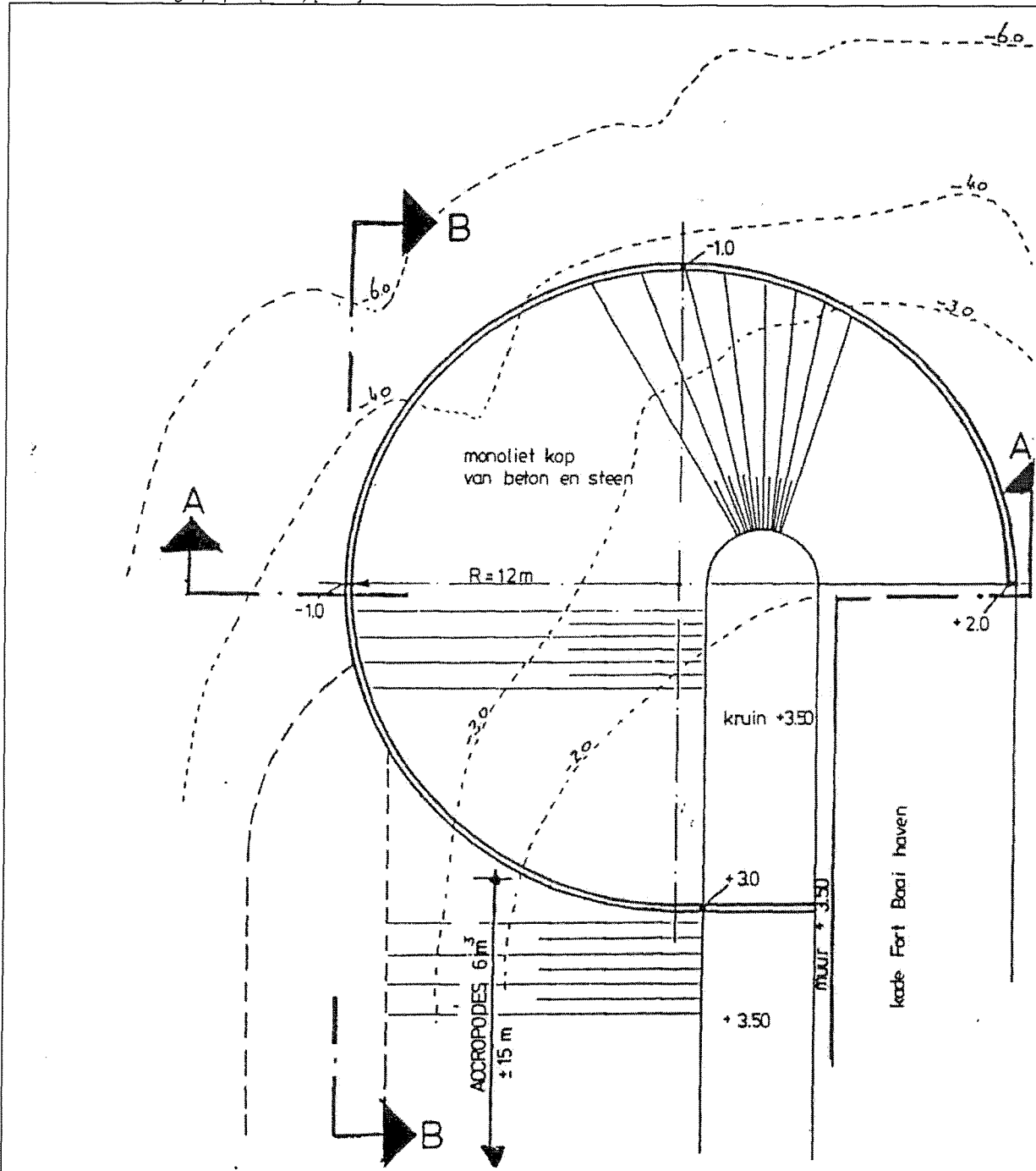
Figure 52: Top view of monolithic main breakwater head from CEC (design 1990)

monoliet kop van beton en steen

bovenzijde damwand
(bekisting)

+3.50

kade +2.30

+2.0

-1.0

4 à 5 m

grof kemmateriaal
(100 kg)

aanwezige steenbodem
penetreren met beton

Cross-section A-A

talud monoliet kop

kruin +3.50

bovenzijde damwand

kade +2.30

-1.00

ACCROPODES 6m³

(berm niet aangegeven)

damwand (bekisting)

fundering bestaande caissons

Front view B-B

Figure 53: Front view and cross-section of monolithic main breakwater head from CEC (design 1990)

ANNEX II   PROBABILITIES OF EXCEEDANCE WL DELFT HYDRAULICS (1988)

Source: WL/Delft Hydraulics wave climate study (1988) [Lit 11]
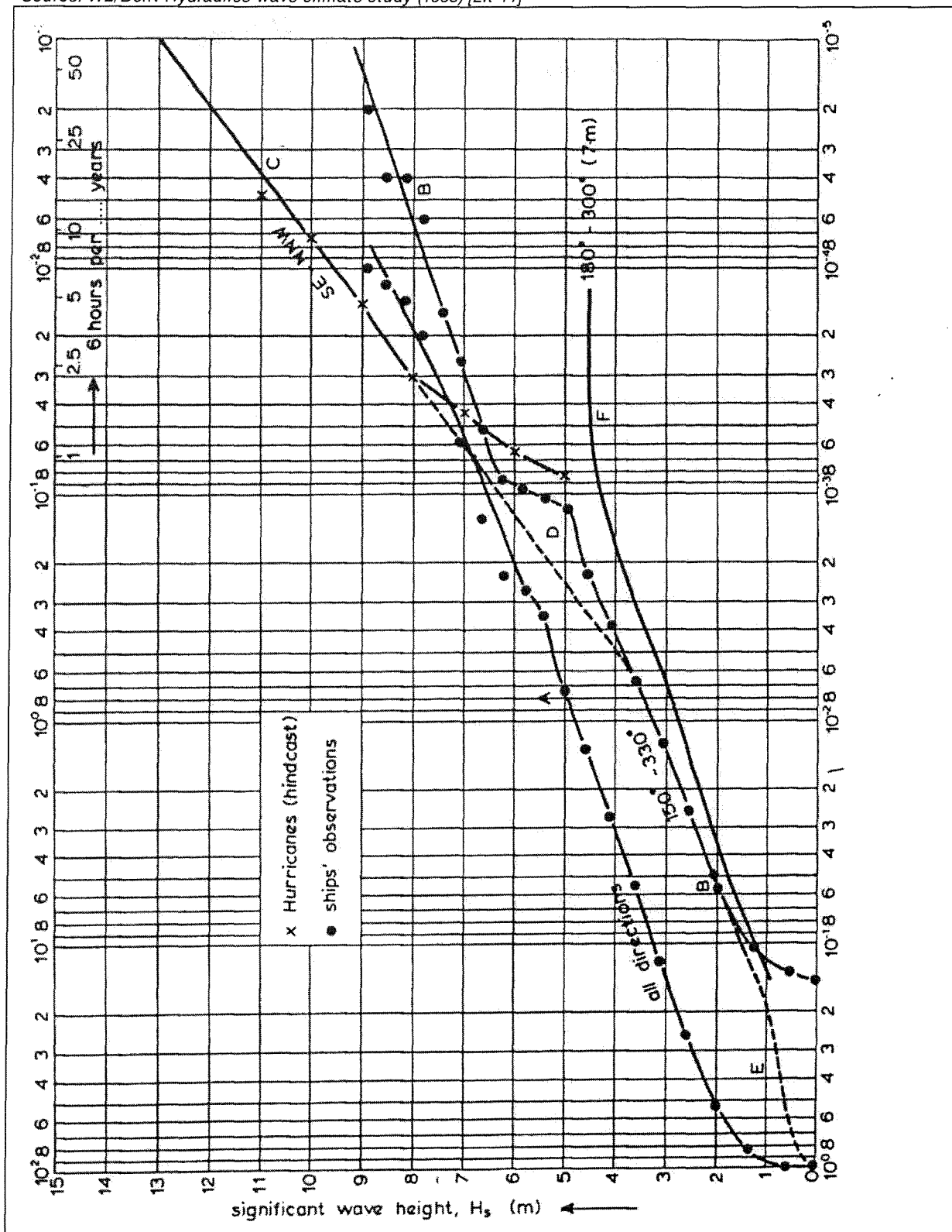
Figure 54: Diagram with probabilities of exceedance WL/Delft Hydraulics (1988)

ANNEX III   SOGREAH ACCROPODE

TOE MOUND WITH ACCROPODE® UNITS

NORMAL SOLUTION

DIMENSIONS

Volume of block (m³)	Height (m)	Weight to d=2.4 (t)	Volume of concrete per m² of facing (m³/m²)	Prefabrication area required per block (m²)	Number of blocks stored per 100 m²
0.8	1.33	1.92	0.61	4.1	81.5
1.5	1.64	3.6	0.75	5.1	53
2.5	1.95	6.0	0.89	6.0	38
4	2.27	9.6	1.04	7.0	27
6.3	2.65	15.12	1.20	8.2	20
9	2.96	21.6	1.36	9.2	16
12	3.28	28.8	1.50	10.1	13
16	3.61	38.4	1.64	11.1	11
21	3.95	50.4	1.79	12.2	9
27	4.30	64.8	1.96	13.1	8
34	4.64	81.6	2.13	14.2	7
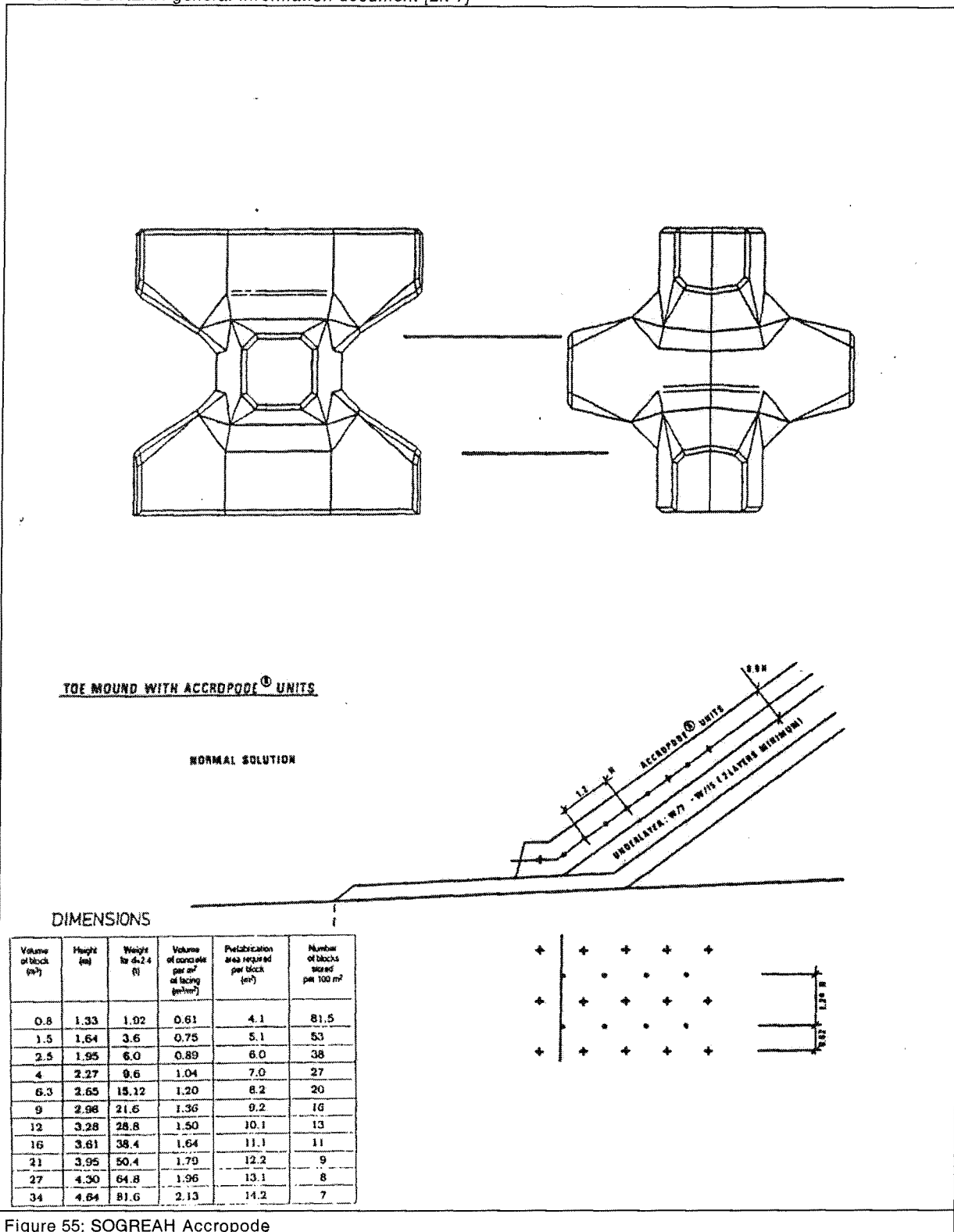
Figure 55: SOGREAH Accropode

ANNEX IV   SAFFIR-SIMPSON SCALE

Fort Bay harbour, Saba. A study on hurricane conditions

82

The Saffir-Simpson Hurricane Intensity Scale

(Source: *Saffir-Simpson* Hurricane Intesity Scale internet site [Lit 23])

When a tropical cyclone reaches hurricane strength, its intensity is rated by the *Saffir-Simpson* Scale. The *Saffir-Simpson* scale approximately starts where the *Beaufort* scale ends.

Category 1 - Sustained Winds 74-95 [mph] (64-83 [knt], 33-43 [m/s]), minimum pressure less than or equal to 980 [mb] and a storm surge of 3-5 [feet].
- Damage primarily to shrubbery, trees, foliage, and unanchored mobile homes.
- Some damage to poorly constructed signs.
- Coastal roads inundated minor pier damage.
- Small craft with exposed anchorage torn from moorings.
- No significant damage to other structures.

Category 2 - Sustained Winds 96-110 [mph] (84-96 [knt], 44-49 [m/s]), minimum pressure 981-965 [mb] and a storm surge of 6-8 [feet].
- Considerable damage to shrubbery and tree foliage, some trees blown down.
- Major damage to exposed mobile homes.
- Extensive damage to poorly constructed signs.
- Some damage to roofs, windows, and doors.
- Coastal roads may be cut by high water 2 to 3 hours before the storm arrives.
- Considerable damage to piers.
- Marina's flooded.
- Small craft with unprotected anchorage torn from moorings.
- Evacuation of the coastline and other low-lying areas may be necessary.
- No major damage to buildings.

Category 3 - Sustained Winds 111-130 [mph] (97-113 [knt], 50-58 [m/s]), minimum pressure 964-945 [mb] and a storm surge of 9-12 [feet].
- Foliage torn from trees, large trees blown down.
- Mobile homes destroyed.
- All poorly constructed signs blown down.
- Some damage to roofs, windows, and doors.
- Some structural damage to small buildings.
- Serious flooding along coastline.
- Small structures on coast destroyed, larger structures damaged by wave action.
- Low level areas (5 feet and less above sea level) flooded inland 8 miles or farther.
- Coastal roads may be cut by high water 3 to 5 hours before the storm arrives.
- Evacuation of low-lying coastline area possibly required.

Category 4 - Sustained Winds 131-155 [mph] (114-135 [knt], 59-69 [m/s]), minimum pressure 944-920 [mb] and a storm surge of 13-18 [feet].
- Most all shrubs and trees blown down.
- All signs blown down.
- Extensive damage to roofs, windows, and doors, roofs on small homes destroyed.
- Complete destruction of most all mobile homes.
- Major damage to coastline structures due to flooding, wave action, and floating debris.
- Low level areas (10 feet or less above sea level) flooded inland 6 miles or farther.
- Coastal roads cut by high water 3 to 5 hours before the storm center arrives.
- Major erosion of beaches.
- Major evacuation of low-lying coastline area, and low ground up to 2 mile inland required.

Category 5 - Sustained Winds Greater than 155 [mph] (135 [knt], 69 [m/s]), minimum pressure less than 920 [mb] and a storm surge over 18 [feet].
- All shrubs and trees blown down.
- All signs blown down.
- Complete failure of roofs on residences and most industrial buildings.
- Extensive shattering of glass windows and doors.
- Severe and extensive damage to doors.
- Some complete building failure, smaller buildings overturned or blown away.
- Complete destruction of mobile homes.
- Major damage to structures less than 15 above sea level due to flooding, wave action, and floating debris.
- Coastal roads inundated by high water 3 to 5 hours before the storm center arrives, cutting off all evacuation routes.
- Massive evacuation of entire population in low-lying areas within 5 to 10 miles of coastline.

ANNEX V   THEORY OF DOLPHIN-B1

Fort Bay harbour, Saba. A study on hurricane conditions

85

Theory of *DOLPHIN-B1*

In *DOLPHIN-B1* a varying energy density spectrum is used to derive wave conditions at a certain prediction or hindcast location at a certain time. Hereafter first an explanation of the wave energy density spectrum is given. Secondly the mathematical description of the spectrum and formulae used in *DOLPHIN-B1* are presented.

Wave energy density spectrum
An example of a wave field registration is given in Figure 56.
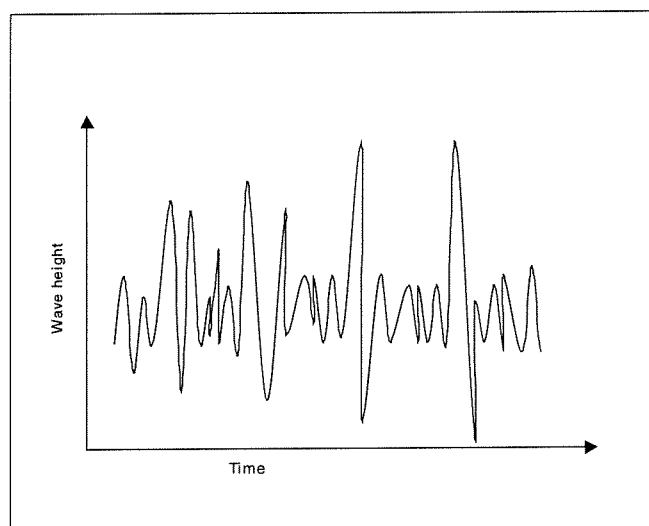
Figure 56: Example of registration of wave field

The wave field is taken to consist of a large number of sinus-shaped waves of differing energy (height) and differing frequency (period) with random beginning phase. The division of energy over the frequency is recorded in the (energy density) spectrum. The parameters characterizing the spectrum are called the spectral parameters. In the frequency domain, the wave height signal (see Figure 56) is transformed via a mathematical conversion (Fourier transform) into a large number of sinus shaped wave movements, each with a different frequency and with each frequency another height.

Frequency is the reverse of (wave) period, thus in the time domain, we demarcate wind-generated waves between 2 and 30 [sec], and we fix the limits for these sorts of waves at between 0.03 and 0.5 [Hz]. In the frequency domain it is also normal not to use the wave height, but the amplitude (half height). The squared amplitude is (proportional to) the energy of the wave. The set of energy values per frequency is the energy density spectrum. An example of such a one-dimensional spectrum is given in Figure 57. When the wave energy density spectrum is presented as function of frequency and wave direction, a two-dimensional spectrum can be constructed, see Figure 58.
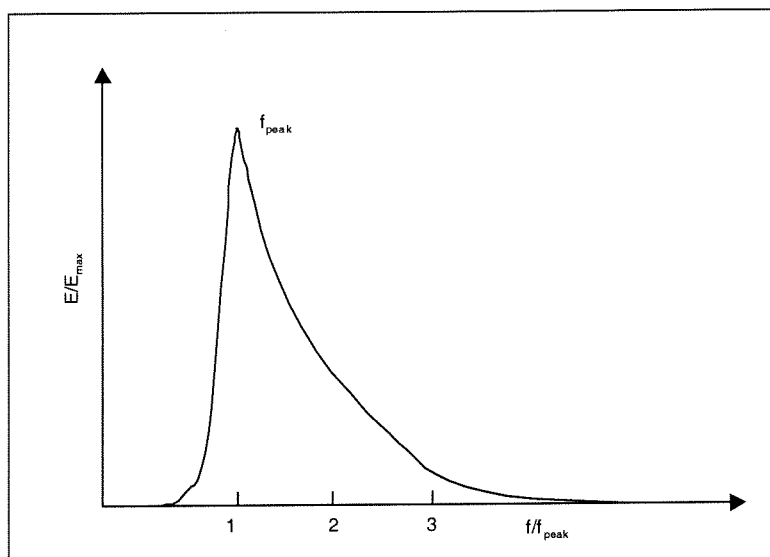
Figure 57: Example of one-dimensional spectrum
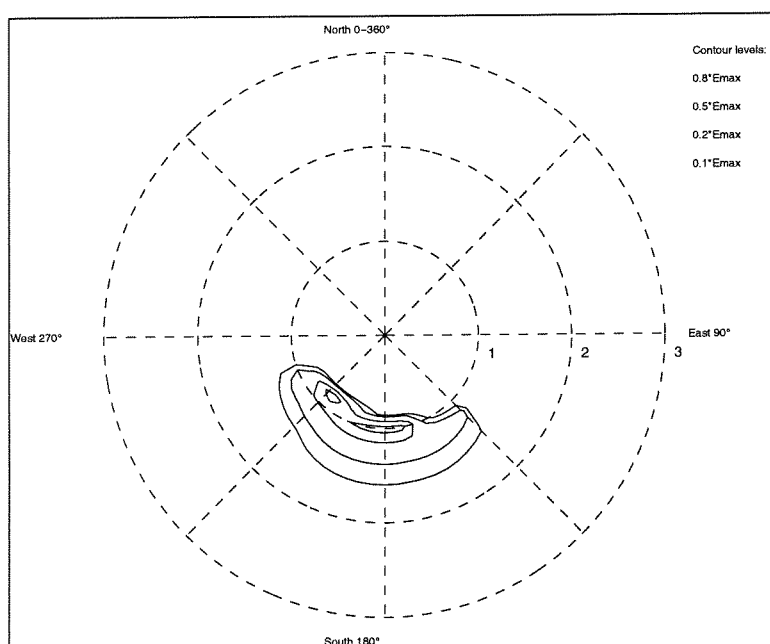
Figure 58: Example of two-dimensional spectrum

The spectrum shows how the energy density is spread over the frequencies. With larger wave heights, the entire spectrum from Figure 57 will be pushed towards the lower frequencies; it will also be higher and therefore contain more energy. With lower wave heights, the spectrum will be pushed more to the right (higher frequencies) and will be lower. The spectrum gives a good, though complex description of the wave field. For this reason, summarizing parameters (spectral parameters) have been developed to characterize the spectrum. These parameters are based on the moments of the spectrum, mostly on the zeroth, first and second moment.

Frequently used spectral parameters are:

Wave height: $H_{m0} = 4 * \sqrt{m_0}$

Wave height: $H_{TE3} = 4 * \sqrt{m_{0(3)}}$ where $m_{0(3)}$ is calculated from the low frequency part of the spectrum

Wave period: $T_{m2} = m_0 / m_2$

Wave period T_p = wave period that belongs to the value of the highest energy density in the spectrum

In the frequency domain, the wave height H_{m0} is equivalent to the wave height $H_{1/3}$ or H_s. The wave period T_{m2} is approximately equivalent to the mean wave period in the time domain (T_m). The wave height H_{TE3} indicates the amount of swell in the wave field.

Mathematical description of the wave energy spectrum
A single wave (in three dimensions x, y, t) can be described as:

$$\eta(x,y,t) = a\cos(\omega t - kx\cos\theta - ky\sin\theta + \alpha)$$

Equation 42

The sum of a large number of these waves can be expressed as a stochastical value:

$$\underline{\eta}(x,y,t) = \sum_{i=1}^{N}\sum_{j=1}^{M}\left\{\underline{a}_{i,j}\cos(\omega_i t - k_i x\cos\theta_j - k_i y\sin\theta_j + \underline{\alpha}_{i,j})\right\}$$

Equation 43

The indices for the frequencies ω and the wave number k are equal as they are related with the dispersion relationship.

$$\omega = \sqrt{gk\tanh(kd)}$$

Equation 44

However, for every frequency a large number of components propagate in every direction θ simultaneously (all combinations of frequencies and directions occur). For that reason the index for the direction is independent of the index for the frequency and a double sum is required in the model. Every wave component (characterized with indices i, j) has a stochastic amplitude $\underline{a}_{i,j}$ and a stochastic phase $\underline{\alpha}_{i,j}$. The amplitudes and phases are stochastically independent. The amplitudes are *Rayleigh* distributed and the phases are uniformly distributed.

The variance of the water level elevation is equal to:

$$E\left\{\underline{\eta}^2\right\} = E\left\{\sum_{i=1}^{N}\sum_{j=1}^{M}\tfrac{1}{2}\underline{a}_{i,j}^2\right\}$$

Equation 45

However, only a finite number of discrete frequencies and directions is considered, whereas at sea a continuum of frequencies is present. In other words, in every arbitrary small frequency and direction interval (Δf_n and $\Delta\theta_m$) an infinite number of frequencies and directions at interval δf en $\delta\theta$ is present at sea. To remove the dependency of the variance on the width of the frequency band and the direction band, the variance is divided by the width of the frequency band and the direction band (Δf_n and $\Delta\theta_m$). This gives the discrete variance density:

$$E^{*}(f_n,\theta_m) = \frac{1}{\Delta f_n\Delta\theta_m}E\left\{\sum_{\Delta f_n}\sum_{\Delta\theta_m}\tfrac{1}{2}\underline{a}_{i,j}^2\right\}$$

Equation 46

The continuous variance density is expressed as:

$$E(f,\theta) = \lim_{\Delta f_n \to 0} \lim_{\Delta\theta_m \to 0} \frac{1}{\Delta f_n \Delta\theta_m} E\left\{\sum_{\Delta f_n}\sum_{\Delta\theta_m} \tfrac{1}{2}a_{i,j}^2\right\}$$

Equation 47

By multiplying the variance density spectrum with ρg, the energy density spectrum is obtained

Computation of the energy density spectrum by *DOLPHIN-B1*
As mentioned before, DOLPHIN-B1 uses a varying wave energy density spectrum. From the previous section it is made clear that the energy density at a certain time and location can be described by $E = E(f, \theta)$. Considering a varying energy density spectrum, the formula describing this phenomenon yields:

$$E = E(f, \theta; x, y, t)$$

Equation 48

However, for convenience the varying spectrum is described again as E(f, θ) in the next.

At location x, y and at time t, the wave energy is a function of f en θ. The varying spectrum can also be seen as the summation of a large number of wave components travelling across the surface of the ocean. Or, to put in other words, the spectral energy density for each spectral wave component varies as the component travels across the ocean. In order to predict the spectrum at a certain location and time, one only need to follow all wave components that arrive at that location at that time from their points of inception (a shore line) while accounting for all effects of generation and dissipation. More properly formulated: one need to follow the energy of each such wave components along its wave ray from the inception point of that component to the prediction point (with the propagation speed of the energy: the group velocity) while integrating the energy balance of that component. Figure 59 shows the principle of DOLPHIN-B1.

Fort Bay harbour, Saba. A study on hurricane conditions

89
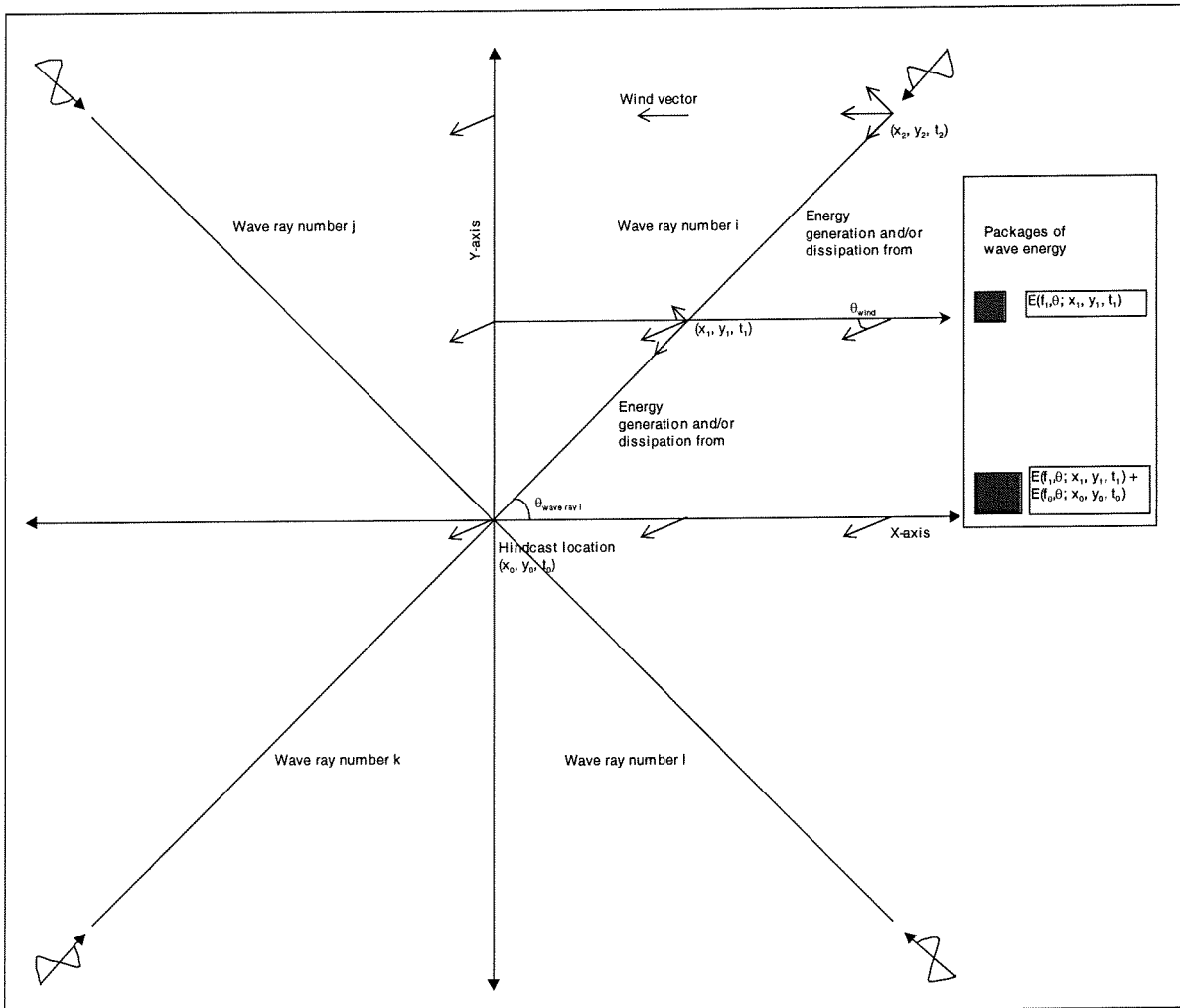
Figure 59: Schematically presentation of *DOLPHIN-B1*

In *DOLPHIN-B1* the following quantity is propagated along the wave rays:

$$E^*(f, \theta) = c_g/kE(f, \theta) \qquad \text{Equation 49}$$

The wave components, which arrive at location (x_0, y_0) at time t_0, are scattered at a previous time t over the ocean in a "sprinkler pattern". The location of each component is being determined by the ray, which is back traced from the prediction point in the direction θ and its propagation time $t_0 - t$ to the prediction point. The distance is determined by the group velocity c_g along the wave ray. The location for each wave component (f, θ) at time t for a given prediction point (x_0, y_0, t_0) is thus determined by f, θ and t only. The time t thus serves both as a time and a location label. This is used explicitly in the model to trace the (propagating) position of all spectral components.

Generation

The generation and/or dissipation of wave energy is accounted for with a source term; then the following equation holds:

$$\frac{d\left(E^*(f,\theta)\right)}{dt} = S^*(f,\theta) = \frac{c_g}{k} S(f,\theta)$$
Equation 50

The source term S^* of the energy balance equation is of the following nature:

$$S^* = A^* + BE^* \qquad \text{for } E<E_{lim}$$
Equation 51

$$S^* = (E^*_{lim} - E^*)/\tau \qquad \text{for } E>E_{lim}$$
Equation 52

A^* represents linear wave growth and BE^* represents exponential wave growth, due to wind input. The variable τ represents the dissipation time scale if E^* becomes higher than E^*_{lim}.

Dissipation

The dissipation of wave energy is represented with the following terms:
- White capping, see Equation 53.

$$S(f,\theta) = -C_{wc} f (k^4 E^*(f,\theta))^2$$
Equation 53

$C_{wc} = $ White capping coefficient (value used in calculations is 1)

- Bottom friction, with Equation 54.

$$S(f,\theta) = -C_f \frac{f^2 E(f,\theta)}{g^2 \sinh^2(kd)}$$
Equation 54

$C_f = $ bottom friction coefficient (value used in calculations is 0.038 m^2/s^3).

ANNEX VI   COMPARISSON KRAFT WITH UNISYS

Fort Bay harbour, Saba. A study on hurricane conditions

92

Quality of the estimations of P_{eye} with formula of Kraft (1971)

The quality of the formula of *Kraft* (1971) is compared with a hurricane record (hurricane *Lenny*) from the *Unisys* database with a complete pressure registration.

Table 28: P_{eye} of hurricane Lenny, according to Unisys and according to the formula of Kraft

Month	Day	Time [hours]	Lat [deg]	Long [deg]	$U_{g,max,sust}$ [knts]	P_{eye} [mbar]	P_{eye} according to formula of Karft [mbar]
11	13	21	16.5	-81.5	30	1003	1008
11	14	3	15.9	-80.6	30	1003	1008
11	14	9	15.9	-79.8	30	1003	1008
11	14	15	15.9	-79.5	30	1002	1008
11	14	19	16.4	-79.3	55	992	998
11	14	21	16.4	-78.9	60	988	995
11	15	0	16.2	-78.6	70	988	988
11	15	3	16.1	-78.3	70	988	988
11	15	6	15.6	-77.6	70	988	988
11	15	9	15.4	-77.1	85	971	976
11	15	12	15.4	-76.7	85	971	976
11	15	15	15	-76.2	85	971	976
11	15	18	14.8	-74.9	85	983	976
11	15	21	14.9	-74.1	75	984	984
11	16	0	15	-73.5	75	982	984
11	16	3	15.2	-73	70	982	988
11	16	6	15.2	-72.1	75	977	984
11	16	9	15.2	-71.5	85	971	976
11	16	12	15.2	-70.6	85	971	976
11	16	15	15.3	-69.8	85	973	976
11	16	18	15.4	-69.1	85	973	976
11	16	21	15.8	-68.2	100	965	962
11	17	0	15.9	-67.6	100	960	962
11	17	3	16.2	-67	100	958	962
11	17	5	16.3	-66.7	100	958	962
11	17	7	16.5	-66.2	105	952	957
11	17	9	16.7	-66	110	950	951
11	17	11	16.8	-65.7	110	949	951
11	17	13	16.9	-65.4	115	948	946
11	17	15	17.1	-65.1	115	942	946
11	17	17	17.2	-64.8	120	933	940
11	17	19	17.5	-64.7	130	936	927
11	17	21	17.6	-64.3	130	934	927
11	17	23	17.7	-64.2	130	929	927
11	18	1	17.7	-64.1	130	939	927
11	18	3	17.7	-64.1	125	939	933
11	18	5	17.7	-64	125	944	933
11	18	7	17.7	-63.8	125	944	933
11	18	9	17.8	-63.6	125	947	933
To be continued							

Continued							
11	18	11	17.8	-63.6	115	951	946
11	18	13	17.8	-63.6	115	952	946
11	18	15	17.8	-63.6	115	952	946
11	18	17	17.9	-63.2	115	955	946
11	18	19	18	-63.2	115	966	946
11	18	21	18.1	-63.1	105	966	957
11	19	0	18.1	-63.1	100	975	962
11	19	6	18	-62.9	95	978	967
11	19	6	18	-62.9	95	978	967
11	19	9	18.1	-62.8	85	982	976
11	19	12	17.9	-63	80	986	980
11	19	15	18	-62.8	80	986	980
11	19	18	17.5	-62.5	65	987	991
11	19	21	17.5	-62.2	60	994	995
11	20	0	17.4	-61.9	60	994	995
11	20	3	17.1	-61.8	60	995	995
11	20	6	17.1	-61.3	50	999	1000
11	20	9	16.9	-60.9	50	995	1000
11	20	15	16	-59.7	50	996	1000
11	20	21	15.6	-59.3	45	998	1003
11	21	3	15.5	-58.9	40	998	1005
11	21	9	16.6	-57.8	30	998	1008
11	21	15	17.6	-56.6	30	1000	1008
11	21	21	18.3	-56.1	25	1003	1010
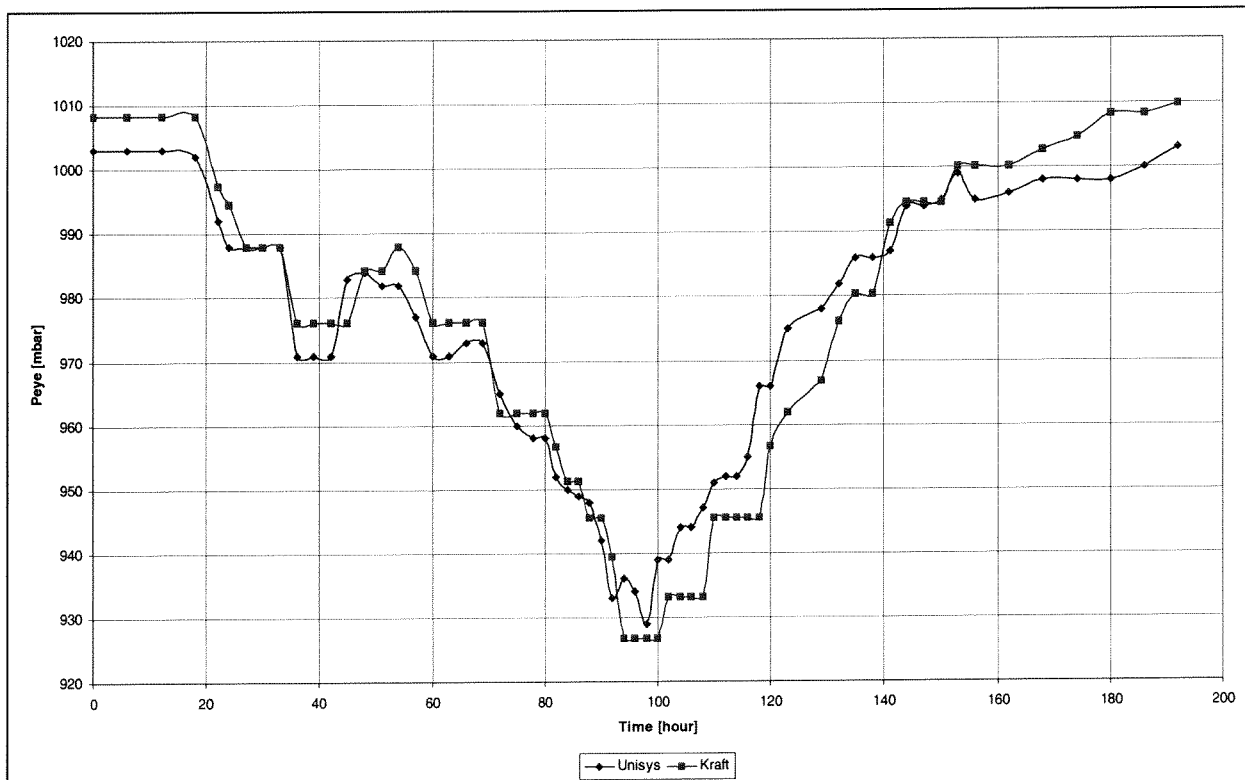
Figure 60: P_{eye} of hurricane Lenny, according to Unisys and according to the formula of Kraft

The quality of the results from *Kraft* can be expressed in terms of the Root-Mean-Square difference (RMS) as well as a relative difference with the *Unisys* values.

The general form of the RMS difference is given in Equation 55.

$$RMS = \sqrt{\frac{1}{N} \sum_{i=1}^{N} \left(D_{T,i} - D_{R,i}\right)^2}$$

Equation 55

$D_{T,i}$ = Data sample from the test data set
$D_{R,i}$ = Data sample from the reference data set
i   = Sample number
N   = Number of samples in D_T or D_R

The general form of the relative difference is given in Equation 56

$$Relative\ deviation = \sqrt{\frac{\sum_{i=1}^{N} \left(D_{T,i} - D_{R,i}\right)^2}{\sum_{i=1}^{N} \left(D_{R,i}\right)^2}}$$

Equation 56

Considering D_R equal with P_{eye} values from *Unisys* and D_T equal with P_{eye} values resulting from *Kraft*, both differences become:

RMS difference   = 6.91 [mbar]
Relative difference   = 0.7 [%]

ANNEX VII   BATHYMETRY OF *SABA* AND THE *SABA BANK*

Fort Bay harbour, Saba. A study on hurricane conditions

96

Source: [Lit 26]
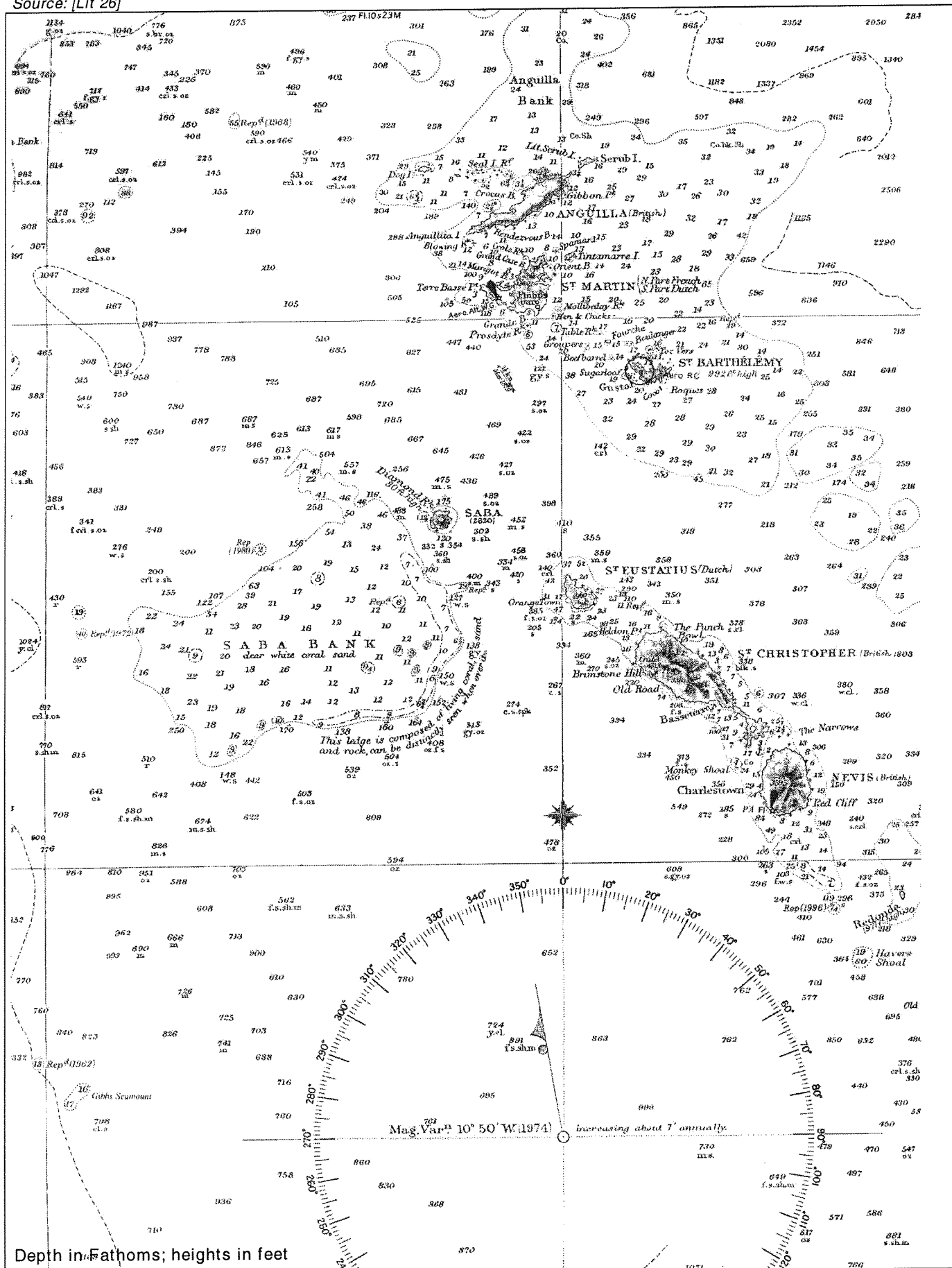
Depth in Fathoms; heights in feet

Figure 61: Bathymetry of the Caribbean Sea in the area of Saba

Fort Bay harbour, Saba. A study on hurricane conditions

97
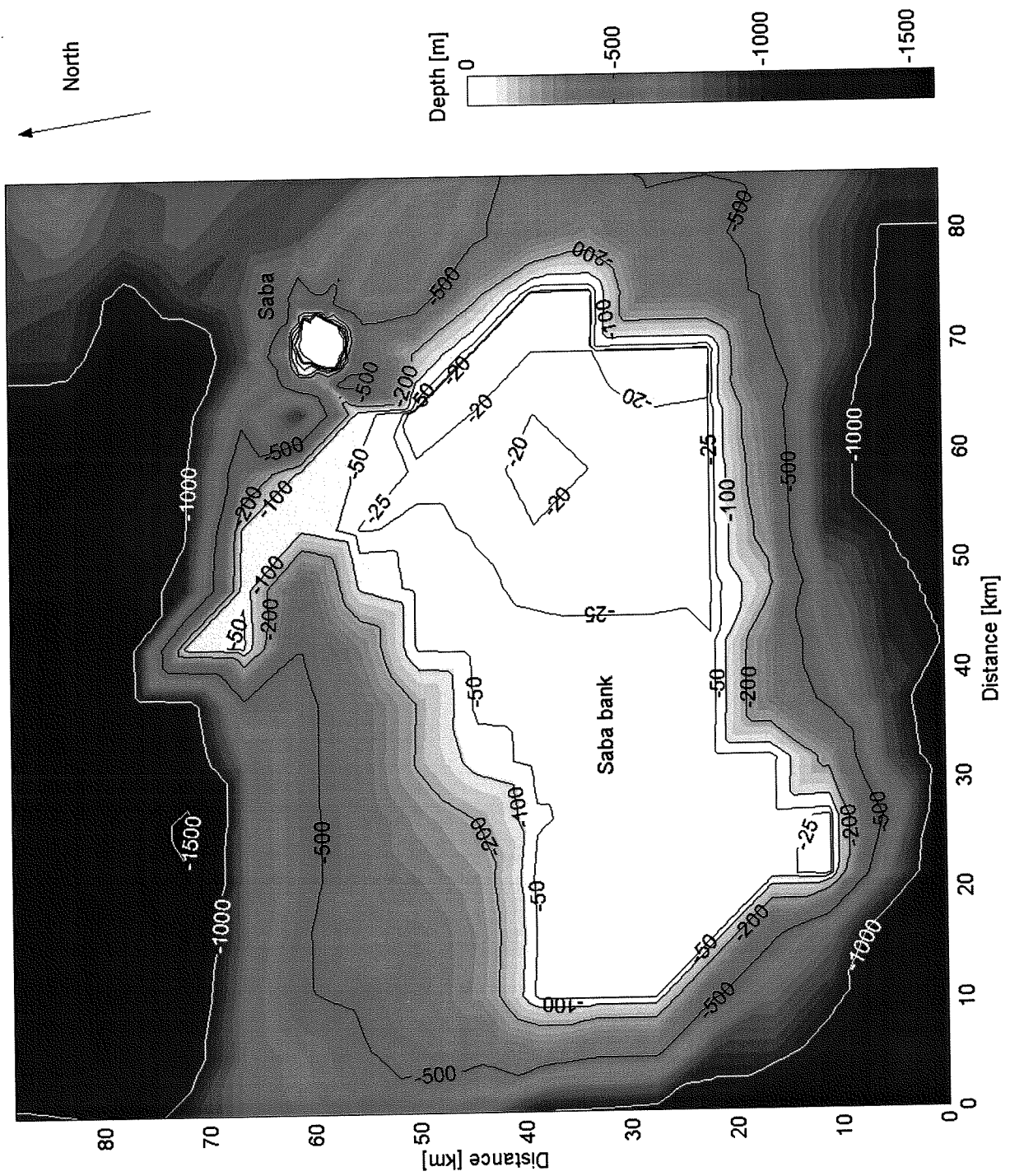
Figure 62: Digitised bathymetry of Saba and the Saba bank, as used in DOLPHIN-B1

Fort Bay harbour, Saba. A study on hurricane conditions

98
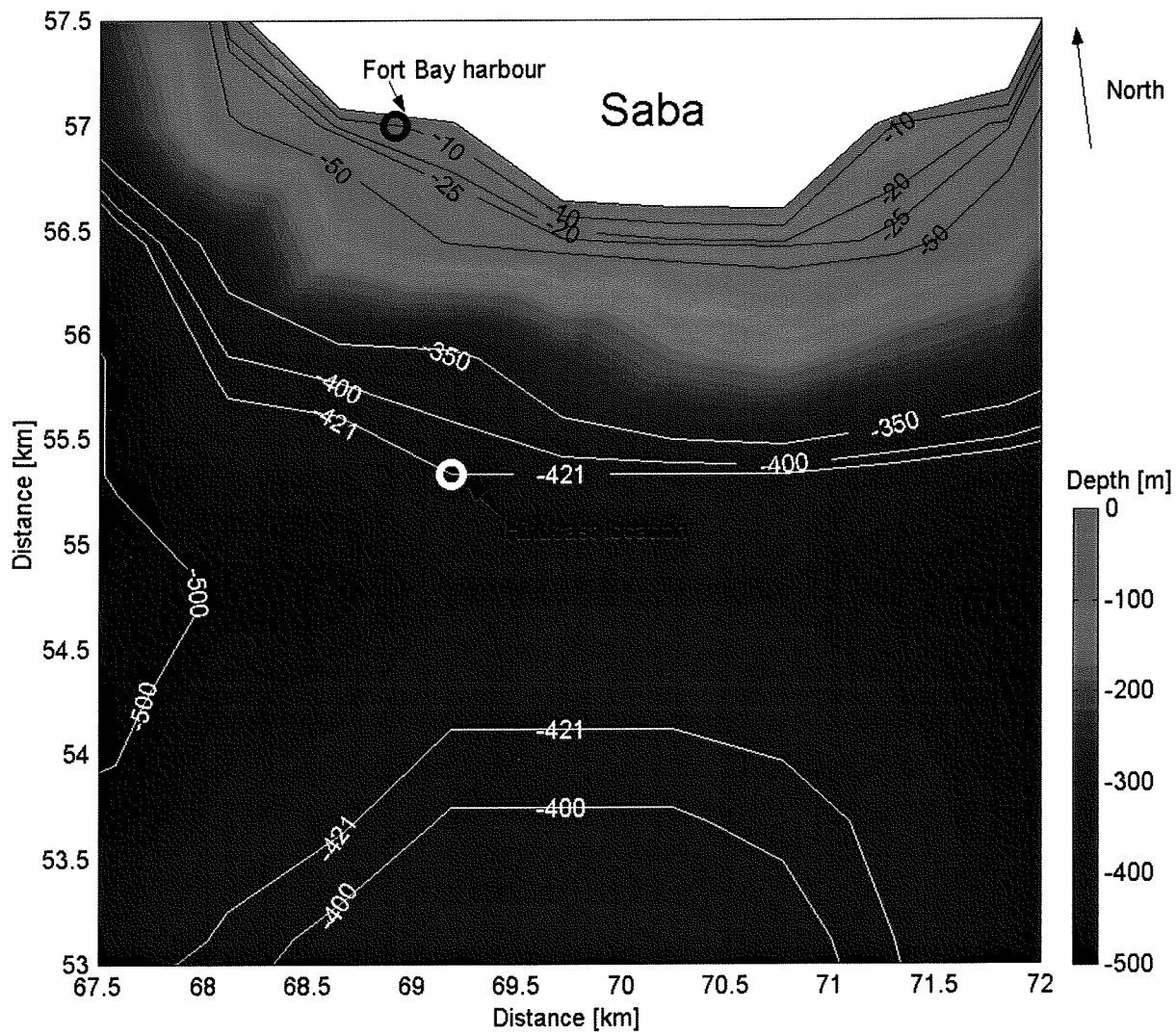
Figure 63: Digitised bathymetry of the area near Fort Bay and the hindcast location, as used in DOLPHIN-B1

ANNEX VIII   COMPARISON OF DOLPHIN-B1 WITH REFERENCES 1 AND 2

Reference 1:   A hindcast of wave conditions generated by hurricanes, carried out by *Oceanroutes Inc.* (Part of the wave climate study near the breakwater of *Oranje Bay* at *St Eustatius*" from *WL| Delft Hydraulics* (1988) [Lit 11]);

Reference 2:   Satellite observations of wave conditions during hurricanes, available from *ARGOSS*.

Comparison of H$_s$ with Oceanroutes Inc.

In the following graphs *WL* must be read as *Oceanroutes Inc.*

Hurricane #3 August 1924 id=?

Hurricane NN September 1906 id=159

Hurricane NN March 1908 id=172

Hurricane NN September 1922 id=249

Hurricane NN September 1926 id=274

Hurricane NN September 1928 id=290

Hurricane NN September 1932 id=313

Hurricane NN September 1947 id=459

Hurricane Baker August 1950 id=488

Hurricane Dog September 1950 id=490

In the following graphs *WL* must be read as *Oceanroutes Inc.*

Fort Bay harbour, Saba. A study on hurricane conditions

102

Comparison of θ with Oceanroutes Inc.

In the following graphs *WL* must be read as *Oceanroutes Inc.*

Fort Bay harbour, Saba. A study on hurricane conditions

103
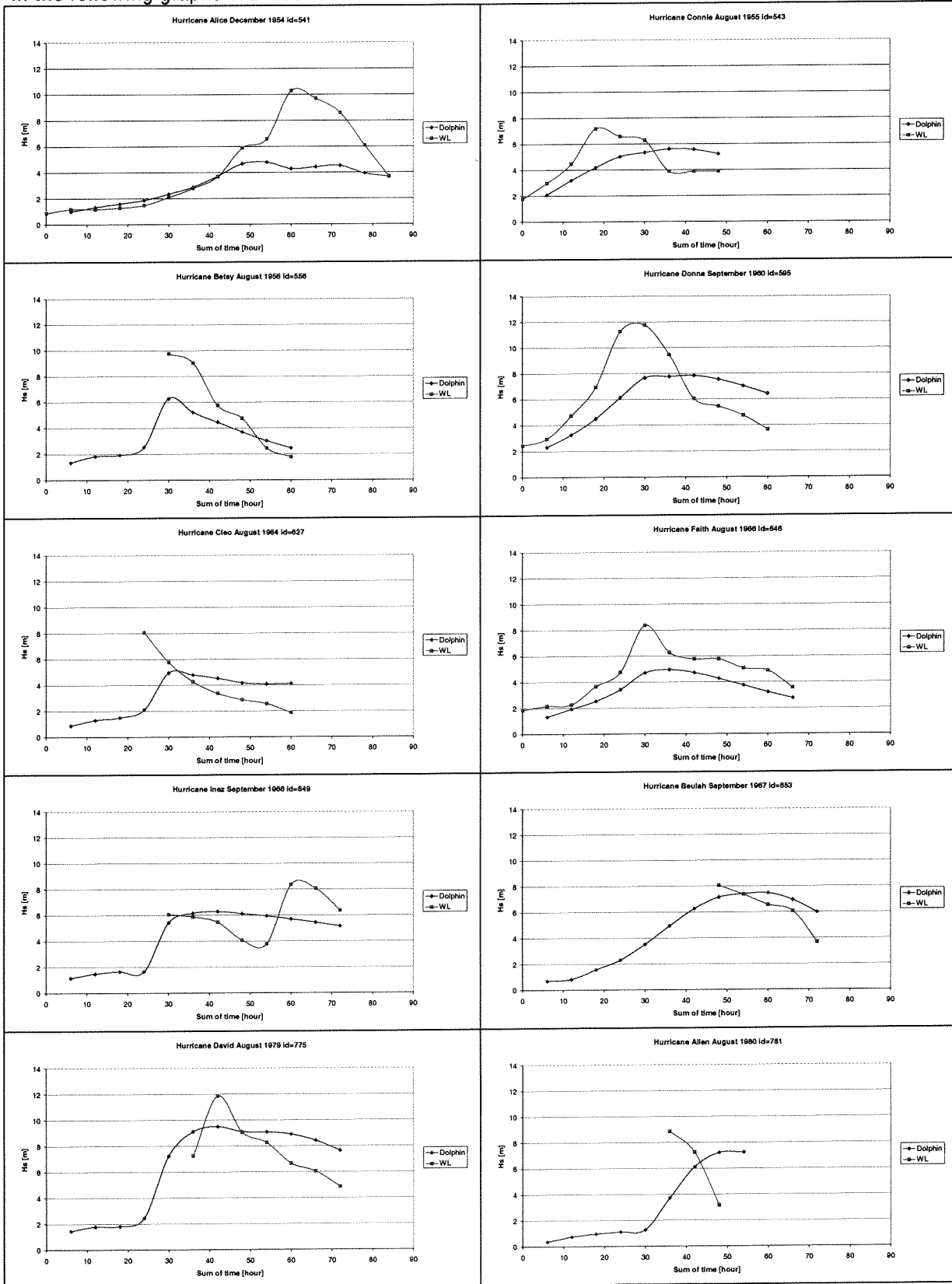
In the following graphs *WL* must be read as *Oceanroutes Inc.*
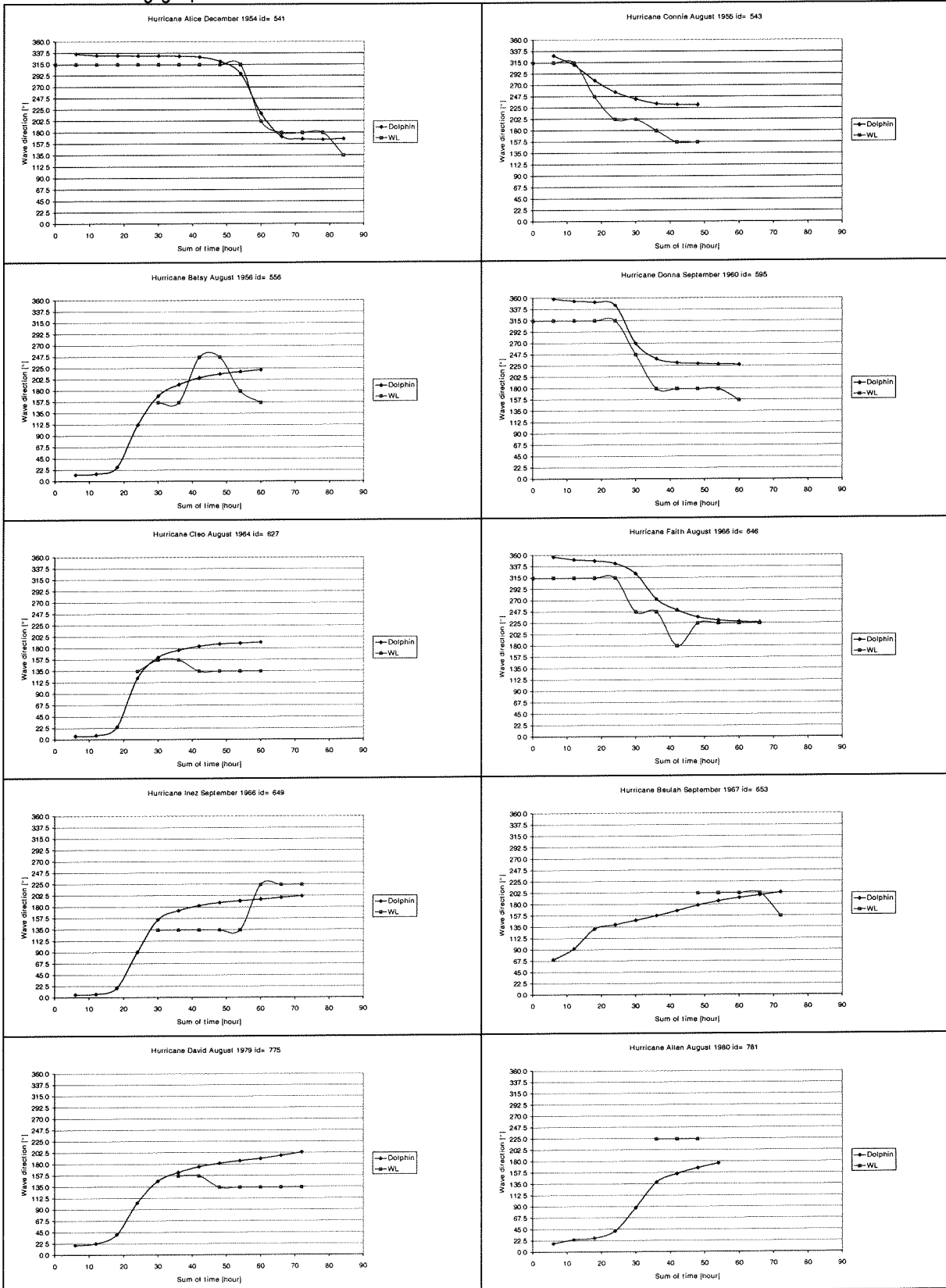
Comparison of the wind speeds with satellite observations

Number 72: Hurricane Marilyn (1995)

Source: ARGOSS [Lit 19]

Figure 64: Satellite observations of wind speed, hurricane Marilyn (1995)

Table 29: Wind speeds of hurricane Marilyn (According to satellite observations and Dolphin-B1)

Observation number	Satellite observation of wind speed [m/s]			DOLPHIN-B1 hindcast of wind speed [m/s]
	Max.	**Med.**	**Min.**	
1	6.8	6.8	6	Not available
2	6.5	6.5	6.4	Not available
3	8	7	6.8	Not available
4	21	21	21	23
5	12.5	12	11	18
6	7.5	7	6.8	9.8
7	5	5	4.9	6.1
8	9	7	5	5.6
9	7.5	7.5	7	Not available

Figure 65: Wind speeds of hurricane Marilyn (According to satellite observations and Dolphin-B1)

Fort Bay harbour, Saba. A study on hurricane conditions

105

Number 80: Hurricane Hortense (1996)

Figure 66: Satellite observations of wind speed, hurricane Hortense (1996)

Table 30: Wind speeds of hurricane Hortense (According to satellite observations and Dolphin-B1)

Observation number	Satellite observation of wind speed [m/s]			DOLPHIN-B1 hindcast of wind speed [m/s]
	Max.	Med.	Min.	
1	8.5	8.5	8.3	Not available
2	8	7.8	7.6	6.7
3	14.7	14.5	13.5	14.4
4	16.3	14.9	11.8	16.1
5	12.8	11.8	10.8	12.3
6	13.1	12.6	11	10.2
7	9.5	8.9	8.9	11.1
8	5.1	5	5	7.9
9	8.8	8	7.8	Not available

Figure 67: Wind speeds of hurricane Hortense (According to satellite observations and Dolphin-B1)

Number 87: Hurricane Georges (1998)

Figure 68: Satellite observations of wind speed, hurricane Georges (1998)

Table 31: Wind speeds of hurricane Georges (According to satellite observations and Dolphin-B1)

Observation number	Satellite observation of wind speed [m/s]			DOLPHIN-B1 hindcast of wind speed [m/s]
	Max.	Med.	Min.	
1	7	6.8	6.7	Not available
2	7.4	7.4	7.3	5.9
3	8.5	8.5	8.3	14
4	12	12	11.9	12.4
5	6.4	6	5.8	5.3
6	7	6.8	6	5.1
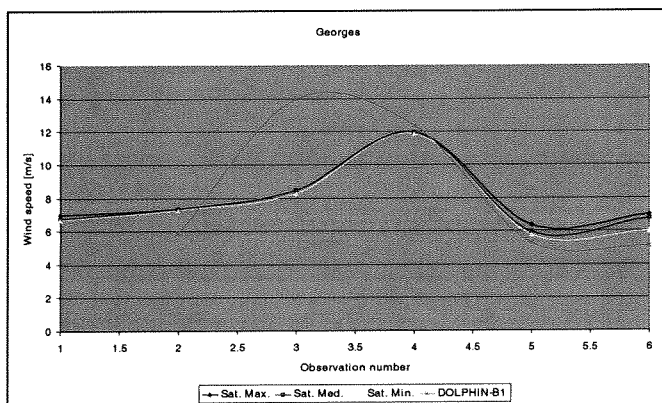
Figure 69: Wind speeds of hurricane Georges (According to satellite observations and Dolphin-B1)

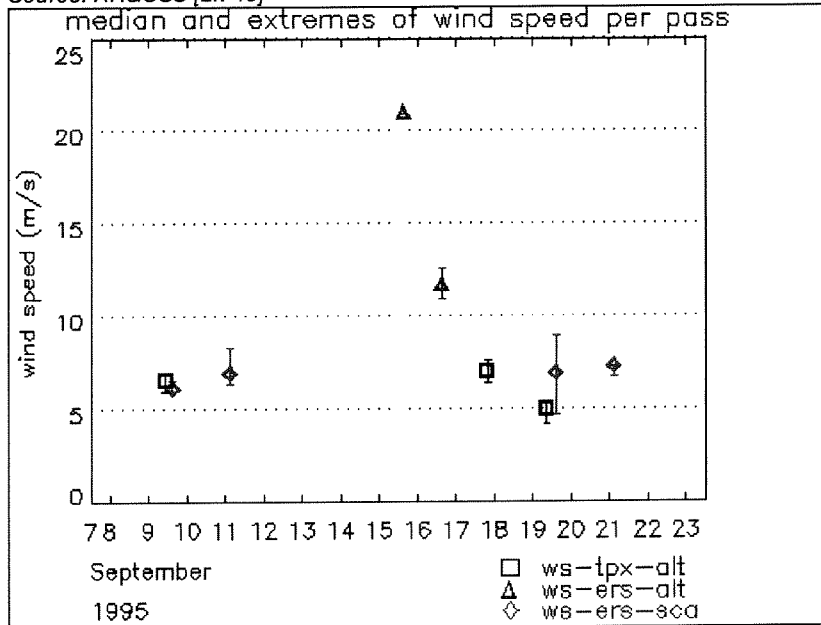# Comparison of H$_s$ with satellite observations

Number 72: Hurricane Marilyn (1995)
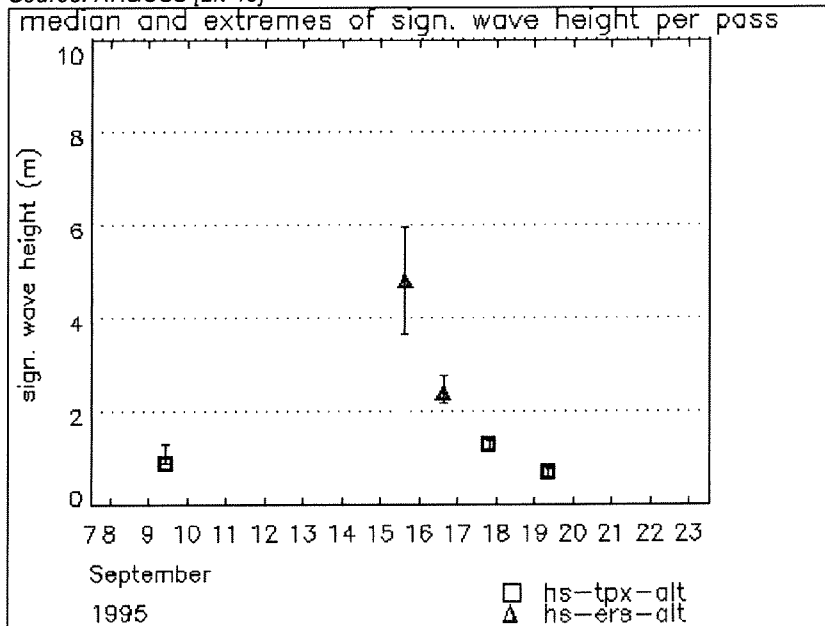
Figure 70: Satellite observations of H$_s$, hurricane Marilyn (1995)

Table 32: H$_s$ of hurricane Marilyn (According to satellite observations and Dolphin-B1)

Observation number	Satellite observation of H$_s$ [m/s]			DOLPHIN-B1 hindcast of H$_s$ [m/s]
	Max.	Med.	Min.	
1	1.4	1	1	Not available
2	6	4.8	3.8	5.7
3	2.8	2.4	2.1	5.7
4	1.7	1.6	1.6	2.4
5	0.9	0.8	0.75	1
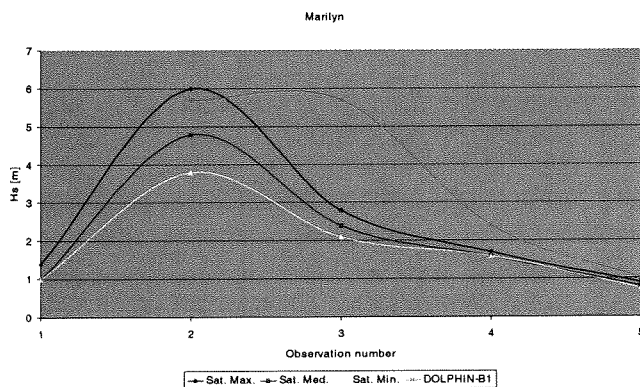
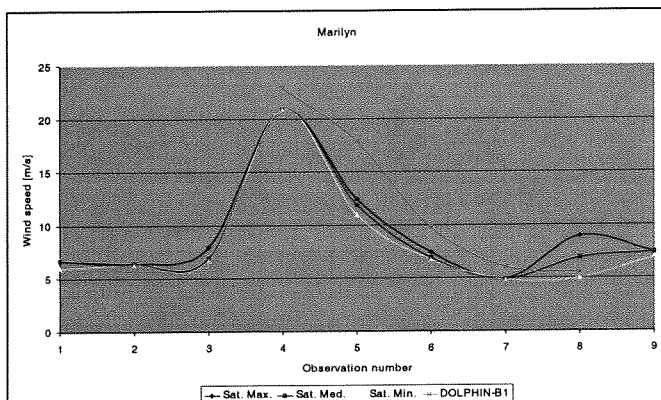Figure 71: H$_s$ of hurricane Marilyn (According to satellite observations and Dolphin-B1)

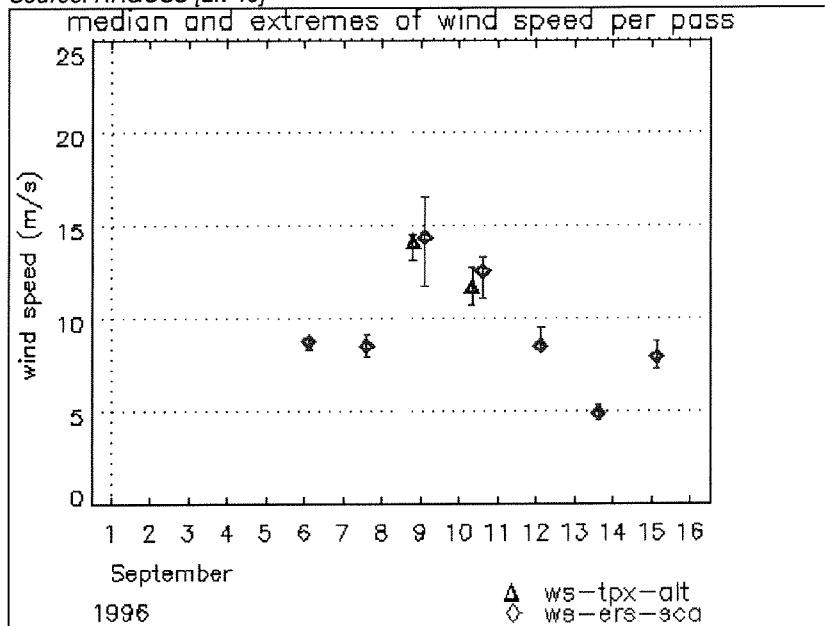**Number 80: Hurricane Hortense (1996)**

Source: ARGOSS [Lit 19]
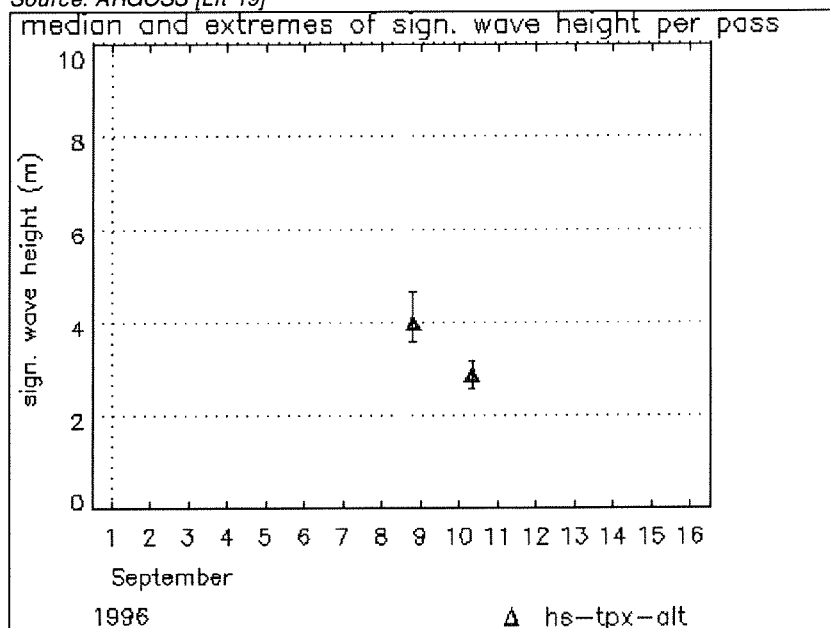
Figure 72: Satellite observations of H_s, hurricane Hortense (1996)

Table 33: H_s of hurricane Hortense (According to satellite observations and Dolphin-B1)

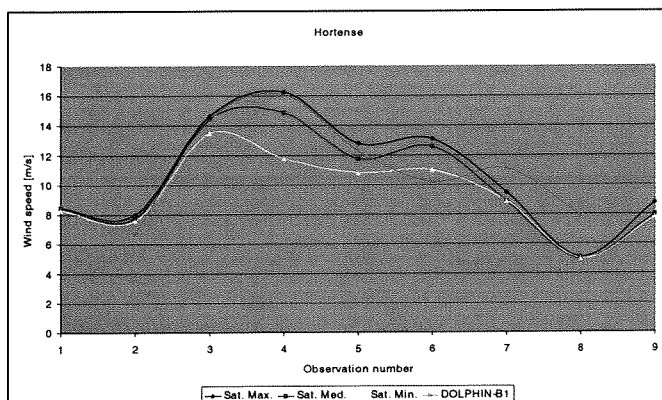| Observation number	Satellite observation of H_s [m/s]			DOLPHIN-B1 hindcast of H_s [m/s]
	Max.	Med.	Min.	
1	4.7	3.95	3.7	4.1
2	3.4	2.9	2.8	3.2
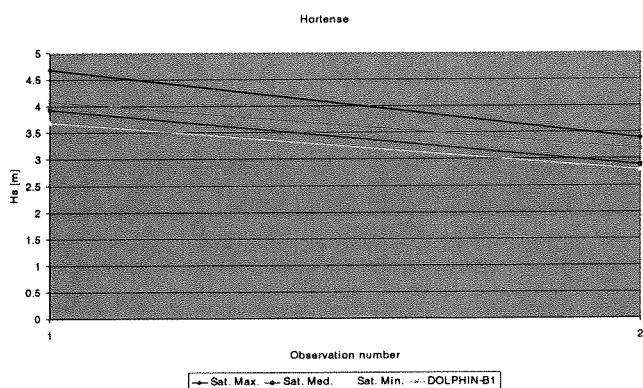
Figure 73: H_s of hurricane Hortense (According to satellite observations and Dolphin-B1)

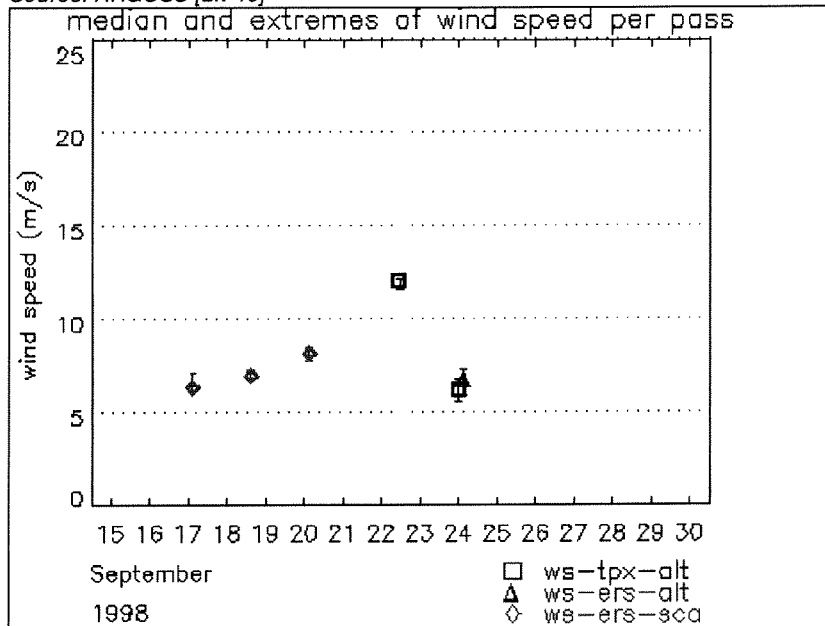**Number 87: Hurricane Georges (1998)**

Source: ARGOSS [Lit 19]
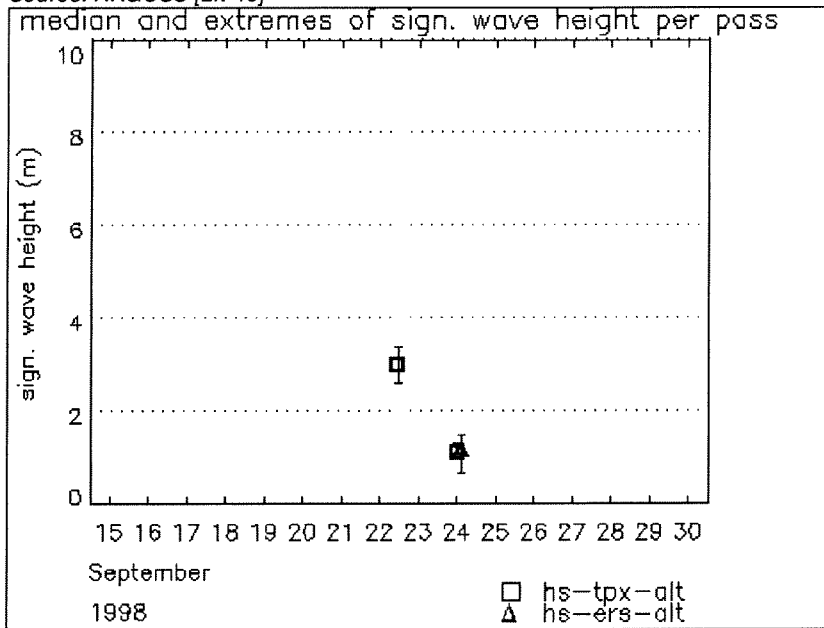
Figure 74: Satellite observations of H_s, hurricane Georges (1998)

Table 34: H_s of hurricane Georges (According to satellite observations and Dolphin-B1)

Observation number	Satellite observation of H_s [m/s]			DOLPHIN-B1 hindcast of H_s [m/s]
	Max.	Med.	Min.	
1	3.4	3	2.6	5
2	1.2	1.1	1	1.2
3	1.4	1.1	0.6	1.2
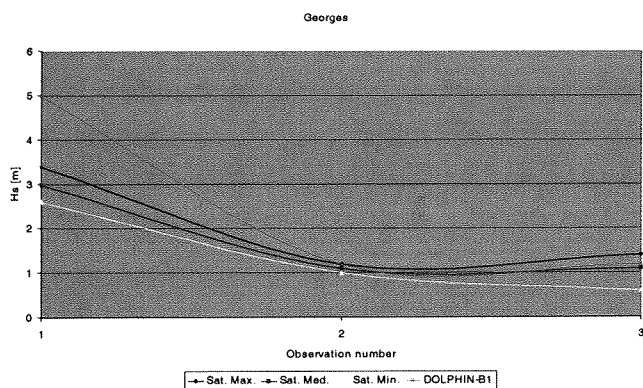
Figure 75: H_s of hurricane Georges (According to satellite observations and Dolphin-B1)

Fort Bay harbour, Saba. A study on hurricane conditions

110

ANNEX IX   EXPLANATION SATELLITE OBSERVATIONS

Fort Bay harbour, Saba. A study on hurricane conditions

111

Satellite altimetry

(Source: AVISIO Internet site [Lit 20])

The wave observations by satellites are carried out with a special instrument on board of the satellite. The instrument is called "altimeter". Therefore this kind of technique is called also "satellite altimetry".

Satellite altimetry means measuring the range from the satellite to the sea surface. Altimeter satellites regularly map the global ocean topography. From the results, also sometimes called the dynamic topography, the mean sea level, wave height, wind velocity, currents and tides can be monitored. The principle of satellite altimetry is explained in Figure 76.
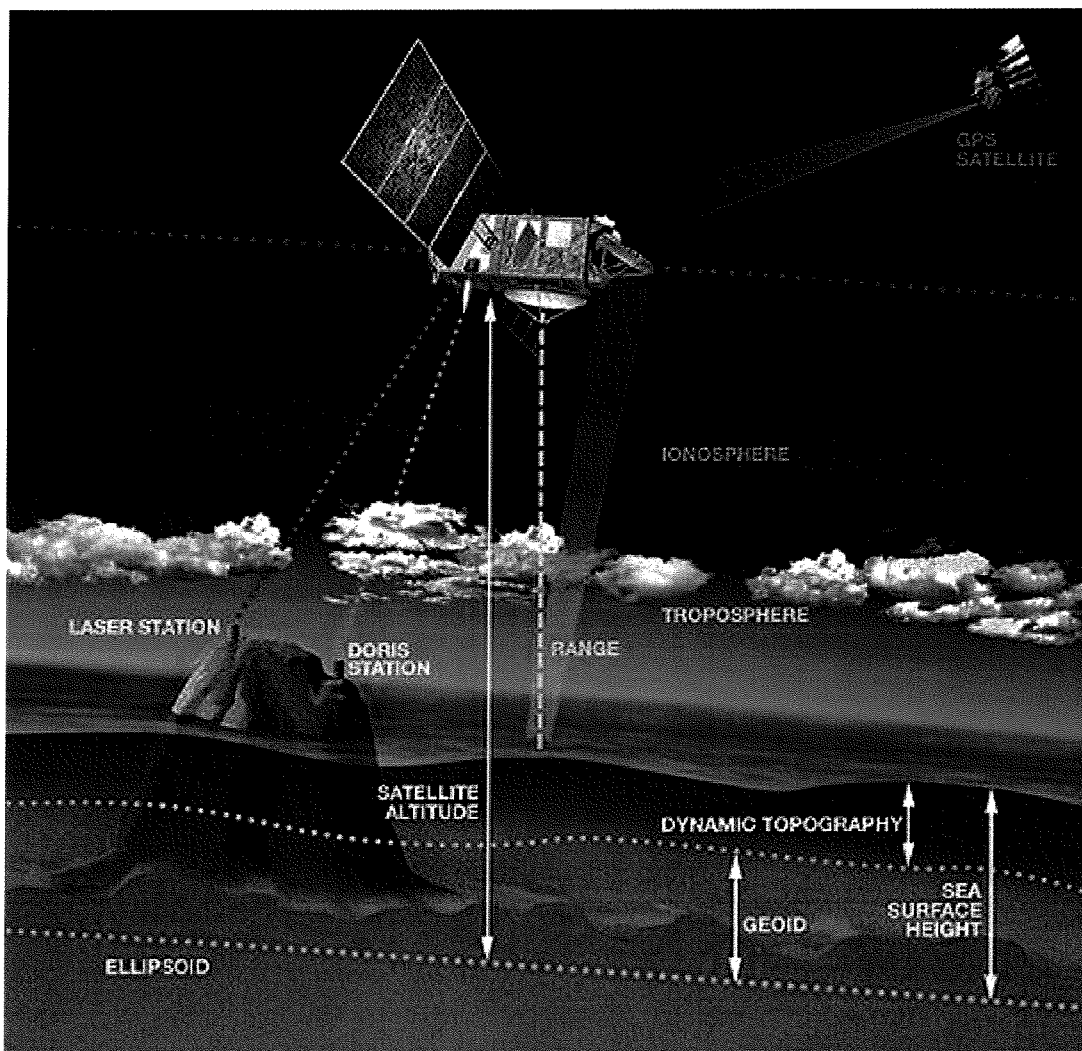
Figure 76: Altimeter on board of a satellite

From radar altimeter to altimeter range (satellite-to-ocean range (Range))
Radar altimeters on board the satellite permanently transmit signals at high frequency (over 1700 pulses per second) to the Earth, and receive the echo from the sea surface. This is analysed to derive a precise measurement of the round-trip time between the satellite and the sea surface. The time measurement, scaled by the speed of light (at which electromagnetic waves travel), yields a range measurement. By averaging the estimates over a second, this produces a very accurate measurement of the satellite-to-ocean range.

However, as electromagnetic waves travel through the atmosphere, they can be decelerated by water vapour or by ionisation. Once these phenomena are corrected for, the final range R is estimated within 2 cm.
The ultimate aim is to measure sea level relative to a terrestrial reference frame. This requires independent measurements of the satellite orbital trajectory, i.e. exact latitude, longitude and altitude coordinates.

Satellite orbit and tracking (Sat)

The critical orbital parameters for satellite altimeter missions are altitude, inclination and period. Take the TOPEX/POSEIDON satellite. It flies at an altitude of 1330km, on an orbit inclined at 66° to Earth's polar axis; this is why it can "see" only up to 66° North and South. The satellite on its so-called "repeat orbit" passes over the same ground position every ten days, uniformly sampling the Earth's surface. The satellite can be accurately tracked in a number of ways. The Doris system on board TOPEX/POSEIDON uses a network of 50 ground beacons, worldwide, transmitting to the satellite. It was developed by CNES. Doris uses the Doppler shift on the beacon signals to accurately determine the velocity of the satellite on its orbit, and dynamic orbitography models to deduce the satellite trajectory relative to Earth.

Reference ellipsoid

This position is determined relative to an arbitrary reference surface, an ellipsoid. This reference ellipsoid is a raw approximation of Earth's surface, a sphere flattened at the poles. The satellite altitude above the refrence ellipsoid, distance S, is available to within 3 cm.

Sea surface height (SSH)

The sea surface height (SSH), is the range at a given instant from the sea surface to a reference ellipsoid. Since the sea depth is not known accurately everywhere, this reference provides accurate, homogeneous measurements. The sea level is simply the difference between the satellite height and the altimetric range, see

$$SSH = Sat - Range \hspace{4cm} \text{Equation 57}$$

The SSH value takes account of such effects as:
- The sea surface height which would exist without any disturbances (wind, currents, tides, etc.). This surface, called the **geoid**, is due to gravity variations around the world, which are in turn due to major mass and density differences on the seafloor. For example, a denser rock zone on the seafloor would deform sea level by tens of metres, and be visible as a hill on the geoid.
- The ocean circulation, or **dynamic topography**. The ocean circulation, which comprises a permanent stationary component (permanent circulation linked to Earth's rotation, permanent winds, etc.) and a highly variable component (due to wind, tides, seasonal variations, etc.). The mean effect is on the order of one metre.

To derive the dynamic topography, D, the easiest way would be to subtract the geoid HEIGHT, G, from SSH. In practice, the geoid is not yet known accurately enough, and mean sea level is subtracted instead. This yields the variable part of the ocean signal.

Significant wave height

Although the altimeter is mostly used to measure the distance between the satellite and the sea surface, it is also possible to derive the significant wave height (H_s) from the reflected radar signal. Most of the time the radar return signal is somehow distorted by the presence of the waves and this distorsion can be used to estimate a significant wave height.

ANNEX X   DEEP WATER WAVE CONDITIONS NEAR *FORT BAY* HARBOUR

Hindcasted hurricanes with DOLPHIN-B1

Hindcast location: Long: 63.25 °W Lat: 17.6 °N								
Id	Hurricane number	Name	Year	Shortest distance between the hindcast location and the hurricane track [km]	$H_{s,max}$ [m]	f_p [1/sec]	f_m [1/sec]	θ [°]
Start of year 1972								
719	1	Christine	1973	62.711	1.463	0.2	0.2567	182.98
727	2	Alma	1974	814.946	0.216	0.3807	0.5079	85.7
729	3	Carmen	1974	129.229	1.441	0.0761	0.0862	262.79
731	4	Elaine	1974	317.704	0.751	0.2349	0.2985	280.59
732	5	Fifi	1974	324.472	0.842	0.0894	0.0974	261.37
733	6	Gertrude	1974	545.151	0.345	0.1234	0.3914	113.62
737	7	Caroline	1975	901.282	0.152	0.5253	0.6009	191.66
739	8	Eloise	1975	108.335	1.97	0.145	0.1856	209.31
740	9	Faye	1975	806.493	1.18	0.1703	0.2429	272.11
741	10	Gladys	1975	513.905	2.38	0.145	0.178	260.26
749	11	Emmy	1976	317.082	1.986	0.145	0.1938	282.77
750	12	Frances	1976	999.540	1.548	0.1703	0.2049	302.66
752	13	Gloria	1976	833.730	0.993	0.2	0.2594	282.1
753	14	Holly	1976	794.912	0.941	0.2	0.2609	295.71
763	15	Cora	1978	627.513	0.338	0.3241	0.4365	83.39
765	16	Ella	1978	1022.247	0.202	0.4472	0.5278	291.33
766	17	Flossie	1978	566.282	0.731	0.2349	0.3011	284.31
767	18	Greta	1978	695.406	0.841	0.2349	0.2781	180.69
770	19	Juliet	1978	253.648	1.825	0.1703	0.204	286.27
772	20	Ana	1979	406.318	0.28	0.3807	0.4631	79.46
774	21	Claudette	1979	88.792	1.735	0.2	0.2356	262.01
775	22	David	1979	210.205	9.645	0.0761	0.0936	172.56
777	23	Frederic	1979	52.415	2.689	0.1703	0.2013	236.3
781	24	Allen	1980	403.543	7.533	0.0761	0.0962	177.29
787	25	Georges	1980	449.652	0.198	0.4472	0.5477	277.37
795	26	Dennis	1981	277.099	0.396	0.3241	0.4204	104.53
797	27	Floyd	1981	82.146	2.496	0.1234	0.1705	232.23
798	28	Gert	1981	125.053	2.812	0.1234	0.1636	183.87
799	29	Harvey	1981	586.462	2.945	0.1234	0.1607	271.35
800	30	Irene	1981	890.171	2.19	0.145	0.1786	298.81
806	31	Beryl	1982	262.782	0.832	0.2349	0.289	275.25
808	32	Deby	1982	736.219	1.523	0.1703	0.2161	251.49
809	33	Ernesto	1982	832.099	0.575	0.2759	0.3471	256.04
815	34	Arthur	1984	213.353	1.071	0.2	0.252	289.42
824	35	Josephine	1984	955.222	0.984	0.2	0.2647	240.37
825	36	Klaus	1984	214.047	4.285	0.1051	0.1413	270.96
826	37	Lili	1984	380.032	1.364	0.1703	0.2291	281.2
832	38	Fabian	1985	984.265	0.517	0.2759	0.3561	277.38
833	39	Gloria	1985	300.487	4.107	0.1051	0.1311	229.31
835	40	Isabel	1985	662.545	0.506	0.2759	0.3621	227
To be continued								

				Continued				
837	41	Kate	1985	390.575	3.313	0.1234	0.1514	231.14
841	42	Danielle	1986	500.984	0.676	0.0894	0.2854	137.49
843	43	Frances	1986	576.567	1.165	0.1703	0.2424	284.8
				Start of year 1987				
849	44	Emily	1987	383.783	4.614	0.0894	0.1235	177.53
853	45	Chris	1988	102.236	1.311	0.1703	0.2294	170.72
858	46	Gilbert	1988	275.983	3.365	0.1051	0.1411	182.49
860	47	Isaac	1988	665.408	0.198	0.4472	0.5241	85.81
861	48	Joan	1988	616.436	1.306	0.0894	0.1833	204.98
864	49	Barry	1989	850.402	0.243	0.3807	0.4623	309.34
866	50	Dean	1989	195.031	4.04	0.1234	0.1456	268.42
869	51	Gabrielle	1989	735.464	3.542	0.1234	0.148	296.5
870	52	Hugo	1989	86.109	8.426	0.0894	0.1077	189.05
871	53	Iris	1989	422.497	1.323	0.1703	0.2189	306.2
874	54	Arthur	1990	478.494	1.333	0.0894	0.202	146.25
879	55	Fran	1990	853.301	0.172	0.4472	0.5545	88.51
880	56	Gustav	1990	561.244	1.878	0.145	0.1781	315.41
884	57	Klaus	1990	130.938	3.156	0.1234	0.1664	286.07
887	58	Nana	1990	499.107	2.209	0.145	0.1832	266.97
891	59	Danny	1991	599.188	0.155	0.3807	0.5401	9.43
897	60	Andrew	1992	495.980	2.906	0.1234	0.1577	217.34
902	61	Frances	1992	1000.836	0.808	0.2349	0.2857	283.91
904	62	Bret	1993	764.668	0.418	0.3241	0.409	94.32
905	63	Cindy	1993	271.563	0.892	0.145	0.2603	152.89
907	64	Emily	1993	921.188	1.439	0.1703	0.2252	260.9
908	65	Floyd	1993	917.211	0.239	0.3807	0.5049	243.13
913	66	Chris	1994	885.275	0.829	0.2	0.2653	307.7
914	67	Debby	1994	336.250	1.726	0.1051	0.1825	154.86
920	68	Chantal	1995	264.748	0.953	0.2	0.2679	288.04
923	69	Felix	1995	74.442	3.794	0.1234	0.1473	287.67
926	70	Iris	1995	139.077	3.044	0.1234	0.1622	281.66
929	71	Luis	1995	89.622	7.217	0.0894	0.1199	267.85
930	72	Marilyn	1995	96.649	6.146	0.0894	0.1213	211.49
933	73	Pablo	1995	885.679	0.152	0.4472	0.5594	57.49
935	74	Sebastien	1995	65.598	1.912	0.1703	0.2224	257.74
936	75	Tanya	1995	895.206	0.464	0.2759	0.3683	291.89
938	76	Bertha	1996	50.250	4.366	0.1051	0.1347	220.25
939	77	Cesar	1996	651.721	0.319	0.3807	0.4324	165.58
941	78	Edouard	1996	442.259	4.802	0.1051	0.1334	294.45
942	79	Fran	1996	409.406	2.697	0.145	0.17	267.82
944	80	Hortense	1996	174.657	4.167	0.1051	0.1322	170.1
955	81	Erika	1997	217.707	4.56	0.1051	0.136	272.76
956	82	Fabian	1997	743.363	0.207	0.4472	0.5335	270.28
957	83	Grace	1997	417.115	1.043	0.2	0.2606	246.88
958	84	Alex	1998	506.913	0.485	0.2349	0.3275	314.35
959	85	Bonnie	1998	184.623	2.339	0.1234	0.1741	220.95
961	86	Danielle	1998	556.982	2.826	0.1234	0.1657	265.99
964	87	Georges	1998	47.470	5.337	0.1051	0.1337	192.91
976	88	Dennis	1999	681.778	0.901	0.1703	0.2496	245.89
977	89	Emily	1999	672.864	0.132	0.4472	0.5804	48.01
979	90	Floyd	1999	467.292	4.968	0.0894	0.122	227.63
980	91	Gert	1999	783.459	3.306	0.1234	0.1534	287.06
				To be continued				

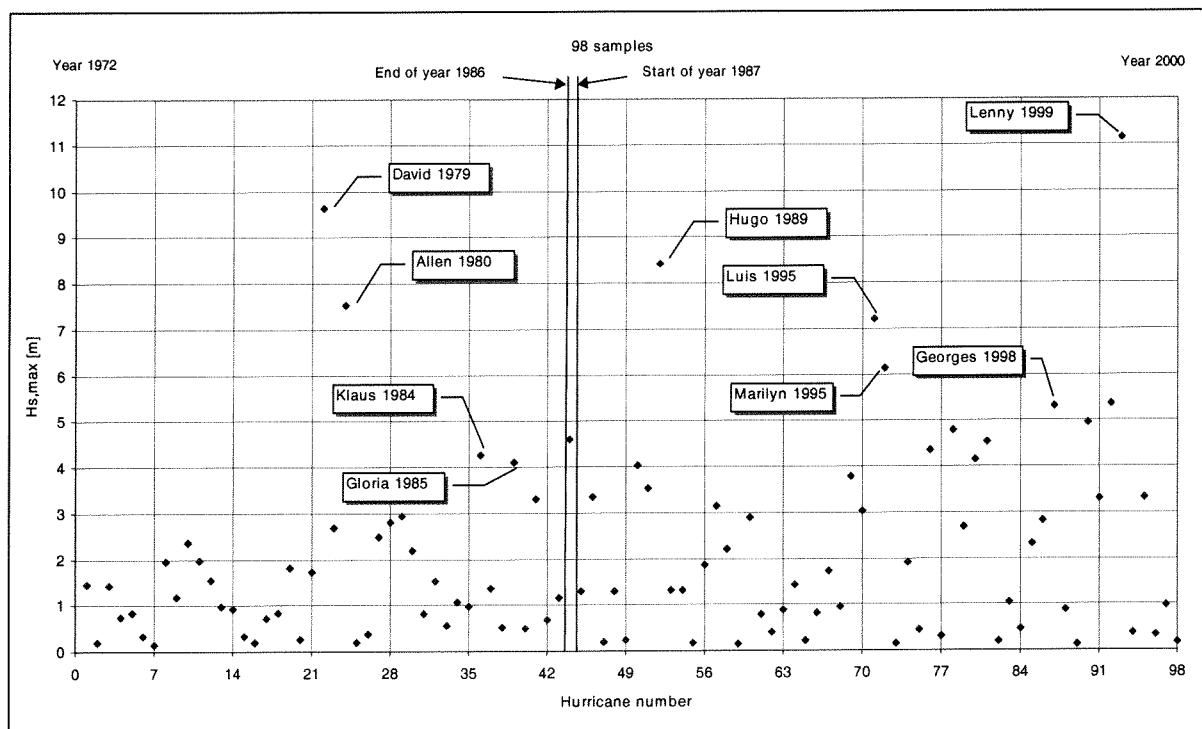|				7Continued				
985	92	Jose	1999	32.681	5.38	0.1051	0.1377	227.85
987	93	Lenny	1999	30.330	11.164	0.0761	0.0939	189.15
993	94	Chris	2000	261.085	0.378	0.2759	0.3881	316.07
994	95	Debby	2000	69.616	3.334	0.145	0.1749	241.01
995	96	Ernesto	2000	539.756	0.336	0.3241	0.402	311.41
999	97	Helene	2000	609.790	0.987	0.2	0.2759	160.88
1001	98	Joyce	2000	623.684	0.173	0.3807	0.5154	29.64
				End of year 2000				

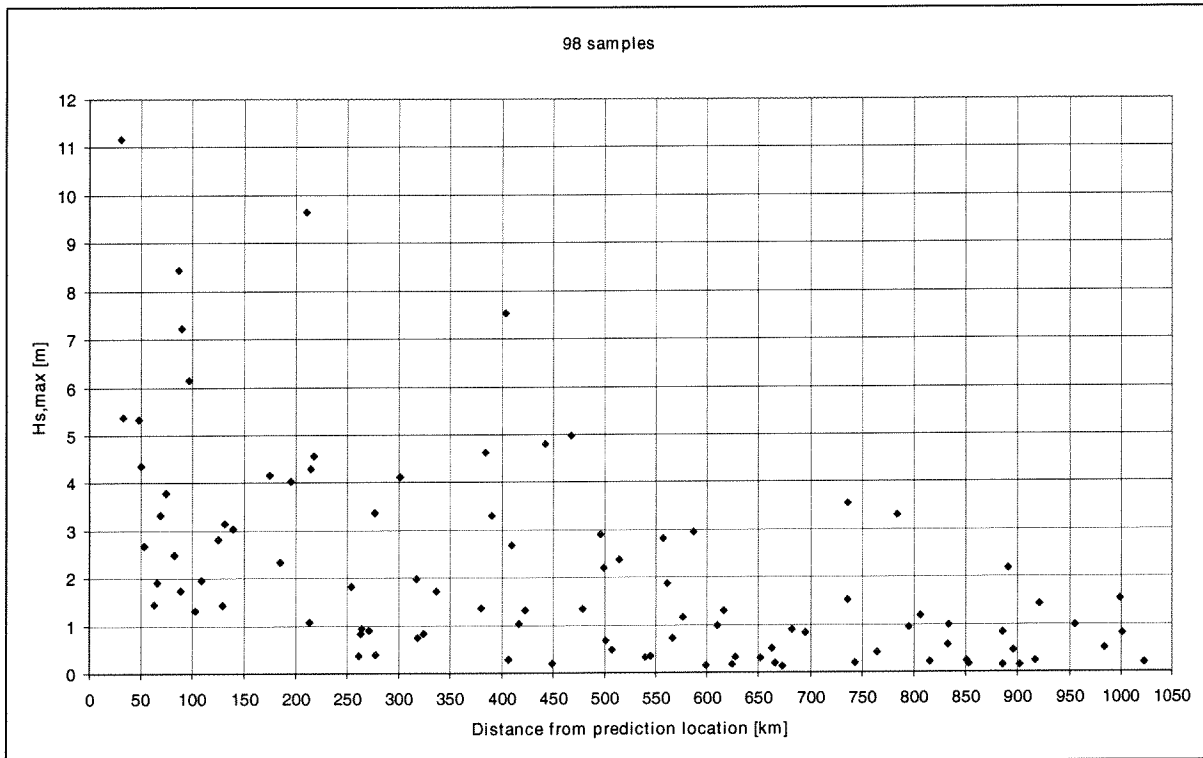Figure 77: $H_{s,max}$ hindcasted with DOLPHIN-B1, in order of appearance

Figure 78: $H_{s,max}$ hindcasted with DOLPHIN-B1, in order of the distance from Fort Bay harbour
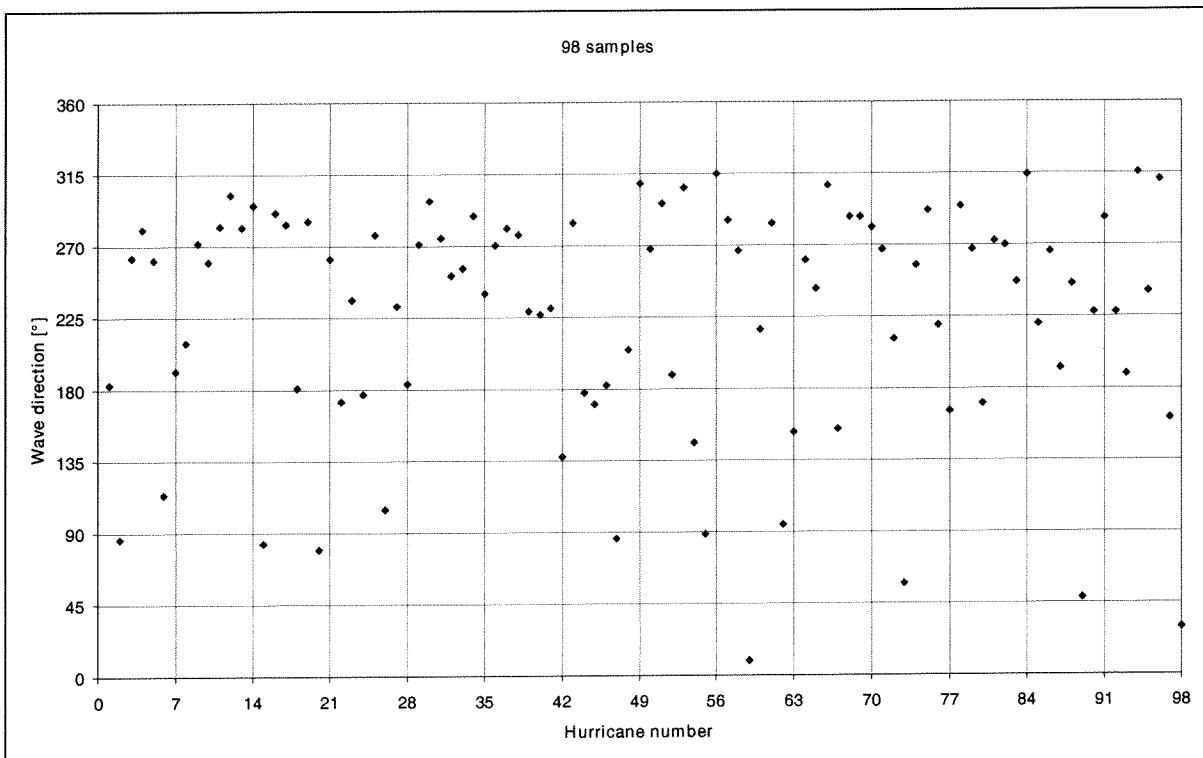
Figure 79: Wave directions hindcasted with DOLPHIN-B1, in order of appearance

Period 1972 till 1986, Hs,max against wave direction [°]

North 0–360°

West 270°

East 90°

Hs,max [m]

43 samples

South 180°

Figure 80: $H_{s,max}$ vs. θ period 1972 till 1986

Period 1987 till 2000, Hs,max against wave direction [°]

North 0–360°

West 270°

East 90°

Hs,max [m]

55 samples

South 180°
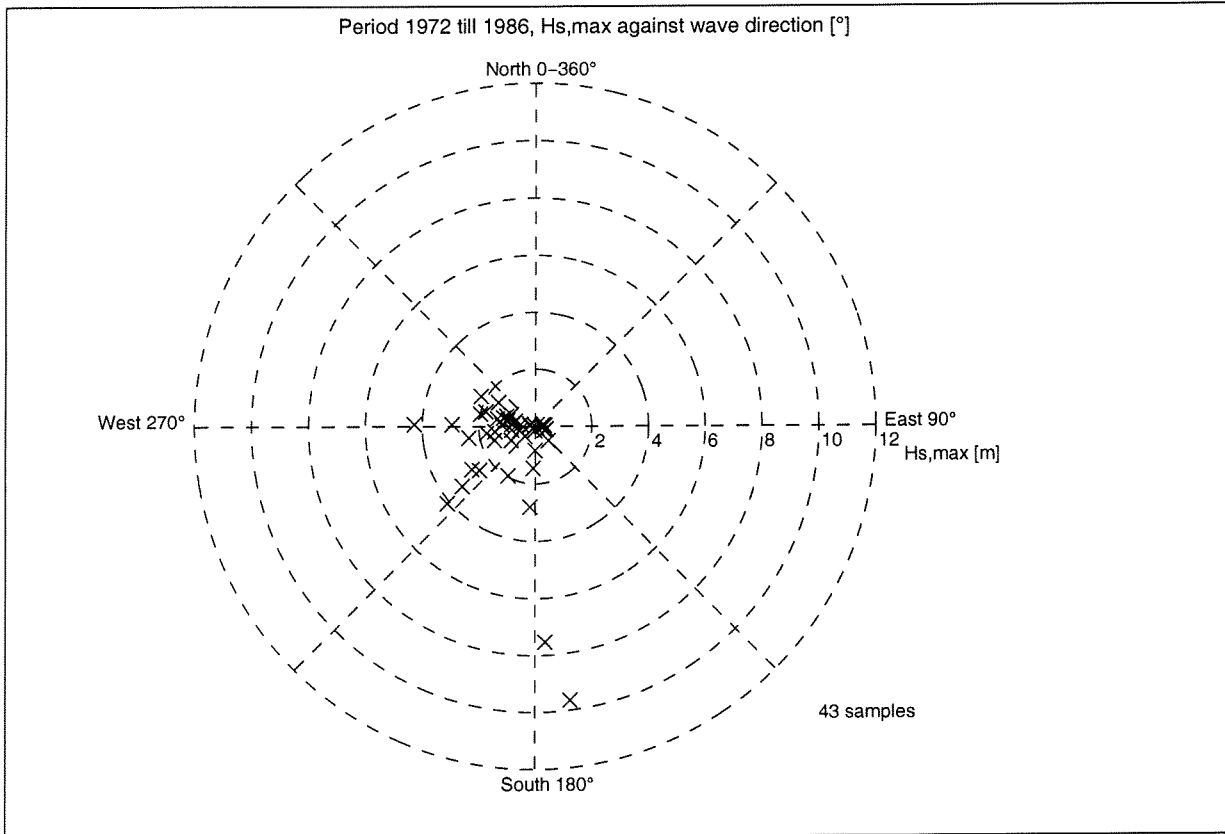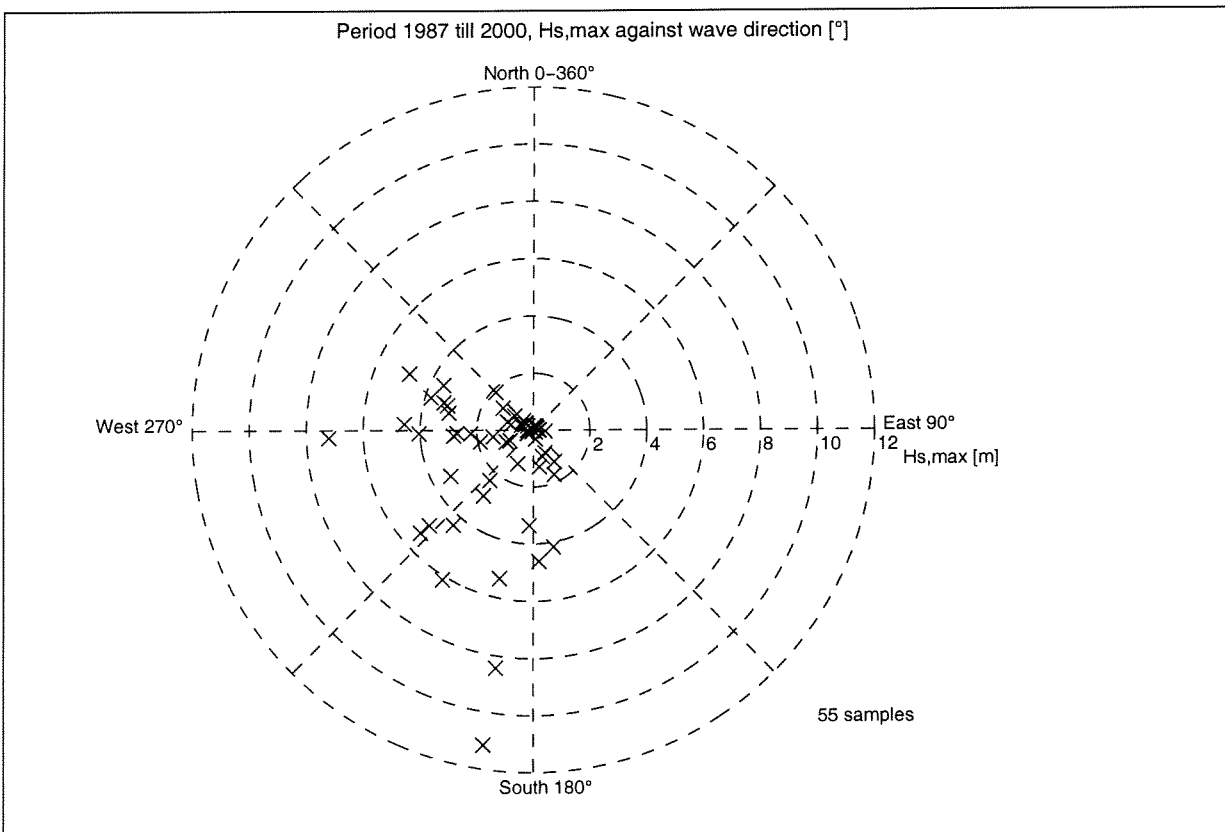
Figure 81: $H_{s,max}$ vs. θ period 1987 till 2000

ANNEX XI   STUDENTIZED BOOTSTRAP

For convenience $H_{s,max}$ are described as H_s.
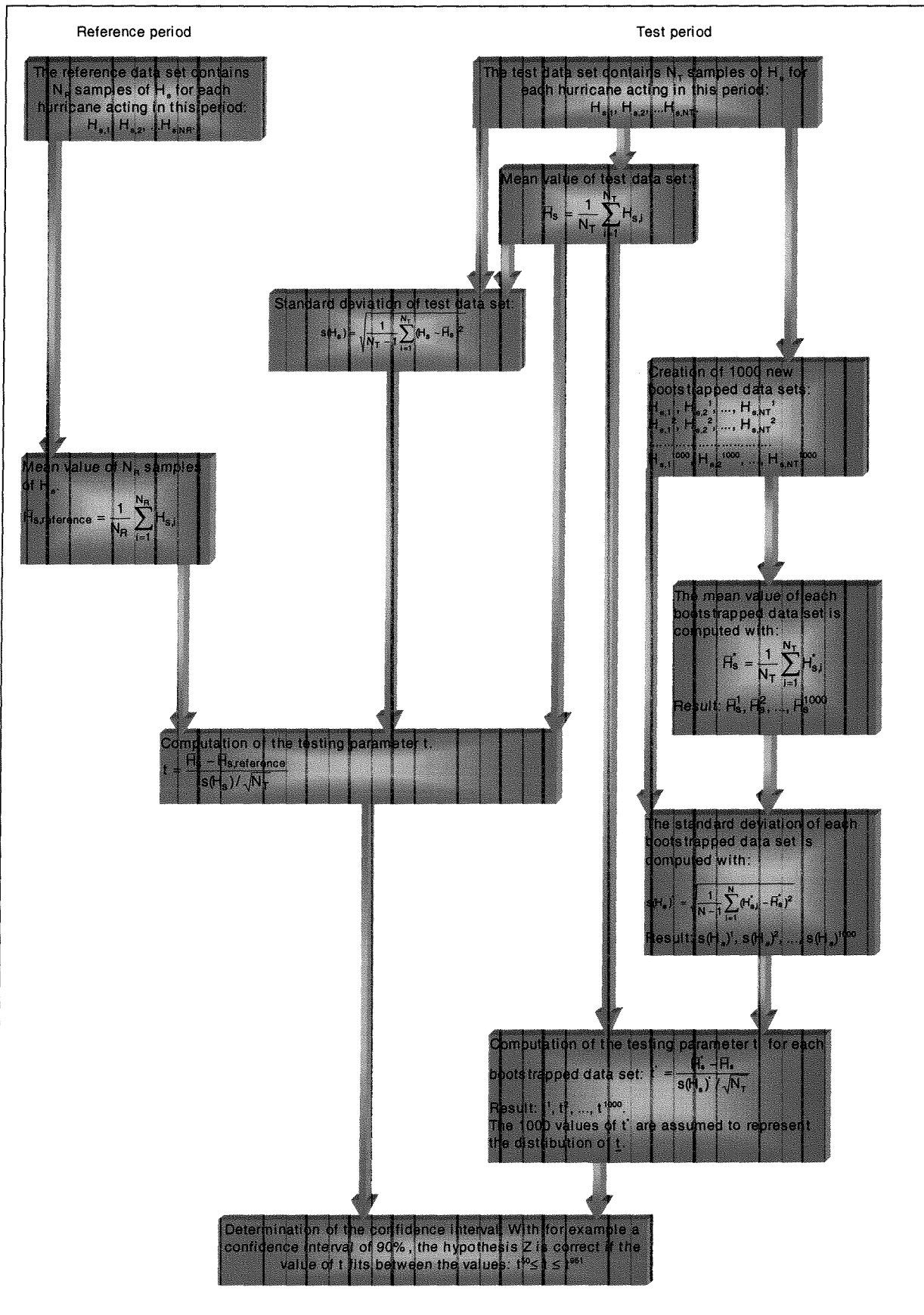
Figure 82: Scheme of the studentized bootstrap

ANNEX XII   MATLAB FILES

Fort Bay harbour, Saba. A study on hurricane conditions

122

```
%Function to carry out a studentized bootstrap.
%1000 bootstraps are made
%Hs1 = reference data set
%Hs2 = test data set
%Function nescessary to run studentboot:
%student.m
%bootstrp.m (Matlab function from Statistical toolbox)
%Wouter van Vilsteren 2001


function studentboot(Hs1, Hs2)

format short;

n = length(Hs2);
[boott,bootsam] = bootstrp(1000,'student',Hs2,mean(Hs2),n);
hist(boott,32);
[frc,x] = hist(boott,32);
frc1=(frc / 1000) / ((max(x) - min(x)) /31);
bar(x,frc1,1,'g');
ylabel('Probability density');
xlabel('Value of t*');
grid on;
hold on;
boott1 = sort(boott);
boundary1 = boott1(50);
boundary2 = boott1(951);
xboundary1 = [boundary1; boundary1];
yboundary1 = [0; 0.18];
plot(xboundary1,yboundary1);
xboundary2 = [boundary2; boundary2];
yboundary2 = [0; 0.18];
plot(xboundary2,yboundary2);
t1 = (mean(Hs2) - mean(Hs1)) / (std(Hs2) / sqrt(length(Hs2)));
text(boundary1 - 1.1,0.19,['Confidence boundary'],'FontSize',9);
text(boundary1 - 1.1,0.18,['at t=',num2str(boundary1)],'FontSize',9);
text(boundary2 + 0.1,0.19,['Confidence boundary'],'FontSize',9);
text(boundary2 + 0.1,0.18,['at t=',num2str(boundary2)],'FontSize',9);
xt = [t1; t1];
yt = [0; 0.3];
plot(xt,yt);
text(t1 + 0.1,0.29,['t=',num2str(t1)],'FontSize',9);
```

```
%Calculates the testing parameter t, used for the
%Student's t-Test

function t = student(x,m,n)

t = (mean(x)-m)/(std(x)/(sqrt(n)));
```

```
%Determination of the threshold value for the maximum significant wave heights
%The following function is nescessary to run the program:
%- weib(); gives the parameters of the Weibull function;
%Wouter van Vilsteren 2001
```

```
function thresholddet(Hs)

Hssort = sort(Hs);
t2      = 1;

for threshold = 0:0.01:Hssort((length(Hssort)) - 5)      %Varying of the threshold till the
fifth                                                     %highest sample in the data set
    clear Hs_threshold;
    clear Hs_adjust;
    clear Hs_adjust1;

    t = 1;                                               %Selecting samples with values above
the                                                       %threshold
    for k = 1:length(Hssort)
        if Hssort(k) > threshold
            Hs_threshold(t) = Hssort(k);
            t = t + 1;
        end
    end

    t1 = 1;
    Hs_adjust = Hs_threshold-threshold;                  %Adjusting of selected samples to the
    for k = 1:length(Hs_adjust)                          %threshold value
        if Hs_adjust(k) > 0
            Hs_adjust1(t1) = Hs_adjust(k);
            t1 = t1 + 1;
        end
    end


    [alfa,sigma] = weib(Hs_adjust1);                     %Determination of the Weibull
parameters

    a = 0.3  + (0.18 / alfa);                            %Coefficients in plotting rule
    b = 0.21 + (0.32 / alfa);                            %according to [lit 14]

    Hs_adjust1 = (Hs_adjust1).*(-1);                     %Changing the ascending order of the
    Hs_adjust1 = sort(Hs_adjust1);                       %samples into a descending order
    Hs_adjust1 = (Hs_adjust1).*(-1);
    i = 1:length(Hs_adjust1);

    dat_prob  = 1 - ((i - a) / (length(Hs_adjust1) + b));%Probabilities from plotting rule
    weib_prob = 1 - exp(-(Hs_adjust1./sigma).^alfa);     %Probabilities from Weibull
    dev2      = (dat_prob - weib_prob).^2;
    sumdev2   = sum(dev2);
    dev(t2)   = sqrt((1 / length(Hs_adjust1)) * sumdev2);%RMS difference
    t2 = t2 + 1;
end

mindev = min(dev);
i = 1;
while dev(i) > mindev
    i = i + 1;
end

Optimal_threshold = (i - 1) * 0.01;                      %Selection of the optimal threshold

clear Hs_threshold;
```

```
clear Hs_adjust;
clear Hs_adjust1;

t = 1;                                              %Selecting samples with values above
the
    for k = 1:length(Hssort)                        %optimal threshold
        if Hssort(k) > Optimal_threshold
            Hs_threshold(t) = Hssort(k);
            t = t + 1;
        end
    end


t1 = 1;
    Hs_adjust = Hs_threshold - Optimal_threshold;   %Adjusting of selected samples to the
    for k = 1:length(Hs_adjust)                     %optimal threshold value
        if Hs_adjust(k) > 0
            Hs_adjust1(t1) = Hs_adjust(k);
            t1 = t1 + 1;
        end
    end


[alfa,sigma] = weib(Hs_adjust1);                         %Determination of the Weibull
parameters
                                                %belonging to the optimal threshold
plot(0:0.01:Hssort((length(Hssort)) - 5),dev);        %Plot of RMS difference against
threshold
xlabel('Threshold defined as Hs,max [m]');
ylabel('RMS Probability difference');
text(0.1,max(dev),['Optimal threshold = ',num2str(Optimal_threshold)],'FontSize',9);
text(0.1,max(dev) - 0.01,['sigma = ',num2str(sigma)],'FontSize',9);
text(0.1,max(dev) - 0.02,['alfa = ',num2str(alfa)],'FontSize',9);
grid on;
```

```
%Maximum likelyhood estimation of the
%Weibull parameters
%Wouter van Vilsteren 2001

function [alfa,sigma]=weib(x)

n = length(x);

alfa = 1;
diff = 1;
while abs(diff)>1e-6
    lnx = log(x);
    xa  = x.^alfa;

    beta = n/sum(xa);
    dL   = n/alfa + sum(lnx) -beta*sum(xa.*lnx);
    S1   = sum(xa.*lnx.*lnx)/sum(xa);
    S2   = sum(xa.*lnx)/sum(xa);
    ddL  = -n*( 1/(alfa*alfa) + S1 - S2*S2 );
    aoud = alfa;
    alfa = aoud - dL/ddL;
    diff = alfa-aoud;
end

beta  = n/sum(x.^alfa);
```

```
sigma = (1/beta)^(1/alfa);
```

ANNEX XIII   INFORMATION ON CD-ROM